DEPARTMENT OF THE INTERIOR
U.S. GEOLOGICAL SURVEY

Composition of Co-Rich Ferromanganese Crusts and Substrate Rocks from the NW Marshall Islands and International Waters to the North, Tunes 6 Cruise

by

James R. Hein[1], Susan E. Zielinski[1], Hubert Staudigel[2], Se-Won Chang[3]
Michelle Greene[1], and Malcolm S. Pringle[4]

Open File Report 97-482

1997

[1]U.S. Geological Survey, Menlo Park, CA
[2]University of California, Scripps Institute of Oceanography, La Jolla, CA
[3]Korea Institute of Geology, Mining, and Materials, Taejon, Korea
[4]Scottish Universities Research and Reactor Centre, Kilbride, UK

INTRODUCTION

Thirteen northwest Pacific seamounts and guyots were dredged during the Tunes 6 cruise, which took place from 31 October to 2 December, 1991 aboard the R.V. Thomas Washington under the direction of H. Staudigel. The primary objectives of the cruise were to study seamount ages and basalt chemistry in order to better understand the long term history of the South Pacific thermal anomaly (SOPITA). Representative ferromanganese oxyhydroxide crusts (Fe-Mn crusts) from most dredges were collected for this study, which extends our previous work on Fe-Mn crusts collected from the Marshall Islands and Federated States of Micronesia to seamounts located farther north (Hein, Kang et al., 1990; Hein, Ahn et al., 1992).

Most dredge recoveries were from 11 seamounts located in international waters north of the Marshall Islands Exclusive Economic Zone (EEZ), whereas only one seamount was sampled within the EEZ of the Marshall Islands (Fig. 1; Table 1). A total of 35 dredges were attempted and 23 recovered Fe-Mn crust samples and substrate rocks. One or two dredge hauls recovered samples from most guyots, however, Vlinder and Batiza Guyots yielded five and four dredge haul recoveries, respectively. Several guyots had previous bathymetric surveys (Batiza, Jennings, Maloney, Missy, Golden Dragon), or were crossed because they were close to the ship's track (Alcatraz, Bellevue) and therefore only minor additional bathymetric surveys were conducted during Tunes 6.

Most volcanic edifices studied are flat-topped guyots and many of those appear from seismic-reflection records to be devoid of summit reefs. However, Jennings Guyot yielded Cretaceous shallow-water limestone and five other guyots (mostly at the western end of the Marcus-Wake seamount group) yielded carbonates. Bellevue, Alcatraz, and Seth Guyots have steep and smooth upper flanks that are morphologically uniform to great depths, indicating carbonate thicknesses up to 1000 m. Drowned atolls typically have steep upper flanks that slope at 24-36° and the reefs form a 20-40 m rim around the summit platform. Vlinder Guyot has a volcanic cone projecting through the summit platform, indicating rejuvenation of volcanism. Guyots without limestones typically have summits that slope at low angles from a central high to the main break in slope between the summit and flanks. Below the main slope break, flanks slope at 12-20° down to the abyssal seafloor.

This report presents data for those dredge hauls from which Fe-Mn crusts were studied. Data include sample descriptions, detailed chemical (major, minor, Pt-group, and rare earth elements) and mineralogical analyses of bulk Fe-Mn crusts and individual crust layers, and major oxide compositions and mineralogy for substrate rocks collected during the Tunes 6 cruise. Correlation coefficients are used to determine relationships between elements and Q-mode factor analysis to determine the grouping of elements with various crust phases.

METHODS

X-ray diffraction was completed on a Philips diffractometer using Cukα radiation and a curved-crystal carbon monochromator. Abundances of major oxides in substrate rocks were determined by X-ray fluorescence spectroscopy (Taggart et al., 1987), Fe(II) by colorimetric titration (Peck, 1964), CO_2 by coulometric titration (Engleman et al., 1985), H_2O^+ by water evolved at 925°C as determined coulometrically by Karl-Fischer titration (Jackson et al., 1987), and H_2O^- by sample weight difference at 110°C for greater than one hour (Shapiro, 1975). The low totals for the phosphorite samples occur because fluorine and sulfur were not determined and therefore are not included in the totals. High fluorine (to 4.4%) and sulfur (to 2.1% SO_3) contents are typical of marine carbonate fluorapatite (Cullen and Burnett, 1986; Burnett et al., 1987; Hein et al., 1993). For Fe-Mn crusts, the concentrations of most major and minor elements were determined by inductively coupled

plasma-atomic emission spectrometry, except those of K, Zn, and Pb, which were determined by flame atomic-absorption spectroscopy, and those of As, Cr, and Cd, determined by graphite-furnace atomic absorption spectroscopy on air-dried samples (Aruscavage et al., 1989). Concentrations of platinum-group elements (PGEs) and rare earth elements (REEs) for Fe-Mn crusts were determined by inductively coupled plasma-mass spectrometry (Lichte et al., 1987a,b).

The usual Pearson product moment correlation coefficient was used to calculate the correlation coefficient matrices. For Q-mode factor analysis, each variable percentage was scaled to the percent of the maximum value before the values were row-normalized and cosine theta coefficients calculated. Factors were derived from orthogonal rotations of principal component eigenvectors using the Varimax method (Klovan and Imbrie, 1971). All communalities are ≥ 0.93. Low factor scores, $\leq |0.2|$, were discarded because they are not statistically significant.

SUBSTRATE ROCK DESCRIPTIONS AND COMPOSITION

Substrate rocks in decreasing order of abundance are basalt, breccia, phosphorite, hyaloclastite, limestone, volcaniclastic siltstone and sandstone, and mudstone (Table 1). As many as five different rock types were recovered in a single dredge haul. As seen in hand samples, breccias most commonly consist of basalt clasts in a hyaloclastite matrix, and/or carbonate fluorapatite (CFA) cement. Many samples have Mn oxide impregnations that commonly form dendrites. Volcanogenic clasts in breccias and volcaniclastic rocks are commonly replaced by clay minerals and iron oxides. Basalts are aphanitic with common plagioclase phenocrysts and CFA infilling fractures and vesicles. Some samples have vesicles filled with carbonate mud or Fe-Mn oxides. Reef limestones consist of rounded carbonate clasts with calcite cement and moldic porosity; pelagic limestones are micritic and bioturbated to massive. Mudstones are mostly bioturbated with Fe-Mn oxides lining some burrows. Phosphorites have carbonate mud in cracks and Fe-Mn oxide impregnations.

X-ray Diffraction Mineralogy and Petrography

Primary volcanogenic and sedimentary minerals include plagioclase, pyroxene, magnetite, and calcite; and secondary minerals include CFA, smectite, calcite, phillipsite, clinoptilolite, goethite, hematite, barite, and potassium feldspar (Table 2). Secondary CFA is the most abundant mineral in these samples and occurs in 73% of the samples as a major or moderate constituent, regardless of rock type (Table 2).

Hyaloclastite and hyaloclastite breccias consist chiefly of CFA and phillipsite (Table 2), with moderate to minor amounts of plagioclase, pyroxene, and magnetite. Most samples contain minor amounts of smectite. One sample consists predominantly of goethite. Hyaloclastites are predominantly completely altered to phillipsite, clinoptilolite, smectite, and Fe oxides, which in turn are cemented by CFA and/or replaced in varying degrees by CFA. Consequently, all gradations exist from altered hyaloclastite to phosphorite with relict hyaloclastite textures. Vesicles are lined with smectite and infilled by zeolites.

Mineralogically, most basalts consist chiefly of plagioclase and pyroxene, although some contain large amounts of CFA, hematite, and goethite. One sample (D21-2) is almost completely replaced by goethite and hematite, whereas another sample (D38-2) is nearly completely replaced by CFA, but shows a relict basalt microcrystalline texture. A wide range of basalt types were collected with variable amounts and combinations of plagioclase, pyroxene, olivine, and rarely amphibole phenocrysts. Groundmass textures include holocrystalline, subophitic, intersertal, microcrystalline, aphanitic, and doleritic. Samples range from highly vesicular to massive. Detailed descriptions of the basalts are available from H. Staudigel, Scripps Institution of Oceanography (see also Koppers, 1997).

Rocks identified as limestones from hand samples are overwhelmingly CFA mineralogically, with moderate amounts of plagioclase, calcite, barite, phillipsite, and potassium feldspar and trace amounts of chlorite, smectite, and quartz. Calcite is primary and the other minerals are due to various admixtures of volcanogenic grains and their alteration products, or to cementation and replacement. Barite forms veins and lenses. All gradations exist from unaltered limestone to phosphorite with relict limestone textures, especially CFA-replaced foraminiferal sands, some with abundant relict radiolarians.

Three types of mudstones were sampled from this region. The first type is composed mainly of magnetite, hematite, and smectite with lesser amounts of phillipsite and clinoptilolite. The second type of mudstone consists of variable amounts of CFA, potassium feldspar, smectite, phillipsite, and plagioclase, whereas the third type is composed solely of smectite. The first type is most likely either an altered ash or altered fine-grained hyaloclastite. The second type is a CFA-replaced altered volcaniclastic mudstone and the third type is bentonite.

Phosphorites are composed of CFA with plagioclase, smectite, and other minerals (Table 2). CFA commonly cements all of the clastic rock types and variably replaces grains in all rock types from incipient to complete replacement. The most commonly replaced rock type is pelagic limestone, where the foraminifera, radiolarians, other grains, and presumably the nannofossil matrix have been completely replaced by CFA. The grains (except the nannofossils) occur as ghosts. Barite veins and lenses commonly occur in the phosphatized pelagic limestone. In addition, shallow-water limestone, volcaniclastic rocks, hyaloclastite, and rarely basalt are completely replaced by CFA, thereby forming phosphorite.

Chemistry

The most P_2O_5 rich CFA-replaced sedimentary rocks have CaO/P_2O_5 ratios of 1.60 to 1.66 (Table 3), whereas theoretical chemical compositions for CFA range from 1.5 to 1.6 (Manheim and Gulbrandsen, 1979). The slight excess Ca over P in some of our samples is due to additional Ca associated with minor contamination by volcanogenic plagioclase, phillipsite cement (an alteration product of volcanic debris), and to relict calcite in the phosphatized limestone.

Smectite occurs in major to moderate amounts in 29% of the samples analyzed, and is especially abundant in the mudstones. It is found in at least trace amounts in over 70% of the samples analyzed. The one sample of nearly pure smectite (D33-3) has relatively high Al, Fe, and Mg contents and low Ca content, indicative of an iron-rich montmorillonite.

Phillipsite is also a common mineral, occurring in major to moderate abundances in 26% of the samples, primarily in the breccias and phosphatized limestones. The samples measured for chemistry, which have abundant phillipsite, have Si/Al ratios ranging from 3.0 to 3.4, which is higher than the range for most marine phillipsites (2.3-2.8) and significantly higher than the values for mafic igneous rocks (1.3-2.4; Kastner, 1979). These high values are the result of contamination by Si-rich volcanogenic and other phases.

Most of the basalt and basalt clasts in breccia are altered to smectite and goethite and are rarely replaced by phosphorite and phillipsite. Alteration is best characterized by increases in Fe_2O_3 and water and decreases in FeO and K_2O contents (Table 3). Volcaniclastic mudstones and hyaloclastites have compositions comparable to highly altered basalts.

FERROMANGANESE CRUSTS

Fe-Mn crusts studied here vary in thickness from 3 to 114 mm (Tables 1, 4), although crusts were collected during Tunes 6 that range from a patina to 200 mm or more (D18,

South Wake Guyot). The thickest crust studied (114 mm) was dredged from the western flank of Vlinder Guyot in dredge D27. The thickest crust average from the various dredge hauls is 49 mm collected from Neen Koiaak Guyot in dredge D12. Limited availability of personnel on the Tunes 6 cruise did not allow for detailed records to be kept of maximum and average crust thicknesses for each dredge and the values listed in this report are predominately for samples analyzed here and from sketchy notes in the original logs.

Thicker crusts are composed of two or more layers, six being the maximum and two being the most common. Polished thin sections show that various layers are typically botryoidal, columnar, mottled, and laminated, in that order of abundance and are typical of other central Pacific crusts (Hein et al., 1992a). If the substrate rock has an irregular surface, then the first Fe-Mn oxyhydroxide layer is botryoidal, with initial points of growth being on the projections. If the substrate rock has a smooth surface, the first oxyhydroxide layer may be laminated, massive, or mottled. Mottled layers are porous and commonly have the most contamination by detrital minerals relative to the other layer types. Detrital minerals also accumulate between columns and are the chief cause for the directed growth of the columnar structure.

Growth Rates and Ages

Because the flux of Co into Fe-Mn crusts is relatively constant over time, growth rates can be determined from the Co content using the equation of Puteanus and Halbach (1988):

$$\text{Growth Rate (mm/Ma)} = 1.28 / (\text{Co\%} - 0.24) \qquad (1)$$

The faster a crust grows, the lower the Co concentration. Crusts in which the older parts have been heavily phosphatized (>1 weight % P), however, do not have such a simple relationship because P dilutes the Co and likely mobilizes many of the metals within that older crust generation (Hein, Kang, et al., 1990; Koschinsky and Halbach, 1995). Growth rates in phosphatized parts of crusts may be determined using Co, Mn, and P contents and another set of equations of Puteanus and Halbach (1988):

$$Co^{(x)'} = Co^{(x)m} (Mn / Co^{(x)}) / (Mn / Co^{(b)}) \qquad (2)$$

$$Co^{(x)''} = Co^{(x)'} (1 - 0.05\ \Delta P)^{-1} \qquad (3)$$

where $Co^{(x)'}$ is the Co concentration corrected for phosphate dilution; $Co^{(x)m}$ is the Co concentration measured in layer (x); $Mn/Co^{(x)}$ and $Mn/Co^{(b)}$ are the Mn/Co ratios measured in layer (x) and the boundary layer, respectively; ΔP is the difference between the CFA fraction of layer (x) and the average of the younger crust; and $Co^{(x)''}$ is the doubly corrected Co concentration in layer (x). Based on Co content for samples with less than one weight percent P and based on Co, P, and Mn contents for the remaining crust samples, growth rates for bulk crusts varied from 2.1 mm/Ma to 9.8 mm/Ma (Table 4). The average growth rate for bulk crusts was 5.0 mm/Ma, which is within the range of growth rates for hydrogenetic crusts (Hein et al., 1987b; 1990), but is a somewhat faster mean rate than for crusts from areas to the south and southeast. Growth rates for Tunes 6 crusts generally decrease with decreasing latitude, with the highest growth rates calculated for crusts from Oma Vlinder and Missy Guyots. Individual crust layers grew at rates from 2.2 to 14.3 mm/Ma.

The five thickest crusts analyzed, D27-5 (114 mm), D15-4 (95 mm), D 36-3 (81 mm), D25-3 (80 mm), and D41-1 (73 mm) began growing at 24.4, 37.5, 21.5, 15.8, and 13.0 Ma respectively, based on the growth rates of individual layers and the thickness of each

layer (Table 4). These ages of initiation of crust growth are minimum ages because the technique does not take into account dissolution and erosional unconformities which can add another several million years to the age of the crusts (Futa et al., 1988; Ingram et al., 1990; Ling et al., 1997). The oldest crust, from Aean Kan Guyot, is of late Eocene age (37.5 Ma), but is still 37-67 Ma younger than ages typical of central Pacific Cretaceous seamounts.

X-ray Diffraction Mineralogy

Great care was taken in sampling crusts for chemical and mineralogical analyses. All contamination from recent sediments was removed, which was especially critical in porous crust layers. Also, special attention was paid to obtaining a clean separation of the lower crust layers from the substrate. Any minerals or elements determined to exist in the various crust layers were incorporated into those layers during deposition or diagenesis and are not due to sampling procedures or post-depositional infiltration of sediment. Finally, all encrusting organisms and other debris were cleaned from the crust surfaces before sampling. Bulk always refers to the entire crust thickness, whether composed of layers or not.

All but two of the 79 samples of Fe-Mn crusts contain greater than 90% δ–MnO_2 (vernadite; Table 5), which has only two X-ray reflections at about 2.42Å and 1.41Å. X-ray amorphous Fe oxyhydroxide epitaxially intergrown with the δ–MnO_2 is also a dominant phase in these crusts, but is not included with the crystalline phases listed in Table 2. This X-ray amorphous iron phase crystallized to goethite in three of the bulk crusts and two of the individual layers analyzed. In the individual layers, goethite was present only in the innermost layer, indicating that those layers have undergone the most advanced diagenetic alteration. Two more samples, one an innermost layer (D41-1C) and the other a thin bulk crust (D14-17A), contain hematite, which is likely due to contamination by altered volcanogenic debris in the thin bulk crust, but may instead be due to diagenesis in the inner layer of the thick crust. CFA occurs in 24% of the bulk crusts and 19% of the layers analyzed. Layered samples contain up to 19% CFA, always within the innermost one or two layers of the crust. CFA is not found in the outer layers.

Quartz was found in all but three crusts. Of those samples that contain quartz, all but five have three percent or less quartz, whereas the other five have 4-5% quartz. Plagioclase (trace to 5%) was found in 75% of the samples. The quartz and some of the plagioclase are of eolian origin, carried by the westerlies from Asia, as there is no local or regional source for quartz in the west-central Pacific. The Marshall Islands are south of the main westerly wind belt which is reflected in lower quartz contents compared to crusts from higher latitudes (Hein et al., 1985a,b; 1987a; 1990). The remainder of the plagioclase, as well as the phillipsite, pyroxene, and calcite are reworked from local outcrops and incorporated into the crusts during precipitation of the Fe-Mn oxyhydroxides.

Calcite occurs in trace amounts in only two bulk samples of thin crusts and none of the layers. Calcite probably occurs from incorporation of biogenic calcite in the outermost millimeter of those crusts during accretion of the oxyhydroxides. The calcite is replaced by the oxyhydroxides once the incorporated calcite is buried by accretion of additional layers.

Todorokite is rare in hydrogenetic seamount crusts (Hein et al., 1987a), but occurs questionably in one of the samples analyzed here (D15-1B, Aean-Kan Guyot). Todorokite may form under different redox conditions than the more oxidized δ–MnO_2 phase, either during initial precipitation, during diagenesis, or during low-temperature hydrothermal precipitation. A diagenetic origin for D15-1 todorokite is unlikely because the crust is too thin for significant diagenesis.

Chemistry

Bulk Crusts: Chemical analyses for 84 samples and subsamples of crusts are presented in Tables 6 and 7 (normalized to 0% H_2O^-). General statistics for each dataset are presented in Tables 8, 9, and 10.

Water-normalized contents are often used because hygroscopic water varies with humidity in the lab in which samples are analyzed. Therefore, H_2O^-, and consequently the abundances of other elements, will vary accordingly and significantly as hygroscopic water contents can be as high as 30%. Compositions normalized to 0% H_2O^- (Table 7) can be more meaningfully compared and may also more closely represent the grade of the potential ore. Consequently, the following discussion is based on hygroscopic water-free data.

The mean Fe and Mn contents of the 46 bulk crust samples are 16.7% and 22.1%, respectively (Table 9). The mean Fe/Mn ratio (0.76) is comparable to the mean ratio for the entire central Pacific region (0.77; Hein et al., 1992b), but is somewhat higher than the mean ratio for the Marshall Islands EEZ (0.65; Hein, Kang, et al., 1990). Mean Fe content is less and Mn somewhat less compared to bulk crust samples from the Marshall Islands EEZ, 15.3% and 23.6%, respectively. The mean contents of the economically important metals Co (0.52%), Ni (0.40%), and Pt (0.50 ppm) are somewhat less than the Marshall Islands EEZ mean contents of 0.66%, 0.50%, and 0.58 ppm, respectively. The mean Co content is less, Ni about the same, and Pt much higher than mean contents for the equatorial Pacific. Phosphorus, a potential byproduct for mining, has a low mean value of 0.72% compared to the central Pacific mean of more than 1% and the Marshall Islands EEZ mean of nearly 2%.

Analysis of a large number of thick crusts lowers the mean contents of most metals (except platinum), and that is probably why this study shows mean concentrations below the regional and Marshall Islands means. Studies that include only analyses of thin crusts yield mean concentrations higher than those of regional means (for example, Pichocki and Hoffert, 1987; see Hein et al., 1992b for discussion).

Layers: In general, Co contents decrease from the outer surface to the substrate through Fe-Mn crusts (Halbach et al., 1982; Hein et al., 1985b); but in Tunes 6 samples, only about half show that decrease (Tables 6,7), whereas in the other half Co increases with depth; in one sample, the Co content remains unchanged with depth in the crust. This geographic area is unique in having so many samples that show an increase in Co with depth in the crusts. Other elements also change with depth in the crusts. Although there are exceptions, the following changes typically occur with depth in the Tunes 6 crusts: Fe, Si, Al, Pb, Cr, and As decrease, while Mn, Ni, Cu, Zn, Ba, Ce, and Pt increase.

Those trends indicate that, in general, elements representative of the aluminosilicate detrital fraction decrease toward the substrate (with notable exceptions), in contrast to the trend found in other studies. This decreasing trend with depth in the crusts is also true for the Fe oxyhydroxide phase and associated elements, whereas the Mn oxyhydroxide phase and associated elements show the opposite trend. Most of the PGEs increase toward the substrate, which is typical of the trend observed in other studies. Phosphorus remains relatively constant in thin crusts and increases significantly in the lower layers of thick crusts. Strongly phosphatized crusts disrupt the trends in the elements as noted above. A few crusts have the highest concentrations of elements in one of the internal layers.

Thinner crusts are similar chemically to the outer parts of thicker crusts. Thinner crusts (<15 mm) have less Mn and Co than thicker crusts and significantly less P, Cu, Mo, and Ni, but more Fe than thicker crusts. These trends are similar to those reported by Hein, Ahn, et al. (1992) for Micronesian crusts, but contrast with trends in crusts from other areas. These differences probably are related to milder phosphatization of Tunes 6 crusts compared to those from other areas. Phosphatization dilutes these elements with depth in the crusts, making their overall grades lower than for thinner, non-phosphatized crusts. In addition to those element trends, thin crusts have higher Al, Si, K, and Cr and much lower

Pt concentrations than thick crusts. The Pt contents of two inner layers of thick crusts are extremely high, among the highest measured in any Pacific crusts, 2.1 ppm (D25-3D) and 2.7 ppm (D32-9H). The other PGEs are also very high in these crust layers.

Platinum Group Elements (PGEs)

We report the concentrations of Pt, Pd, Rh, Ru, and Ir for 19 bulk crusts and 33 crust layers (Tables 6, 7). This is the fourth report of Ru and Ir contents in Fe-Mn crusts (see Hein, Kang, et al., 1990; Hein, Ahn, et al., 1992; Hein, Gramm-Osipov, et al., 1994). Platinum contents vary from 0.133 ppm to 0.874 ppm for bulk crusts and from 0.133 ppm to 2.65 ppm for crust layers (Tables 9, 10). Palladium is below the limit of detection of 4 ppb (based on the original hygroscopic water-bearing dataset); the other PGEs vary by factors of three to nine: Rh (9.8-97.6 ppb), Ru (8.7-32.3 ppb), and Ir (4.1-22.3 ppb). The maximum values for each PGE (except Pd) are extremely high compared to those in other crusts analyzed to date. However, the mean values of bulk crusts are significantly less than mean values of Marshall Islands EEZ crusts for Ir, somewhat less for Pt and Rh, and somewhat more for Ru. The Tunes 6 PGE contents are significantly enriched over lithospheric and seawater abundances, but not over chondrite abundances (Figs. 2, 3; Parthé and Crocket, 1978; Hodge et al., 1986; Goldberg, 1987; Anders and Grevesse, 1989; Colodner, 1991; Bertine et al., 1993). For comparison, the sample with the highest PGE enrichment (D32-9H, layer 50-60 mm) is plotted in Fig. 3. Relative to chondrites, Ir and Ru ratios are a few times greater in D32-9H compared to the mean values for bulk crusts, Rh an order of magnitude greater, and Pt is enriched by three orders of magnitude. Relative to surface seawater, Ir is the most enriched for the mean bulk crust dataset, whereas Pt is the most enriched for sample D32-9H, but only somewhat more enriched than Ir, Ru, and Rh. Pd probably has about the same enrichment for both mean crust and most enriched crust datasets.

The highest Pt, Rh, and Ir concentrations occur in the inner layer of crust D32-9H, which was recovered from the deepest water dredge site, whereas the highest Ru content is in the innermost layer of crust D18-1C. Enrichment of PGEs in the inner parts of crusts is common for central Pacific crusts. The highest Pd and Ru concentrations occur in crusts from the Yap and Mariana arcs, as do other elements indicative of clastic input. As shown in previous studies, Pt, Ir, and Rh are derived predominantly from seawater, whereas Pd and much of the Ru are derived from clastic debris, the remainder of the Ru being derived from seawater. The extraterrestrial component (meteorite debris) in the bulk crusts is small. However, meteorite debris may be concentrated locally in the crusts by formation of dissolution unconformities, or by proximity of the crust to meteorite fallout during formation of the layer. Localized extraterrestrial debris-rich horizons, however, do not alter the overall hydrogenetic signature of the PGEs in the crusts. The high Pt contents in three crusts studied here occur over many millimeters of the inner crusts, which represent millions of years of accretion of Fe-Mn oxyhydroxides and therefore cannot be explained as the result of meteorite impacts, as those are essentially instantaneous events and would form only a very thin lamina in the crusts. In addition, the PGE ratios are non-chondritic, with Fe-Mn crust compositions showing more than an order of magnitude more Pt relative to Ir and Rh relative to Ir. More likely, Pt is a redox sensitive element and its changing concentration reflects changing redox conditions and diagenesis (see Hein et al., 1997).

Rare Earth Elements (REEs)

The concentrations of REEs are reported for 19 bulk crust samples and 33 individual crust layers (Table 11). For bulk crusts, ΣREEs range from 0.13% to 0.32%, with a mean

of 0.21%. Nearly the same range is found for individual layers (0.14-0.35%) (Table 11). Out of 13 samples in which layers were analyzed, 11 of those show increases of ΣREEs with depth in the crusts; the other two samples show the opposite trend although the differences in percentages of ΣREEs between layers is quite small in those two samples. For crusts D18-1, D23-1, D37-4, and D41-1, the outer layer of each crust has the highest concentration of each REE, except Ce, which is highest in the middle layer. This is the same trend reported by Hein, Ahn, et al. (1992) for crusts from Micronesia. D15-4 and D27-1 show the same trends, but also have inner layers with the highest Yb contents. For crusts D25-3, D27-5, D32-9, D36-3, and D42-1, the innermost layers have the highest concentrations of all REEs. D-32-8 has the highest concentrations of all the REEs except Ce in the middle layer.

Chondrite (Anders and Grevesse, 1989)-normalized patterns show a positive Ce anomaly (2Ce/La+Pr from chondrite-normalized data), light REE enrichment, and a slight decrease in heavy REEs with increasing atomic number; whereas, post-Archean Australian shale (PAAS; McLennan, 1989)-normalized patterns show nearly flat heavy REEs, light REE depletion, and positive Ce anomaly (Fig. 4). Normalized REE patterns for bulk crusts and layers are shown in Figures 4-17. Patterns for individual samples (Figs. 5-17), in additional to the above characteristics, show a small positive Gd anomaly, typical of hydrogenetic Fe-Mn crusts and of seawater (Hein et al., 1988). In crusts where two layers were analyzed, the largest Ce anomaly occurs in the inner layer as does the highest enrichment of Ce relative to chondrites. When more than two layers were analyzed, the largest Ce anomaly was either in an interior layer or the innermost layer, whereas the greatest enrichment relative to chondrites occurred in the innermost layer.

Interelement Relationships

Correlation coefficient matrices were constructed from the chemical compositions of 46 bulk crusts (Table 12), nine thick bulk crusts (≥70 mm; Table 13), five thin bulk crusts (≤11 mm; Table 14), five layers from D27-5 (Table 15), and five layers from D32-9 (Table 16). In addition to 28 elements, all matrices include H_2O^+, H_2O^-, CO_2, LOI, and the tables for bulk crusts include longitude, latitude, water depth, and crust thickness.

For the 46 bulk crusts, statistically significant positive correlations at the 99% confidence level are found among the following selected elements, listed in order of decreasing significance for each element (Table 12): **Mn:** Mo, H_2O^+, LOI, Ni, Zn, H_2O^-, Cu, Co, Cd, V, Ti; **Fe:** Na, As, Si, V; **Si:** Al, Na, K, Mg, Cr, As; **P:** CO_2, Ca, Y, Sr, Mo; **Ba:** Ce, Sr, V, Mo, Pb, Y, Zn, Ti, Ca; **Pt:** Rh, Ir.

All elements are associated with one or more mineral phase(s) in the crusts. We interpret these correlations and others in Table 12 to indicate the following phases and their associated elements: **δ-MnO_2:** Mn, Ni, Co, Mo, Cd, Cu, V, Ti; **Fe oxyhydroxide:** Fe, V, As; **aluminosilicate:** Si, Al, K, Na, Mg, Cr, As; **CFA:** Ca, P, Y, CO_2, Sr; **residual biogenic:** Ba, Zn, V, Cu, Ce, Sr, Y, Ca. In general, these interelement associations are similar to those determined for crusts from other areas of the central Pacific, although regional differences do occur (Hein et al., 1990, 1992b; Hein, Kang, et al., 1990).

Weak correlations exist for dredge haul locations and crust compositions. Y increases with increasing **latitude** (to the north) and Zn, Mn, Fe, Co, and V increase with increasing **longitude** (to the east), whereas Co and Zn decrease with increasing latitude. Only Ti increases with increasing **water depth**. Most PGEs (Pt, Ir, Rh), the CFA phase, and Ni increase with increasing **crust thickness**, whereas the iron and aluminosilicate phases decrease with increasing crust thickness.

For the nine bulk crusts thicker than 70 mm (Table 13), the following positive correlations between elements are found: **Mn:** Zn, Na, Pb, As, Co, H_2O^+; **Fe:** Ba, Mg,

Ti, Cu, H_2O^-, Si, Na, K, Al, LOI; **Si:** K, Fe, H_2O^-, Al, Ti, Ba, Cu, Mg, Ce, LOI; **P:** Ca, CO_2, Sr, Y; **Ba:** Fe, Si, Na, Mg, Ti, H_2O^-, Cu, Zn, Ru; **Pt:** Co, Ir. Notable differences from the entire bulk crust dataset are the correlations of Pb with Mn and Cu with Fe. Fe and Ti are more strongly associated with the aluminosilicate phase and there has been a transfer of elements between the residual biogenic and iron oxyhydroxide phases. These differences indicate that diagenesis has affected the thicker crusts. The CFA phase and crust thickness decrease with increasing latitude. Co increases and Ce decreases with increasing longitude. With increasing water depth, Al, K, Ti, Si, Cu, Ce, and Cr increase and Ni, Co, Sr, and Cd decrease.

The five thin bulk crusts (<11 mm) have statistically significant positive correlations between the following elements (Table 14): **Mn:** H_2O^-, Ca, Ba, LOI, Co, and at just below the 95% confidence level, Ni and Mo; **Fe:** P, Sr, Pb, As; **Si:** none; **P:** Fe, Sr, V, As; **Ba:** Mo, Mn, LOI, Y. These thin crusts have no CFA mineralization and P is correlated with Fe, and Ca with the Mn phase. These correlations indicate that there are at least two mechanisms that incorporate P into crusts: Syndepositional adsorption and later-stage diagenesis. No elements are correlated with crust thickness, water depth, or latitude. With increasing **longitude**, Mo, Ba, LOI, Y, V, and CO_2 increase, whereas Si, Al, and Cu decrease.

For the five layers of crust D27-5 (west side of Vlinder Guyot), the following elements have statistically significant positive correlations (Table 15): **Mn:** H_2O^-, LOI, Ni, Cu, Rh, Ir; **Fe:** H_2O^+, As; **Si:** H_2O^+; **P:** Ca, Y, CO_2, Sr, Ba; **Ba:** Ca, P, Sr, Ce; **Pt:** Rh, Ir, Zn, Cu. There is a strong negative correlation between layer thickness and Si and H_2O^+. The hydrogenetic PGEs may be associated with the Mn phase.

The five crust layers from D32-9 (Oma Vlinder Guyot) have the following positive element correlations (Table 16): **Mn:** Ti; **Fe and Si** have none; **P:** Ca, Ba, Y, Pt, Rh, Ir; **Ba:** Ir, Rh, Pt, Ca, P, Ce, Al; **Pt:** Rh, Ba, Ir, Ce, Ca, P, Al, Y. The interesting aspect of these correlations is the possible association of the PGEs with the CFA phase; or the CFA phase and some other PGE-bearing phase may simply co-vary. However, Ir and Rh have perfect correlations with Ba.

The only association common to all of these groups is the composition of CFA, with Ca, P, Y, CO_2, and Sr being consistently positively correlated.

Grouping of Elements: Q-Mode Factor Analysis

Q-mode factor analysis was completed on chemical data for the 46 bulk crusts (Figs. 18, 19). Grouped elements are assigned to five factors, four of which are essentially the same as those interpreted from the correlation coefficient data. Factor analysis did not identify a group of elements that we interpret as a residual biogenic phase from correlation coefficients. Instead, factor 2 is a PGE-bearing phase that may or may not be a residual biogenic phase. Two elements that have factor scores somewhat less than the |0.2| cutoff are Sr and Mg, which are commonly part of a residual biogenic (loosely bound) phase and support the interpretation of factor 2 as a residual biogenic phase. Differences are minor in elements assigned to the other four phases through interpretation of correlation coefficients and Q-mode factor assignments. Q-mode factor analysis does not include V, Ti, and Cu in the δ-MnO_2 phase; V in the FeOOH phase; Cr and As in the aluminosilicate phase; and Sr in the CFA phase. Factor analysis additionally includes Ba in the FeOOH phase; Ti and Fe in the aluminosilicate phase; and Mo in the CFA phase.

The statistical data show that the partitioning of elements in crusts is complex and that many elements occur in several crust phases. Element distributions depend on the location of Fe-Mn crust formation--that is both geographic and water depth locations. Distributions also depend on crust thickness, which reflects changes in growth rates with time and

diagenesis within the thicker crusts. Compositions further depend on global oceanic and atmospheric changes, which manifest in temporal changes in seawater chemistry.

RESOURCE CONSIDERATIONS

The commonly cited cut off grade for potential economic development is 0.8% Co and the cut off thickness is 40 mm. On a water-free basis, these samples are high in Pt (0.50 ppm); high in Mn (22.1%); and moderate in Ni (0.40%), Co (0.52%), and Cu (0.14 %), with a mean Co+Ni+Cu content of 1.06%. The mean crust thickness is 40 mm, but the true mean crust thickness from each dredge is poorly known.

REFERENCES

Anders, E. and Grevesse, N., 1989, Abundances of the elements: Meteoritic and solar. Geochimica et Cosmochimica Acta, v. 53, p. 197-214.

Aruscavage, P.J., Kirschenbaum, H., and Brown, F., 1989, Analytical methods: The determination of 27 elements in ferromanganese materials: *in* Manheim, F.T. and Lane-Bostwick, C.M. (eds.), Chemical Composition of Ferromanganese Crusts in the World Ocean: A Review and Comprehensive Database. U.S. Geological Survey Open File Report 89-020, 200 p. plus 3 appendices.

Bertine, K.K., Koide, M., and Goldberg, E.D., 1993, Aspects of rhodium marine chemistry. Marine Chemistry, v. 42, p. 199-210.

Burnett, W.C., Cullen, D.J., and McMurtry, G.M., 1987, Open-ocean phosphorites--in a class by themselves? *in* Teleki, P.G., Dobson, M.R., Moore, J.R., and von Stackelberg, U. (eds.), Marine Minerals, D. Reidel, Dordrecht, p. 119-134.

Colodner, D.C., Boyle, E.A., and Edmond, J.M., 1991, Platinum in seawater: Abstracts and Program, 1992 Ocean Sciences Meeting, EOS, Transactions of the American Geophysical Union, v. 72, no. 51, p. 44.

Cook, H.E., Johnson, P.D., Matti, J.C., and Zemmels, I., 1975, Methods of sample preparation and X-ray diffraction data analysis (X-ray mineralogy laboratory, Deep Sea Drilling Project, University of California Riverside): *in* Hays, D.E., Frakes. L.A., et al., Initial Reports of the Deep Sea Drilling Project, U.S. Government Printing Office, Washington, D.C., v. 28, p. 999-1007.

Cullen, D.J. and Burnett, W.C., 1986, Phosphorite associations on seamounts in the tropical southwest Pacific Ocean. Marine Geology, v. 71, p. 215-236.

Engleman, E.E., Jackson, L.L., and Norton, D.R., 1985, Determination of carbonate carbon in geological materials by coulometric titration. Chemical Geology, v. 53, p. 125-128.

Futa, K., Peterman, Z.E., and Hein, J.R., 1988, Sr and Nd isotopic variations in ferromanganese crusts from the central Pacific: Implications for age and source provenance. Geochimica et Cosmochimica Acta, v. 52, p. 2229-2233.

Goldberg, E.D., 1987, Heavy metal analyses in the marine environment--approaches to quality control. Marine Chemistry, v. 22, p. 117-124.

Halbach, P., Manheim, F.T., and Otten, P., 1982, Co-rich ferromanganese deposits in the marginal seamount regions of the central Pacific basin--results of the Midpac '81: Erzmetall, v. 35, p. 447-453.

Hein, J.R., Manheim, F.T., Schwab, W.C., and Davis, A.S., 1985a, Ferromanganese crusts from Necker Ridge, Horizon Guyot, and S.P. Lee Guyot: Geological considerations. Marine Geology, v. 69, p. 25-54.

Hein, J.R., Manheim, F.T., Schwab, W.C., Davis, A.S., Daniel, C.L., Bouse, R.M., Morgenson, L.A., Sliney, R.E., Clague, D.A., Tate, G.B., and Cacchione, D.A., 1985b, Geological and geochemical data for seamounts and associated ferromanganese

crusts in and near the Hawaiian, Johnston Island, and Palmyra Island Exclusive Economic Zones. U.S. Geological Survey Open-File Report 85-292, 129 p.

Hein, J.R., Morgenson, L.A., Clague, D.A., and Koski, R.A., 1987a, Cobalt-rich ferromanganese crusts from the Exclusive Economic Zone of the United States and nodules from the oceanic Pacific: *in* Scholl, D.W., Grantz, A., and Vedder, J.G. (eds.), Geology and Resource Potential of the Continental Margin of Western North America and Adjacent Ocean Basins-Beaufort Sea to Baja California. Circum-Pacific Council for Energy and Mineral Resources, Earth Science Series, Houston, Texas, v. 6, p. 753-771.

Hein, J.R., Schwab, W.C., Foot, D.G., Masuda, Y., Usui, A., Davis, A.S., Fleishman, C.L., Barna, D.L., Pickthorn, L.-B., Larson, D.A., Ruzzi, P., Benninger, L.M., and Gein, L.M., 1987b, Farnella cruise F7-86-HW, cobalt-rich ferromanganese crust data report for Karin Ridge and Johnston Island, central Pacific. U.S. Geological Survey Open File Report 87-663, 34 p.

Hein, J.R., Schwab, W.C. and Davis, A.S., 1988, Cobalt and platinum-rich ferromanganese crusts and associated substrate rocks from the Marshall Islands. Marine Geology, v. 78, p. 255-283.

Hein, J.R., Kang, J.-K., Schulz, M.S., Park, B.-K., Kirschenbaum, H., Yoon, S.-H., Olson, R.L., Smith, V.K., Park., D.-W., Riddle, G.O., Quinterno, P.J., Lee, Y.-O., Davis, A.S., Kim, S.R., Pringle, M.S., Choi, D.-L., Pickthorn, L., Schlanger, S.O., Duennebier, F.K., Bergersen, D.D. and Lincoln, J.M., 1990, Geological, geochemical, geophysical, and oceanographic data and interpretations of seamounts and Co-rich ferromanganese crusts from the Marshall Islands, KORDI-USGS R.V. Farnella Cruise F10-89-CP. U.S. Geological Survey Open File Report 90-407, 246 p.

Hein, J.R., Kirschenbaum, H., Schwab, W.C., Usui, A., Taggart, J.E., Stewart, K.C., Davis, A.S., Terashima, S., Quinterno, P.J., Olson, R.L., Pickthorn, L.G., Schulz, M.S., Morgan, C.L., 1990, Mineralogy and geochemistry of Co-rich ferromanganese crusts and substrate rocks from Karin Ridge and Johnston Island, Farnella Cruise F7-86-HW. U.S. Geological Survey Open File Report 90-298, 80 pp.

Hein, J.R., Ahn, J.-H., Wong, J.C., Kang, J-K., Smith, V.K., Yoon, S-H., d'Angelo, W.M., Yoo, S-O., Gibbs, A.E., Kim, H-J., Quinterno, P.J., Jung, M.-Y., Davis, A.S., Park, B.-K., Gillison, J.R., Marlow, M.S., Schulz, M.S., Siems, D.F., Taggart, J.E., Rait, N., Gray, L., Malcolm, M.J., Kavulak, M.G., Yeh, H.-W., Mann, D.M., Noble, M., Riddle, G.O., Roushey, B.H., and Smith, H., 1992, Geology, geophysics, geochemistry, and deep-sea mineral deposits, Federated States of Micronesia: KORDI-USGS R.V. Farnella cruise F11-90-CP. U.S. Geological Survey Open File Report 92-218, 191 pp.

Hein, J.R., Bohrson, W.A., Schulz, M.S., Noble, M., and Clague, D.A., 1992a, Variations in the fine-scale composition of a central Pacific ferromanganese crust: Paleoceanographic implications. Paleoceanography, v. 7, p. 63-77.

Hein, J. R., Schulz, M. S., Gein, L. M., 1992b, Central Pacific cobalt-rich ferromanganese crusts: Historical perspective and regional variability: *in* Keating, B. H., and Bolton, B. R., (eds.), Geology and Offshore Mineral Resources of the Central Pacific Basin. Circum-Pacific Council for Energy and Mineral Resources, Earth Sciences Series, v. 14, New York, Springer-Verlag, p. 261-283.

Hein, J.R., Yeh, H.-W., Gunn, S.H., Sliter, W.V., Benninger, L.M., and Wang, C.-H., 1993, Two major Cenozoic episodes of phosphogenesis recorded in equatorial Pacific seamount deposits. Paleoceanography, v. 8, p. 293-311.

Hein, J.R., Gramm-Osipov, L., Gibbs, A.E., Kalyagin, A.N., d'Angelo, W.M., Nachaev, V.P., Briggs, P.H., Bychkov, A.S., Davis, A.S., Gusev, V.V., Chezar, H., Gorbarenko, S.A., Bullock, J.H., Kraynikov, G.A., Siems, D.F., Mikhailik, E.V., Smith, H., Eyberman, M.F., Schutt, M.J., Beloglazov, A.I., Mozherovsky, A.V., and Chichkin, R.V., 1994, Description and composition of Fe-Mn crusts, rocks, and sediments collected on Karin Ridge, R.V. Aleksandr Vinogradov cruise 91-AV-

19/2: *in* Hein, J.R., Bychkov, A.S., and Gibbs, A.E. (eds.), Data and results from R.V. Aleksandr Vinogradov cruises 91-AV-19/1, north Pacific hydrochemistry transect; 91-AV-19/2, north equatorial Pacific Karin Ridge Fe-Mn crust studies; and 91-AV-19/4, northwest Pacific and Bering Sea sediment geochemistry and paleoceanographic studies. U.S. Geological Survey Open-File Report 94-230, p. 39-91.

Hein, J.R., Koschinsky, A., Halbach, P., Manheim, F.T., Bau, M., Kang, J.-K., and Lubick, N., 1997, Iron and manganese oxide mineralization in the Pacific: *in* Nicholson, K., Hein, J.R., Bühn, B., and Dasgupta, S. (eds.) Manganese Mineralization: Geochemistry and Mineralogy of Terrestrial and Marine Deposits. Geological Society Special Publication No. 119, London, p. 123-138.

Hodge, V., Stallar, M., Koide, M., and Goldberg, E.D., 1986, Determination of platinum and iridium in marine waters, sediments, and organisms. Analytical Chemistry, v. 58, p. 616-620.

Ingram, B.L., Hein, J.R., and Farmer, G.L., 1990, Age determinations and growth rates of Pacific ferromanganese deposits using strontium isotopes. Geochimica et Cosmochimica Acta, v. 54, p. 1709-1721.

Jackson, L.L., Brown, F.W., and Neil, S.T., 1987, Major and minor elements requiring individual determination, classical whole rock analysis, and rapid rock analysis: *in* Baedecker, P.A. (ed.) Methods for Geochemical Analysis. U.S. Geological Survey Bulletin 1770, p. G1-G23.

Kastner, M., 1979, Zeolites: *in* Burns, R.G. (ed.), Marine Minerals, Mineralogical Society of America Short Course Notes, v. 6, p. 111-122.

Klovan, J.E. and Imbrie, J., 1971, An algorithm and FORTRAN-IV program for large-scale Q-mode factor analysis and calculation of factor scores. Mathematical Geology, v. 3, p. 61-77.\

Koppers, A., 1997, The geochronology of western seamounts and implications for plate motion. Ph.D. thesis, Fee University of Amsterdam, December, 1997.

Koschinsky, A. and Halbach, P., 1995, Sequential leaching of marine ferromanganese precipitates: Genetic implications. Geochimica et Cosmochimica Acta, v. 59, p. 5113-5132.

Lichte, F.E., Golightly, D.W., and Lamothe, P.J., 1987a, Inductively coupled plasma-atomic emission spectrometry: *in* Baedecker, P.A. (ed.), Methods for Geochemical Analysis. U.S. Geological Survey Bulletin 1770, p. B1-B10.

Lichte, F.E., Meier, A.L., and Crock, J.G., 1987b, Determination of the rare earth elements in geological materials by inductively coupled plasma-mass spectrometry. Analytical Chemistry, v. 59, p. 1150-1157.

Ling, H.F., Burton, K.W., O'Nions, R.K., Kamber, B.S., von Blanckenburg, F., Gibbs, A.J., and Hein, J.R., 1997, Evolution of Nd and Pb isotopes in central Pacific seawater from ferromanganese crusts. Earth and Planetary Science Letters, v. 146, p. 1-12.

Manheim, F.T. and Gulbrandsen, R.A., 1979, Marine phosphorites. *in* Burns, R.G. (ed.), Marine Minerals. Mineralogical Society of America Short Course Notes, v. 6, p. 151-173.

McLennan, S.M., 1989, Rare earth elements in sedimentary rocks: Influence of provenance and sedimentary processes: *in* Lipin, B.R. and McKay, G.A. (eds.) Geochemistry and Mineralogy of Rare Earth Elements. Mineralogical Society of America's Reviews in Mineralogy, v. 21, Washington D.C.

Parthé, E. and Crocket, J.H., 1978, Platinum group: *in* Wedepohl, K.H. (ed.) Handbook of Geochemistry, v. II/5, Springer-Verlag, Berlin, p. 78-A1-78-O7.

Peck, L.C., 1964, Systematic analysis of silicates. U.S. Geological Survey Bulletin 1170, 89 p.

Pichochi, C. and Hoffert, M., 1987, Characteristics of Co-rich ferromanganese nodules and crusts sampled in French Polynesia. Marine Geology, v. 77, p. 109-119.

Puteanus, D. and Halbach, P., 1988, Correlation of Co concentration and growth rate: A method for age determination of ferromanganese crusts. Chemical Geology, v. 69, p. 73-85.

Shapiro, L., 1975, Rapid analysis of silicate, carbonate, and phosphate rocks--revised edition. U.S. Geological Survey Bulletin 1401, 76 p.

Taggart, J.E., Lindsay, J.R., Scott, B.A., Vivit, D.V., Bartel, A.J., and Stewart, K.C., 1987, Analysis of geologic materials by wavelength-dispersive X-ray fluorescence spectrometry: *in* Baedecker, P.A. (ed.), Methods for Geochemical Analysis. U.S. Geological Survey Bulletin 1770, p. E1-E19.

Table 1. Location and description of dredge hauls from Tunes 6 cruise

Dredge Number	Latitude (N)	Longitude (E)	Water Depth On-Off Bottom (m)	Guyot	Max Crust Thickness (mm)	Avg. Crust Thickness (mm)	General Description
D 9	12° 06.00' 12° 03.60'	164° 56.25' 164° 56.25'	3000-1500	Wodejebato	110	42	Basalt, volcaniclastic rocks, sedimentary and hyaloclastite breccia, phosphorite, Fe-Mn crust
D 10	12° 07.00' 12° 06.50'	165° 00.70' 165° 01.20'	3000-1500	Wodejebato	65	26	Basalt, sedimentary and hyaloclastite breccia, phosphorite, Fe-Mn crust
D 12	14° 19.70' 14° 20.60'	160° 52.50' 160° 53.20'	1500	Neen Koiaak	120	105	Hyaloclastite, phosphorite, Fe-Mn crust, basalt, clastic rocks showing brecciation and cementation
D 13	14° 17.06' 14° 17.40'	160° 54.60' 160° 55.80'	3200-2000	Neen Koiaak	14	11	Basalt, hyaloclastite, very thin Fe-Mn crust
D 14	14° 47.04' 14° 47.08'	160° 18.23' 160° 18.68'	2800-3035	Aean-Kan	50	22	Basalt, phosphatized hyaloclastite breccia, mudstone, Fe-Mn crust
D 15	14° 52.10' 14° 50.00'	160° 20.97' 160° 18.68'	2200-1430	Aean-Kan	102	40	Basalt, phosphorite, breccia, mudstone, Fe-Mn crust
D 18	19° 30.70' 19° 30.50'	157° 44.70' 157° 45.00'	2700-2200	South Wake	68	24	Volcaniclastics, basalt, breccia, phosphorite, Fe-Mn crust
D 19	19° 43.00' 19° 45.75'	156° 45.50' 156° 45.75'	2800-2250	Batiza	26	18	Basalt, hyaloclastite, phosphorite, Fe-Mn crust
D 21	20° 10.50' 20° 09.98'	156° 40.90' 156° 40.64'	2700-2200	Batiza	20	9	Basalt, hyaloclastite, Fe-Mn crust
D 22	20° 14.32' 20° 13.00'	156° 23.80' 156° 25.00'	2200	Batiza	31	18	Basalt, volcaniclastics, breccia, clastic limastone
D 23	21° 03.40' 21° 03.00'	157° 09.20' 157° 09.60'	2400-2200	Maloney	110	51	Basalt, breccia, hyaloclastite, phosphorite
D 25	20° 26.94' 20° 27.06'	155° 55.25' 155° 55.17'	2300-2100	Batiza	85	42	Fe-Mn crust, basalt, phosphatized limestone, pelagic chalk, hyaloclastite, phosphorite
D 27	16° 59.24' 16° 59.55'	154° 10.06' 154° 01.62'	3100-2900	Vlinder	122	57	Fe-Mn crust, basalt, volcaniclastics, phosphorite, mud
D 28	17° 02.25' 17° 02.26'	154° 02.26' 154° 04.29'	3200-2200	Vlinder	13	7	Basalt, Fe-Mn crust, mudstone
D 30	16° 31.70' 16° 31.50'	154° 21.50' 154° 22.00'	2800-1600	Oma Vlinder	22	14	Fe-Mn crust, phosphorite breccia, Cretaceous reef limestone, pelagic chalk
D 31	16° 30.40' 16° 30.70'	154° 21.70' 154° 22.50'	2400-1800	Oma Vlinder	45	33	Cretaceous reef limestone, palegic chalk, Mn-crust, phosphorite breccia

Table 1 Continued

Dredge Number	Latitude (N)	Longitude (E)	Water Depth On-Off Bottom (m)	Guyot	Max Crust Thickness (mm)	Avg. Crust Thickness (mm)	General Description
D 32	16° 23.80' 16° 25.30'	154° 20.80' 154° 21.10'	3350-3440	Oma Vlinder	75	31	Basalt, hyaloclastite breccia, limestone, phosphorite, Fe-Mn crust
D 33	20° 53.40' 20° 53.30'	154° 52.00' 154° 53.30'	2700-2100	Missy	14	8	Mudstone, Fe-Mn crust, siltstone, phosphorite, basalt
D 36	21° 22.10' 21° 22.45'	153° 08.80' 153° 09.94'	1700-1200	Golden Dragon	105	77	Basalt, Fe-Mn crust, pelagic carbonate, breccia, hyaloclastite, phosphorite
D 37	21° 15.45' 21° 14.85'	153° 02.45' 153° 04.20'	2600-2250	Golden Dragon	60	40	Basalt, hyaloclastite, Mn-crust, minor carbonate, phosphorite
D 38	23° 48.10' 23° 47.80'	150° 30.00' 150° 32.40'	3100-2300	Bellevue	61	32	Hyaloclastite, basalt, Fe-Mn crust and nodules, phosphorite, breccia
D 41	23° 49.20' 23° 49.10'	148° 40.50' 148° 40.60'	3400-3200	Seth	73	60	Volcaniclastics, Fe-Mn crust, basalt
D 42	23° 53.50' 23° 54.20'	148° 41.50' 148° 42.90'	2400-3600	Seth	60	36	Basalt, volcaniclastics, hyaloclastite, phosphatized pelagic limestone, phosphorite, pillow breccia, Fe-Mn crust

Table 2. X-ray diffraction mineralogy of substrate rocks from Tunes 6 cruise

Sample	Major[1]	Moderate	Minor/Trace	Rock/Sediment
D9-22B	CFA[2]	Calcite	Chlorite	Phosphorite (clastic limestone)[3]
D9-24	CFA	Phillipsite, plagioclase	Smectite	CFA-cemented breccia[4]
D10-1B	CFA	Phillipsite	Smectite	CFA-cemented breccia in contact w/ phosphorite (foraminifera sand)
D10-3	CFA	Plagioclase	Smectite	CFA-cemented breccia
D10-5A	CFA	–	Smectite	Phosphorite (breccia)
D12-3B	CFA	Plagioclase	Smectite, quartz	Phosphorite (sandstone)
D13-13B	Plagioclase pyroxene	Magnetite	Smectite	Basalt
D14-17B	K-feldspar magnetite	Hematite, smectite	–	Mudstone
D14-18	Amorphous smectite, CFA	–	–	Mudstone
D15-3	K-feldspar, CFA	Smectite	–	Mudstone
D15-4E	CFA	Barite	–	Phosphorite (micritic limestone)
D18-3	Phillipsite	Magnetite	Smectite plagioclase	Breccia
D18-5B	CFA	–	–	Phosphorite (foraminifera sand)
D21-2	Goethite	Calcite, hematite	–	Yellow-red mineral replacement of basalt
D21-3B	Smectite	–	–	Yellow replacement mineral
D22-1B	Plagioclase smectite	CFA, hematite	–	Amygdaloid basalt
D23-1E	Phillipsite, CFA plagioclase	–	Smectite	CFA-cemented breccia
D23-5B	CFA, goethite	Plagioclase, pyroxene	Smectite	CFA-cemented breccia
D25-2B	CFA	Plagioclase	Smectite, quartz	Phosphorite (volcaniclastic calcareous sandstone)
D25-3E	CFA	Plagioclase	Smectite	Phosphorite (hyaloclastite)
D25-3F	CFA	–	–	Phosphorite
D28-1B	K-feldspar	Pyroxene, CFA phillipsite, plagioclase	Smectite	Mudstone
D31-1B	CFA	–	Smectite, quartz	Phosphorite (limestone)
D32-6A	CFA	Phillipsite, K-feldspar	Smectite clinoptilolite	Phosphorite (limestone)
D32-8A	CFA	Smectite	–	Phosphorite
D32-9A	CFA	–	K-feldspar	White phosphorite
D32-9B	CFA	Barite	–	Brown fracture fill
D33-1B	Clinoptilolite smectite	Magnetite, hematite	Plagioclase	Pale brown mudstone
D33-1C	Smectite	Hematite, phillipsite	Clinoptilolite	Dark brown mudstone
D33-1D	Smectite	–	–	Green mudstone
D33-2B	CFA	Phillipsite	–	Phosphorite (limestone)
D33-3	Smectite	–	–	Mudstone/tuff
D37-1	CFA	–	–	Phosphorite
D38-2-1	CFA	Phillipsite, smectite	–	Phosphorite (basalt)
D42-1D	Phillipsite	–	–	Botryoidal crystals in vug

[1]Major: ≥25%, Moderate: ≥5% to <25%, Minor: <5%
[2]CFA is carbonate fluorapatite
[3]Rock types in parentheses are replaced by phosphorite
[4]All breccias are sedimentary, and most are volcaniclastic

Table 3. Chemical composition in weight percent of substrate rocks from Tunes 6 cruise

	D9-22B	D10-1B	D12-3B	D13-13B	D14-17B	D15-4E	D18-5B	D22-1B	D25-2B
SiO_2	10.1	28.3	7.89	47.0	43.5	3.84	5.76	41.9	6.90
Al_2O_3	3.02	8.21	2.42	15.1	15.5	0.83	1.90	8.86	1.74
FeO	nd	<0.01	0.04	3.2	nd	<0.01	0.04	1.0	nd
Fe_2O_3	3.16	6.97	1.70	9.34	11.4	1.15	1.42	10.6	1.74
MgO	1.06	2.51	0.37	4.49	2.38	0.41	0.38	7.84	0.44
CaO	41.3	21.2	44.2	8.99	1.49	42.2	47.2	12.6	46.2
Na_2O	0.97	1.33	0.99	3.45	1.83	0.83	0.96	1.40	0.70
K_2O	0.70	1.51	0.67	1.44	3.58	0.17	0.29	1.31	0.61
TiO_2	0.35	1.12	0.35	2.68	2.32	0.16	0.32	2.60	0.35
P_2O_5	22.5	12.1	27.5	0.76	0.83	26.3	28.5	2.75	28.9
MnO	0.96	0.32	0.07	0.24	1.88	0.23	0.08	0.15	0.54
LOI 925C°	10.5	13.0	6.45	2.56	14.4	7.07	7.67	8.19	6.55
Total	94.62	96.57	92.65	99.25	99.11	83.19	94.52	99.20	94.67
H_2O^+	2.1	3.7	2.2	1.4	4.5	2.1	2.0	2.0	1.6
H_2O^-	1.6	6.3	0.48	1.4	9.0	0.50	0.78	5.4	1.1
CO_2	7.2	2.3	4.3	0.07	0.10	4.4	5.5	0.20	4.2
CaO/P_2O_5	1.84	1.75	1.61	11.8	1.80	1.60	1.66	4.58	1.60
Rock Type	Phosphorite (clastic ls)	CFA-cemented breccia	Phosphorite (sandstone)	Basalt	Mudstone	Phosphorite (micritic ls)	Phosphorite (ls breccia)	Amygdaloid basalt	Phosphorite (volcaniclastic calcareous ss)

	D25-3E	D28-1B	D31-1B	D32-6A	D33-1B	D33-1C	D33-2B	D33-3
SiO_2	20.1	44.0	3.60	12.70	44.3	36.7	14.0	47.4
Al_2O_3	5.85	13.4	1.02	3.24	12.7	13.6	3.64	12.6
FeO	<0.01	nd	<0.01	<0.01	<0.01	0.20	<0.01	<0.01
Fe_2O_3	5.11	9.16	0.84	3.05	11.3	13.9	3.51	9.15
MgO	1.36	2.22	0.39	0.78	2.67	2.53	0.89	4.15
CaO	30.0	6.09	49.2	37.3	0.53	0.44	37.0	0.43
Na_2O	1.42	2.13	0.77	1.34	3.10	1.78	1.37	2.22
K_2O	1.31	4.21	0.12	0.78	2.57	1.55	0.87	1.35
TiO_2	1.09	1.38	0.08	0.39	1.99	2.66	0.45	1.73
P_2O_5	18.7	3.48	30.3	23.4	0.24	0.24	23.2	0.16
MnO	0.17	0.72	0.41	0.16	0.25	0.1	0.24	0.12
LOI 925C°	11.5	12.1	7.53	12.9	19.3	26.2	10.4	20.6
Total	96.61	98.89	94.26	96.04	98.95	99.90	95.57	99.91
H_2O^+	3.0	4.3	1.9	0.20	5.6	2.5	0.40	4.3
H_2O^-	5.6	4.8	0.80	5.8	11.1	13.5	5.2	13.3
CO_2	2.9	0.42	5.3	1.8	0.03	0.02	3.3	0.02
CaO/P_2O_5	1.60	1.75	1.62	1.59	2.21	1.83	1.59	2.69
Rock Type	Phosphorite (hyaloclastite)	Mudstone	Phosphorite (limestone)	Phosphorite (limestone)	Mudstone	Mudstone	Phosphorite (limestone)	Mudstone/tuff

• Major oxides by X-ray fluorescence; LOI = Loss On Ignition at 925°C; nd= not determined; analysts: H. Smith, J. R. Gillison, C. J. Skeen, U.S. geological Survey
• Low totals are due to the presence of high F, Cl, and S, which is typical of seamount phosphorites
• Rock type in parentheses was replaced by carbonate fluorapatite; ls = limestone; ss = sandstone

Table 4. Calculated growth rates of Fe-Mn crusts from Tunes 6 cruise

Sample	Type & Interval (mm)[1]	Mn (wt.%)	P (wt.%)	Co (ppm)	Growth Rate (mm/Ma)[2]	Crust Age (Ma)
D9-11	Bulk (0-30)	26.0	0.33	8493	2.1	14.3
D9-22A	Bulk (0-41)	21.3	0.45	3856	8.8	4.7
D9-25A	Layer (0-23)	24.1	0.35	6818	2.9	7.9
D9-25B	Layer (23-43)	19.6	0.35	4183	7.2	10.7
D10-1A	Bulk (0-49)	27.1	0.32	5683	3.9	12.6
D12-3A	Bulk (0-45)	24.3	0.39	5676	3.9	11.5
D13-13A	Bulk (0-14)	23.1	0.39	6114	3.5	4.1
D14-11	Bulk (0-30)	22.8	0.32	6166	3.4	8.8
D14-17A	Bulk (0-15)	19.6	0.31	4830	5.3	2.9
D14-19A	Bulk (0-29)	24.0	0.35	5851	3.7	7.8
D15-1A	Bulk (0-29)	20.6	2.19	3732	--[3]	–
D15-1B	Bulk (0-20)	15.3	5.52	2233	–	–
D15-4A	Bulk (0-93)	20.9	2.87	4961	2.5	36.8
D15-4B	Layer (0-33)	25.0	0.36	7371	2.6	12.8
D15-4C	Layer (30-62)	27.6	0.36	7034	2.8	23.3
D15-4D	Layer (62-95)	16.1	6.09	2609	2.3	37.5
D18-1A	Bulk (0-68)	29.0	0.40	6777	2.9	23.3
D18-1B	Layer (0-18)	24.1	0.40	5764	3.8	4.7
D18-1C	Layer (18-56)	30.9	0.32	8298	2.2	22.2
D18-5A	Bulk (0-8)	21.5	0.44	5645	3.9	2.0
D19-1	Bulk (0-26)	19.9	0.37	5033	4.9	5.4
D19-2	Bulk (0-20)	24.2	0.35	6174	3.4	5.9
D21-3A	Bulk (0-15)	18.1	0.36	4774	5.4	2.8
D21-4	Bulk (0-15)	20.0	0.36	4927	5.1	3.0
D22-1A	Bulk (0-30)	20.1	0.40	4947	5.0	6.0
D22-2	Bulk (0-22)	18.7	0.47	5355	4.3	5.1
D23-1A	Bulk (0-70)	23.0	0.39	5142	4.7	15.0
D23-1B,C	Layer (0-25)	21.3	0.36	4267	6.9	3.7
D23-1D	Layer (25-70)	27.6	0.40	6069	3.5	16.6
D23-5A	Bulk (0-40)	25.1	1.85	3038	–	–
D25-1	Bulk (0-55)	23.0	0.36	4865	5.2	10.6
D25-2A	Bulk (0-19)	18.2	0.35	4681	5.6	3.4
D25-3A	Bulk (0-83)	24.5	0.41	5306	4.4	18.8
D25-3B	Layer (0-24)	22.6	0.37	4781	5.4	4.5
D25-3C	Layer (24-46)	28.8	0.37	6319	3.3	11.2
D25-3D	Layer (46-80)	23.4	0.59	4121	7.4	15.8
D27-1A	Bulk (0-62)	22.6	1.46	3595	6.1	10.2
D27-1B	Layer (0-14)	22.7	0.39	4412	6.4	2.2
D27-1C	Layer (14-51)	20.8	2.60	3121	6.0	8.4
D27-4	Bulk (0-18)	19.7	0.38	5125	4.7	3.8
D27-5A	Bulk (0-114)	21.9	1.37	3962	4.7	24.5
D27-5B	Layer (0-11)	18.2	0.43	4935	5.1	2.2
D27-5C	Layer (11-23)	19.7	0.37	5125	4.7	6.9
D27-5D	Layer (23-53)	25.4	0.41	5501	4.1	14.1
D27-5E	Layer (53-84)	21.4	1.47	3217	5.1	20.2
D27-5F	Layer (83-114)	16.4	4.28	2138	7.4	24.4
D28-1A	Bulk (0-11)	18.2	0.32	4799	5.3	2.1

Table 4 Continued

D30-1A	Bulk (0-21)	19.8	0.34	5013	4.9	4.3
D31-1A	Bulk (0-45)	21.4	0.31	6434	3.2	14.2
D32-2	Bulk (0-22)	21.7	0.31	6522	3.1	7.1
D32-5	Bulk (0-72)	26.0	0.41	5328	4.4	16.5
D32-6B	Bulk (0-3)	18.1	0.39	3876	8.7	0.4
D32-8B	Bulk (0-40)	22.6	0.39	5459	4.2	9.6
D32-8C	Layer (0-5)	16.5	0.41	3295	14.3	0.4
D32-8D	Layer (5-20)	21.2	0.38	5305	4.4	3.8
D32-8E	Layer (20-40)	25.5	0.35	6711	3.0	10.5
D32-9C	Bulk (0-60)	23.3	0.41	6036	3.5	17.0
D32-9D	Layer (0-2)	21.2	0.45	3968	8.2	0.3
D32-9E	Layer (2-17)	24.1	0.41	5221	4.5	3.6
D32-9F	Layer (17-30)	28.7	0.36	6019	3.5	7.2
D32-9G	Layer (30-50)	26.3	0.39	6510	3.1	13.7
D32-9H	Layer (50-60)	25.1	0.75	4045	7.8	15.0
D33-1A	Bulk (0-10)	18.4	0.37	4331	6.6	1.5
D33-2A	Bulk (0-10)	16.6	0.41	3713	9.8	1.0
D36-1	Bulk (0-72)	27.5	1.10	5777	–	–
D36-3A	Bulk (0-78)	22.4	1.98	5013	3.8	20.6
D36-3B	Layer (0-18)	21.1	0.51	5277	4.5	4.1
D36-3C	Layer (18-49)	24.5	0.44	5722	3.9	12.1
D36-3D	Layer (49-81)	22.1	3.65	4297	3.4	21.5
D36-4	Bulk (0-76)	26.1	1.37	5761	–	–
D37-2	Bulk (0-50)	21.6	0.53	5405	4.3	11.7
D37-4A	Bulk (0-50)	22.6	0.49	4515	6.1	8.3
D37-4B	Layer (0-30)	21.1	0.40	3826	9.0	3.3
D37-4C	Layer (30-50)	22.9	1.01	4980	5.0	7.4
D38-1A	Bulk (0-55)	22.6	0.53	4927	5.1	10.9
D38-1B	Layer (0-28)	23.3	0.38	5062	4.8	5.8
D38-1C	Layer (28-57)	21.8	0.41	3951	8.3	8.3
D38-2-2A	Bulk (0-13)	22.3	0.43	4849	5.2	2.5
D41-1A	Bulk (0-72)	21.6	0.46	4723	5.5	13.1
D41-1B	Layer (0-32)	21.5	0.39	4570	5.9	5.4
D41-1C	Layer (32-73)	23.0	0.53	4775	5.4	13.0
D42-1A	Bulk (0-20)	19.9	0.44	4122	7.4	2.7
D42-1B	Layer (0-7)	18.6	0.44	3851	8.8	0.8
D42-1C	Layer (7-20)	21.3	0.41	4933	5.1	3.4

[1]Intervals measured from the outer surface of crusts

[2]Growth rates determined via the equations of Puteanus and Halbach (1988); crust age was calculated from growth rate and crust thickness; the age of a layer is for the base of that layer

[3]Growth rates and crust ages could not be determined because samples were heavily phosphatized and no unphosphatized younger layers existed for comparison

Table 5. X-ray diffraction mineralogy of Fe-Mn crusts from Tunes 6 cruise

Sample	Type & Interval (mm)[1]	δ–MnO_2 (%)[2]	Others (%)
D9-11	Bulk (0-30)	98	1-goethite, <1-K-feldspar
D9-22A	Bulk (0-41)	91	8-phillipsite, <1-amphibole, <1-goethite
D9-25A	Layer (0-23)	100	trace-quartz
D9-25B	Layer (23-43)	98	1-goethite, <1-smectite, <1-quartz
D10-1A	Bulk (0-49)	93	6-goethite, <1-smectite(?)
D13-13A	Bulk (0-14)	97	2-quartz, 1-plagioclase
D14-11	Bulk (0-30)	98	1-plagioclase, 1-quartz
D14-17A	Bulk (0-15)	93	3-plagioclase, 2-quartz, 2-hematite
D14-19A	Bulk (0-29)	97	2-palygorskite, 1-plagioclase, <1-quartz
D15-1A	Bulk (0-29)	90	8-CFA, 1-plagioclase, 1-quartz
D15-1B	Layer (0-20)	81	16-CFA, 1-plagioclase, 1-quartz, 1-todorokite (?)
D15-4A	Bulk (0-93)	93	6-CFA, <1-quartz, <1-plagioclase
D15-4B	Layer (0-33)	96	3-quartz, 1-plagioclase
D15-4C	Layer (30-62)	99	<1-plagioclase, <1-quartz
D15-4D	Layer (62-95)	90	9-CFA, <1-geothite, <1-plagioclase, <1-quartz
D18-1A	Bulk (0-68)	98	1-plagioclase, 1-quartz
D18-1B	Layer (0-18)	96	2-CFA, 1-plagioclase, 1-quartz
D18-1C	Layer (18-56)	100	trace-quartz
D18-5A	Bulk (0-8)	97	2-quartz, 1-plagioclase
D19-1	Bulk (0-26)	94	5-quartz, 1-plagioclase
D19-2	Bulk (0-20)	98	1-quartz, <1-plagioclase, <1-smectite
D21-3A	Bulk (0-15)	93	3-quartz, 2-plagioclase, 2-smectite (?)
D21-4	Bulk (0-15)	97	2-quartz, 1-plagioclase
D22-1A	Bulk (0-30)	95	3-quartz, 2-plagioclase
D22-2	Bulk (0-22)	91	5-plagioclase, 2-birnessite, 1-quartz, <1-calcite, <1- smectite
D23-1A	Bulk (0-70)	97	2-plagioclase, 1-quartz
D23-1B,C	Layer (0-25)	97	1-phillipsite, 1-plagioclase, 1-quartz
D23-1D	Layer (25-70)	98	1-plagioclase, 1-quartz
D23-5A	Bulk (0-40)	94	5-CFA, <1-plagioclase, 1-quartz
D25-1	Bulk (0-55)	98	1-plagioclase, <1-quartz, <1-smectite
D25-2A	Bulk (0-19)	90	5-phillipsite, 3-plagioclase, 2-quartz
D25-3A	Bulk (0-83)	97	1-CFA, 1-plagioclase, 1-quartz
D25-3B	Layer (0-24)	98	1-quartz, <1-plagioclase
D25-3C	Layer (24-46)	98	1-plagioclase, 1-quartz
D25-3D	Layer (46-80)	96	2-phillipsite, 1-plagioclase, 1-quartz
D27-1A	Bulk (0-62)	94	6-CFA, <1-quartz
D27-1B	Layer (0-14)	99	1-quartz
D27-1C	Layer (14-51)	93	6-CFA, 1-quartz
D27-4	Bulk (0-18)	98	1-plagioclase, <1-quartz
D27-5A	Bulk (0-114)	95	4-CFA, <1-quartz
D27-5B	Layer (0-11)	97	2-quartz, 1-plagioclase
D27-5C	Layer (11-23)	99	<1-quartz
D27-5D	Layer (23-53)	99	1-quartz
D27-5E	Layer (53-83)	96	3-CFA, 1-quartz
D27-5F	Layer (83-114)	81	19-CFA
D28-1A	Bulk (0-11)	93	5-phillipsite, 1-plagioclase 1-quartz
D31-1A	Bulk (0-45)	96	2-quartz, 1-plagioclase, 1-smectite
D32-2	Bulk (0-22)	98	1-chlorite (?), 1-quartz
D32-5	Bulk (0-72)	97	2-quartz, 1-plagioclase
D32-6B	Bulk (0-3)	93	4-quartz, 2-plagioclase, 1-smectite
D32-8B	Bulk (0-40)	97	2-quartz, 1-plagioclase
D32-8C	Layer (0-5)	92	5-quartz, 3-plagioclase

Table 5 Continued

D32-8D	Layer (5-20)	96	2-quartz, 1-plagioclase, 1-stevensite (?)
D32-8E	Layer (20-40)	99	1-quartz
D32-9C	Bulk (0-60)	99	<1-plagioclase, <1-quartz
D32-9D	Layer (0-2)	97	2-quartz, 1-plagioclase
D32-9E	Layer (2-17)	99	1-quartz
D32-9F	Layer (17-30)	99	<1-clinoptilolite, <1-stevensite
D32-9G	Layer (30-50)	99	1-quartz
D32-9H	Layer (50-60)	98	1-CFA, 1-quartz
D33-1A	Bulk (0-10)	93	4-quartz, 2-plagioclase, <1-calcite (?), <1-smectite
D33-2A	Bulk (0-10)	92	5-quartz, 2-plagioclase
D36-1	Bulk (0-72)	97	2-CFA, <1-plagioclase, <1-quartz
D36-3A	Bulk (0-78)	95	4-CFA, 1-quartz
D36-3B	Layer (0-18)	95	3-quartz, 2-plagioclase
D36-3C	Layer (18-49)	99	1-quartz
D36-3D	Layer (49-81)	83	16-CFA, 1-quartz
D36-4	Bulk (0-76)	96	2-CFA, 1-quartz, 1-plagioclase
D37-2	Bulk (0-50)	94	5-phillipsite, <1-plagioclase, <1-quartz
D37-4A	Bulk (0-50)	97	2-quartz, 1-plagioclase
D37-4C	Layer (30-50)	93	4-phillipsite, 2-CFA, <1-plagioclase, <1-quartz
D38-1A	Bulk (0-55)	99	1-quartz
D38-1B	Layer (0-28)	97	2-quartz, <1-plagioclase, <1-smectite
D38-1C	Layer (28-57)	94	2-plagioclase, 2-quartz, 1-CFA, 1-smectite
D38-2-2A	Bulk (0-13)	95	2-plagioclase, 1-CFA, 1-quartz
D41-1A	Bulk (0-72)	97	2-plagioclase, 1-quartz
D41-1B	Layer (0-32)	99	1-quartz, <1-plagioclase
D41-1C	Layer (32-73)	97	1-hematite, 1-plagioclase, 1-quartz
D42-1A	Bulk (0-20)	98	2-quartz
D42-1B	Layer (0-7)	92	4-plagioclase, 2-pyroxene (?), 2-quartz
D42-1C	Layer (7-20)	97	1-phillipsite, 1-quartz

[1]Intervals measured from the outer surface of crusts

[2]Percentages were determined by using the following weighting factors relative to quartz set at 1: δ-MnO_2 70; todorokite 10; birnessite 12 (Hein et al., 1988); carbonate fluorapatite (CFA) 3.1; plagioclase 2.8; calcite 1.65; smectite 3.0; goethite 7.0; phillipsite 17.0; illite 6.0; pyroxene 5.0; halite 2.0 (Cook et al., 1975); the limit of detection for each mineral falls between 0.2 and 1.0%, except the manganese minerals which are greater, perhaps as much as 10% for δ-MnO_2

Table 6. Chemical composition of Fe-Mn crusts from Tunes 6 cruise

	D9-11	D9-22A	D9-25A[1]	D9-25B	D10-1A	D12-3A	D13-13A	D14-11	D14-17A	D14-19A	D15-1A	D15-1B
Fe Wt%	12	13	13	15	14	14	14	13	13.0	14.0	10.0	7.7
Mn	19.0	16.0	18.0	15.0	20.0	18.0	17.0	17.0	15.0	18.0	16.0	13.0
Fe/Mn	0.63	0.81	0.72	1.00	0.70	0.78	0.82	0.76	0.87	0.78	0.63	0.59
Si	2.4	3.5	3.0	3.9	2.3	3.5	4.1	4.0	5.1	3.8	2.8	1.9
Na	1.2	1.4	1.3	1.3	1.3	1.3	1.3	1.2	1.5	1.0	1.2	1.0
Al	0.41	0.96	0.53	1.1	0.41	0.76	0.65	0.81	1.3	0.73	0.61	0.64
K	0.40	0.49	0.41	0.46	0.39	0.46	0.41	0.45	0.57	0.42	0.39	0.36
Mg	0.68	0.67	0.66	0.67	0.82	0.80	0.80	0.66	0.68	0.80	0.67	0.73
Ca	1.9	2.0	1.9	1.8	2.0	1.9	1.8	1.8	1.8	1.9	5.8	14
Ti	0.88	0.81	0.88	0.95	0.88	0.95	0.72	0.97	0.94	0.98	0.71	0.62
P	0.24	0.34	0.26	0.27	0.24	0.29	0.29	0.24	0.24	0.26	1.7	4.7
H_2O^+	5.8	7.1	8.7	6.6	7.6	7.2	7.0	7.8	7.4	7.3	8.1	5.3
H_2O^-	27.0	24.8	25.2	23.5	26.1	26.0	26.4	25.4	23.4	24.8	22.3	14.9
CO_2	0.34	0.35	0.41	0.31	0.35	0.35	0.38	0.33	0.30	0.39	0.99	2.20
LOI	39.9	37.7	38.5	36.0	39.4	38.5	38.6	38.1	36.2	37.4	34.8	26.1
Ni ppm	4000	3200	3100	2600	3700	3100	2800	2900	2600	2900	3300	4200
Cu	690	2100	980	2100	1600	1900	480	1200	1700	910	1000	1100
Zn	490	570	460	570	680	580	470	480	480	520	620	740
Co	6200	2900	5100	3200	4200	4200	4500	4600	3700	4400	2900	1900
Ba	1100	1700	1100	1700	1600	1600	1100	1200	1300	1400	2200	2100
Mo	370	270	350	260	410	310	340	290	230	340	400	290
Sr	1200	1200	1200	1200	1300	1200	1200	1100	1100	1200	1300	1400
Ce	650	740	700	670	770	880	730	870	920	920	1200	850
Y	140	130	160	160	110	130	150	140	130	150	210	390
V	490	490	510	540	610	540	510	500	460	500	560	440
Pb	1100	920	1100	800	1000	1000	1400	1100	1000	1200	1600	1200
Cr	10.0	9.6	9.1	11	4.8	7.3	8.0	7.5	9.3	5.9	2.8	81
Cd	3.3	2.5	2.3	1.9	2.0	2.0	2.0	2.5	2.3	2.4	2.4	3.7
As	170	170	190	170	190	170	220	170	150	190	140	77
Pt ppb	-	-	-	-	250	350	240	-	-	220	-	-
Pd	-	-	-	-	<4	<4	<4	-	-	<4	-	-
Rh	-	-	-	-	12	15	13	-	-	12	-	-
Ru	-	-	-	-	16	19	18	-	-	16	-	-
Ir	-	-	-	-	4.6	5.5	5.3	-	-	4.3	-	-
Interval[2]	B 0-30	B 0-41	L 0-23	L 23-43	B 0-49	B 0-45	B 0-14	B 0-30	B 0-15	B 0-29	B 0-29	B 0-20
Type	Crust	Crust	Crust	Crust	Crust	Crust	Crust	Crust	Crust	Crust	Crust	Crust

Table 6 Continued

	D15-4A	D15-4B	D15-4C	D15-4D	D18-1A	D18-1B	D18-1C	D18-5A	D19-1	D19-2	D21-3A	D21-4
Fe Wt%	11.0	13.0	12.0	7.4	11.0	14.0	9.6	14.0	13.0	12.0	14.0	13.0
Mn	16.0	18.0	20.0	13.0	21.0	18.0	22.0	16.0	15.0	18.0	14.0	15.0
Fe/Mn	0.69	0.72	0.60	0.60	0.52	0.78	0.44	0.88	0.87	0.67	1.00	0.87
Si	2.6	3.6	2.6	1.5	2.4	3.4	1.5	3.7	5.1	3.8	6.1	4.4
Na	1.1	1.4	0.8	1.1	1.1	1.3	1.0	1.5	1.3	1.3	1.6	1.3
Al	0.58	0.61	0.62	0.48	0.47	0.51	0.33	0.58	0.91	0.83	1.3	0.94
K	0.36	0.44	0.42	0.34	0.45	0.40	0.44	0.42	0.47	0.51	0.57	0.48
Mg	0.77	0.83	0.88	0.65	0.90	0.83	0.93	0.70	0.64	0.72	1.0	0.73
Ca	7.2	1.8	2.0	14	2.1	1.9	2.0	1.9	1.7	1.9	1.8	1.8
Ti	0.74	0.83	1.0	0.49	0.82	0.77	0.94	0.67	0.80	1.0	0.98	0.94
P	2.2	0.26	0.26	4.9	0.29	0.30	0.23	0.33	0.28	0.26	0.28	0.27
H_2O^+	5.8	2.9	6.8	4.0	7.3	6.1	7.3	7.6	6.0	5.9	5.1	7.5
H_2O^-	23.4	28.1	27.5	19.5	27.7	25.4	28.9	25.6	24.5	25.5	22.5	24.9
CO_2	1.10	0.34	0.34	2.20	0.36	0.40	0.34	0.38	0.34	0.34	0.31	0.32
LOI	35.3	40.3	39.9	29.9	40.7	38.1	41.7	38.3	36.3	38.4	33.9	37.5
Ni ppm	3300	3300	4100	3100	4900	3000	5800	2700	2300	3200	2100	2200
Cu	1000	670	1400	1100	1300	590	1600	320	520	1400	980	940
Zn	460	450	560	420	550	440	590	420	420	480	420	410
Co	3800	5300	5100	2100	4900	4300	5900	4200	3800	4600	3700	3700
Ba	1200	1100	1500	1100	1300	1100	1400	9300	1000	1200	1100	1000
Mo	300	350	360	240	440	390	460	360	300	280	210	260
Sr	1300	1200	1300	1300	1200	1300	1200	1200	1100	1100	990	1100
Ce	690	680	830	640	890	710	990	630	760	970	1100	1000
Y	190	120	100	280	170	160	140	170	160	120	150	150
V	410	460	470	310	450	510	430	560	510	490	470	490
Pb	1000	1300	1000	680	1300	1400	1200	1400	1300	1400	1300	1300
Cr	9.6	10	9.0	6.4	7.3	6.2	7.3	5.3	4.4	11	120	27
Cd	2.2	2.5	2.5	2.8	3.1	1.9	3.4	2.2	2.1	2.9	2.3	2.0
As	140	210	180	93	190	230	170	250	210	170	170	190
Pt ppb	470	220	650	590	580	150	840	-	-	-	-	-
Pd	<4	<4	<4	<4	<4	<4	<4	-	-	-	-	-
Rh	18	12	29	19	21	9.6	28	-	-	-	-	-
Ru	16	19	21	12	19	14	23	-	-	-	-	-
Ir	6.3	5.3	8.3	7.0	6.9	4.4	8.8	-	-	-	-	-
Interval[2]	B 0-93	L 0-33	L 30-62	L 62-95	B 0-68	L 0-18	L 18-56	B 0-8	B 0-26	B 0-20	B 0-15	B 0-15
Type	Crust	Crust	Crust	Crust	Crust	Crust	Crust	Crust	Crust	Crust	Crust	Crust

Table 6 Continued

	D22-1A	D22-2	D23-1A	D23-1B,C	D23-1D	D23-5A	D25-1	D25-2A	D25-3A	D25-3B	D25-3C	D25-3D
Fe Wt%	14.0	13.0	13.0	14.0	11.0	13.0	13.0	11.0	13.0	15.0	10.0	11.0
Mn	15.0	14.0	17.0	16.0	20.0	19.0	17.0	14.0	18.0	17.0	21.0	17.0
Fe/Mn	0.93	0.93	0.76	0.88	0.55	0.68	0.76	0.79	0.72	0.88	0.48	0.65
Si	5.6	5.1	4.3	5.6	3.0	1.6	3.6	5.6	3.5	3.8	3.0	4.1
Na	1.4	1.3	1.3	1.3	1.0	1.1	1.4	2.0	1.3	1.6	1.0	1.1
Al	1.1	1.1	0.81	0.88	0.71	0.30	0.66	1.6	0.76	0.58	0.79	1.3
K	0.53	0.53	0.49	0.45	0.51	0.32	0.47	0.85	0.48	0.40	0.53	0.67
Mg	0.91	0.71	0.84	0.76	0.87	0.66	0.70	0.75	0.86	0.81	0.94	0.87
Ca	1.8	2.3	1.9	1.7	2.1	5.3	1.8	1.8	2.0	1.8	2.1	2.4
Ti	0.74	0.69	0.87	0.81	0.96	0.89	0.86	0.82	0.93	0.88	0.96	0.91
P	0.30	0.35	0.29	0.27	0.29	1.4	0.27	0.27	0.30	0.28	0.27	0.43
H_2O^+	6.0	5.5	6.6	6.3	6.7	6.9	6.8	6.9	6.8	7.6	8.0	7.8
H_2O^-	25.2	25.3	26.1	25.0	27.5	24.3	26.0	23.1	26.5	24.7	27.2	26.5
CO_2	0.35	0.98	0.36	0.36	0.35	0.84	0.33	0.31	0.34	0.36	0.32	0.36
LOI	36.8	37.0	38.2	36.2	39.9	36.5	39.0	35.6	39.0	37.8	40.1	38.9
Ni ppm	2500	2700	3300	2300	4400	2300	3000	2800	3300	2400	4800	3500
Cu	690	520	1100	640	1800	880	890	1200	1100	600	1800	1400
Zn	380	380	490	430	570	570	470	430	500	450	570	520
Co	3700	4000	3800	3200	4400	2300	3600	3600	3900	3600	4600	3000
Ba	930	860	1300	1100	1500	2600	1200	1100	1300	1100	1400	1800
Mo	280	260	330	300	360	490	330	240	340	340	380	310
Sr	1100	1000	1200	1100	1100	1600	1100	910	1100	1200	1100	1100
Ce	630	620	1000	840	1200	1700	990	840	1100	950	1100	1300
Y	140	130	150	140	140	300	160	140	160	160	150	220
V	440	460	460	470	430	600	500	430	460	500	420	420
Pb	1200	1200	1300	1400	1100	1900	1300	1200	1300	1400	930	1200
Cr	30	12	6.3	11	5.9	5.7	5.5	12	11	7.2	23	18.0
Cd	1.8	2.4	2.1	2.0	3.0	1.5	2.4	2.3	1.9	2.4	2.9	1.8
As	220	200	190	200	160	180	180	150	180	210	140	140
Pt ppb	210	-	440	150	700	520	-	-	590	120	650	1500
Pd	<4	-	<4	<4	<4	<4	-	-	<4	<4	<4	<4
Rh	12	-	19	10	27	20	-	-	24	8.5	26	55
Ru	17	-	17	15	20	9.9	-	-	16	15	20	20
Ir	5.2	-	6.4	4.1	8.6	6.2	-	-	7.1	3.9	8.0	13
Interval[2]	B 0-30	B 0-22	B 0-70	L 0-25	L 25-70	B 0-40	B 0-55	B 0-19	B 0-83	L 0-24	L 24-46	L 46-80
Type	Crust	Crust	Crust	Crust	Crust	Crust	Crust	Crust	Crust	Crust	Crust	Crust

Table 6 Continued

	D27-1A	D27-1B	D27-1C	D27-4	D27-5A	D27-5B	D27-5C	D27-5D	D27-5E	D27-5F	D28-1A	D30-1
Fe Wt%	13.0	16.0	11.0	12.0	12.0	15.0	14.0	10.0	13.0	11.0	12.0	14.0
Mn	17.0	17.0	16.0	15.0	16.0	14.0	15.0	18.0	16.0	13.0	14.0	15.0
Fe/Mn	0.76	0.94	0.69	0.80	0.75	1.07	0.93	0.56	0.81	0.85	0.86	0.93
Si	2.2	3.6	2.0	4.7	2.6	5.1	4.7	2.9	2.1	1.9	6.5	4.7
Na	1.3	1.3	1.2	1.4	0.9	0.9	1.2	1.0	1.0	0.8	1.2	1.3
Al	0.39	0.55	0.38	1.4	0.57	0.85	0.98	0.84	0.43	0.42	2.0	0.95
K	0.31	0.34	0.30	0.62	0.37	0.41	0.50	0.49	0.32	0.29	1.1	0.49
Mg	0.71	0.81	0.60	0.72	0.68	0.73	0.73	0.85	0.63	0.49	0.69	0.66
Ca	4.4	1.7	5.8	2.0	3.6	1.6	1.7	1.9	3.8	9.0	1.7	1.7
Ti	0.89	0.82	0.92	1.0	0.91	0.82	1.10	0.84	0.94	0.90	0.90	0.83
P	1.1	0.29	2.00	0.29	1.00	0.33	0.28	0.29	1.1	3.40	0.25	0.26
H_2O^+	6.9	7.3	6.1	6.4	5.2	7.9	7.9	5.2	5.8	5.1	7.0	8.1
H_2O^-	24.9	25.2	23.1	23.9	26.8	23.0	23.9	29.1	25.4	20.5	22.9	24.2
CO_2	0.71	0.38	0.95	0.34	0.60	0.39	0.29	0.56	0.59	1.50	0.30	0.35
LOI	37.6	38.4	35.5	36.8	38.8	35.3	35.4	40.8	37.4	31.3	33.7	37.0
Ni ppm	2300	2400	2100	2700	2800	2000	2300	4500	2400	1500	2500	2300
Cu	790	540	910	1300	1100	560	1000	1300	1100	690	1200	680
Zn	510	450	520	490	520	440	460	530	570	490	450	460
Co	2700	3300	2400	3900	2900	3800	3900	3900	2400	1700	3700	3800
Ba	2200	1100	2500	1200	2200	1200	1400	1500	2500	3000	1100	1100
Mo	410	300	430	220	370	250	210	280	450	360	200	270
Sr	1400	1200	1600	980	1300	1200	1200	1100	1500	1700	900	1100
Ce	1400	900	1600	1000	1500	850	1100	1100	1700	1500	910	740
Y	200	160	230	130	190	170	160	160	190	370	130	150
V	550	490	590	420	540	510	460	400	650	560	400	490
Pb	1500	1300	1800	1100	1500	1400	1300	1000	1800	1500	1100	1300
Cr	5.1	6.3	3.4	12	3.5	8.1	9.6	7.0	5.8	< 2	15	6.3
Cd	1.6	2.3	2.0	2.3	1.9	1.9	1.8	3.1	1.7	1.4	2.4	1.9
As	180	210	110	130	150	210	170	140	170	110	130	200
Pt ppb	400	210	350	-	640	120	340	680	750	310	-	-
Pd	<4	<4	<4	-	<4	<4	<4	<4	<4	<4	-	-
Rh	15	13	14	-	27	9.0	20	33	32	11	-	-
Ru	11	15	8.8	-	13	15	23	21	12	6.9	-	-
Ir	5.9	5.0	5.3	-	8.1	3.9	6.5	9.2	8.7	4.4	-	-
Interval[2]	B 0-62	L 0-14	L 14-51	B 0-18	B 0-114	L 0-11	L 11-23	L 23-53	L 53-84	L 83-114	B 0-11	B 0-21
Type	Crust	Crust	Crust	Crust	Crust	Crust	Crust	Crust	Crust	Crust	Crust	Crust

Table 6 Continued

	D31-1A	D32-2	D32-5	D32-6B	D32-8B	D32-8C	D32-8D	D32-8E	D32-9C	D32-9D	D32-9E	D32-9F
Fe Wt%	12.0	13.0	11.0	14.0	12.0	13.0	13.0	11.0	11.0	14.0	13.0	10.0
Mn	16.0	18.0	19.0	14.0	17.0	13.0	16.0	19.0	17.0	16.0	18.0	21.0
Fe/Mn	0.75	0.72	0.58	1.00	0.71	1.00	0.81	0.58	0.65	0.88	0.72	0.48
Si	4.6	2.3	3.0	7.0	4.3	8.4	3.9	2.8	3.4	4.6	2.7	1.5
Na	1.2	1.3	1.0	1.5	1.3	1.6	1.3	1.1	1.1	1.3	1.1	1.3
Al	1.0	0.37	0.67	1.3	0.79	1.4	0.61	0.55	0.75	0.82	0.40	0.25
K	0.51	0.36	0.48	0.43	0.44	0.52	0.39	0.41	0.45	0.41	0.33	0.35
Mg	0.71	0.68	0.76	0.85	0.76	0.72	0.73	0.81	0.81	0.85	0.76	0.79
Ca	2.0	1.8	2.2	1.6	1.7	1.6	1.7	1.9	1.9	1.8	1.9	2.0
Ti	0.94	0.92	0.86	0.75	0.87	0.65	0.90	1.0	0.97	0.67	0.85	0.98
P	0.23	0.25	0.30	0.30	0.29	0.32	0.29	0.26	0.30	0.34	0.31	0.26
H_2O^+	7.6	8.0	7.5	6.4	5.6	5.2	4.7	5.1	4.3	7.6	5.8	6.7
H_2O^-	25.4	26.4	26.8	22.6	24.9	21.1	24.6	25.5	27.1	24.4	25.3	26.9
CO_2	0.31	0.37	0.36	0.32	0.35	0.39	0.37	0.35	0.32	0.41	0.39	0.38
LOI	37.5	40.1	39.3	34.2	37.5	32.0	37.4	38.5	39.4	36.8	38.7	40.3
Ni ppm	3100	2500	4100	2100	3100	1800	2800	4200	3700	2100	3200	4400
Cu	1100	540	1200	1100	900	520	690	1300	1300	640	850	1200
Zn	480	410	540	500	450	390	430	530	500	460	490	510
Co	4800	4800	3900	3000	4100	2600	4000	5000	4400	3000	3900	4400
Ba	1200	1000	1400	1100	1200	1000	1200	1400	1400	910	1300	1300
Mo	270	370	380	220	310	230	330	350	300	280	450	480
Sr	1000	1100	1100	1100	1200	1100	1300	1200	1100	1200	1300	1300
Ce	760	920	1100	800	920	710	890	1200	1100	910	830	940
Y	140	150	180	120	150	150	170	140	170	150	180	140
V	450	530	490	480	480	470	500	470	450	530	600	540
Pb	1200	1300	1300	1500	1300	1400	1500	1300	1300	1500	1500	1400
Cr	6.8	3.4	3.4	5.5	12	8.8	5.4	4.2	5.6	3.6	4.4	< 2
Cd	2.4	2.1	2.8	1.8	2.8	1.7	2.1	2.9	2.8	2.2	2.1	2.9
As	170	200	170	200	180	190	190	170	160	230	210	170
Pt ppb	-	-	-	-	330	140	160	670	550	-	120	150
Pd	-	-	-	-	<4	<4	<4	<4	<4	-	<4	<4
Rh	-	-	-	-	18	8.8	12	29	29	-	8.6	8.8
Ru	-	-	-	-	19	14	16	22	23	-	16	15
Ir	-	-	-	-	5.6	3.2	4.6	7.7	7.9	-	3.7	4.1
Interval[2]	B 0-45	B 0-22	B 0-72	B 0-3	B 0-40	L 0-5	L 5-20	L 20-40	B 0-60	L 0-2	L 2-17	L 17-30
Type	Crust	Crust	Crust	Crust	Crust	Crust	Crust	Crust	Crust	Crust	Crust	Crust

Table 6 Continued

	D32-9G	D32-9H	D33-1A	D33-2A	D36-1	D36-3A	D36-3B	D36-3C	D36-3D	D36-4	D37-2	D37-4A
Fe Wt%	9.6	11.0	13.0	14.0	9.9	10.0	13.0	12.0	7.2	10.0	12.0	13.0
Mn	19.0	18.0	14.0	13.0	20.0	17.0	16.0	18.0	17.0	19.0	16.0	17.0
Fe/Mn	0.51	0.61	0.93	1.08	0.50	0.59	0.81	0.67	0.42	0.53	0.75	0.76
Si	2.6	2.7	6.5	7.0	2.1	2.6	4.7	3.6	1.2	2.7	4.7	3.8
Na	1.0	1.0	1.9	1.8	1.1	1.1	1.0	1.1	1.3	1.2	1.3	1.1
Al	0.63	0.76	1.3	1.30	0.40	0.46	0.83	0.65	0.31	0.51	1.1	0.70
K	0.45	0.46	0.55	0.44	0.42	0.37	0.42	0.42	0.36	0.44	0.57	0.43
Mg	0.82	0.76	0.86	0.82	0.84	0.78	0.76	0.79	0.77	0.83	0.82	0.78
Ca	2.0	2.6	1.7	1.6	3.5	5.0	1.8	1.7	8.2	3.9	2.1	2.0
Ti	0.94	0.90	0.70	0.70	0.79	0.68	0.60	0.74	0.65	0.69	0.98	0.92
P	0.28	0.54	0.28	0.32	0.80	1.5	0.39	0.32	2.8	1.0	0.39	0.37
H_2O^+	5.0	4.1	5.4	3.8	6.6	5.2	2.9	5.9	1.7	5.3	5.6	5.0
H_2O^-	27.8	28.3	23.8	21.9	27.3	24.2	24.2	26.6	23.2	27.1	26.0	24.7
CO_2	0.30	0.38	0.34	0.35	0.56	0.98	0.47	0.40	1.50	0.63	0.34	0.45
LOI	40.5	40.5	35.7	34.0	39.5	36.4	35.7	38.7	35.8	39.2	38.3	37.2
Ni ppm	4800	3400	2100	1800	4600	3800	2400	3300	4500	4200	2600	2900
Cu	1700	1500	740	770	1100	590	290	580	930	630	1100	1000
Zn	580	540	420	530	620	460	340	400	550	510	470	480
Co	4700	2900	3300	2900	4200	3800	4000	4200	3300	4200	4000	3400
Ba	1600	2100	1000	1100	1500	1100	860	1000	1300	1200	1200	1300
Mo	380	330	230	230	450	390	380	370	380	430	270	330
Sr	1200	1200	1000	1100	1300	1300	1200	1200	1300	1300	1100	1200
Ce	1200	1500	750	720	1100	940	680	800	1100	1000	1200	1100
Y	150	280	140	130	250	240	160	130	320	200	180	180
V	460	480	440	470	490	450	520	480	390	460	440	500
Pb	1100	1300	1300	1400	1400	1400	1500	1500	1200	1400	1100	1200
Cr	6.4	3.4	8.0	11.0	4.4	5.2	< 2	7.1	11	12	6.3	8.9
Cd	3.1	2.1	1.7	1.4	3.0	2.7	1.8	3.0	2.9	2.7	2.1	2.1
As	140	130	170	200	180	170	270	220	110	180	150	190
Pt ppb	700	1900	-	180	-	470	200	360	730	-	-	290
Pd	<4	<4	-	<4	-	<4	<4	<4	<4	-	-	<4
Rh	30	70	-	10	-	24	14	21	30	-	-	17
Ru	21	21	-	15	-	14.	15	17	13	-	-	16
Ir	8.4	16	-	4.3	-	7.1	5.1	6.9	8.7	-	-	5.3
Interval[2]	L 30-50	L 50-60	B 0-10	B 0-10	B 0-72	B 0-78	L 0-18	L 18-49	L 18-49	B 0-76	B 0-50	B 0-50
Type	Crust	Crust	Crust	Crust	Crust	Crust	Crust	Crust	Crust	Crust	Crust	Crust

Table 6 Continued

	D37-4B	D37-4C	D38-1A	D38-1B	D38-1C	D38-2-2A	D41-1A	D41-1B	D41-1C	D42-1A	D42-1B	D42-1C
Fe Wt%	14.0	9.4	13.0	14.0	10.0	11.0	12.0	15.0	9.2	15.0	15.0	14.0
Mn	16.0	17.0	17.0	17.0	18.0	17.0	16.0	16.0	17.0	15.0	14.0	16.0
Fe/Mn	0.88	0.55	0.76	0.82	0.56	0.65	0.75	0.94	0.54	1.00	1.07	0.88
Si	3.8	3.8	4.2	3.6	4.7	5.1	3.9	3.2	4.5	3.9	4.1	3.8
Na	1.1	1.1	1.1	1.0	1.0	1.6	1.1	1.0	1.3	1.0	1.3	1.0
Al	0.59	0.98	0.91	0.64	1.3	1.4	1.0	0.66	1.3	0.66	0.84	0.69
K	0.37	0.61	0.52	0.41	0.67	0.68	0.53	0.35	0.68	0.36	0.43	0.37
Mg	0.74	0.85	0.83	0.79	0.90	0.88	0.82	0.77	0.92	0.77	0.78	0.77
Ca	1.8	3.0	2.2	1.8	2.7	2.0	2.0	1.7	2.3	1.7	1.6	1.8
Ti	0.92	0.88	0.95	0.92	0.99	0.93	0.94	1.0	0.87	0.75	0.75	0.89
P	0.30	0.75	0.40	0.28	0.54	0.33	0.34	0.29	0.39	0.33	0.33	0.31
H_2O^+	5.6	3.8	6.3	6.9	5.0	6.7	3.7	6.2	3.3	4.6	5.0	5.7
H_2O^-	24.2	25.7	24.9	26.9	26.6	23.7	25.9	25.6	26.7	24.8	24.7	25.0
CO_2	0.42	0.48	0.41	0.36	0.39	0.31	0.34	0.38	0.31	0.47	0.41	0.45
LOI	36.6	37.7	37.4	39.4	38.0	36.3	37.9	38.0	37.9	37.1	37.0	37.1
Ni ppm	2300	4000	2900	2600	3500	3200	3000	2200	3900	2100	1700	2500
Cu	710	1500	990	580	1400	1600	1100	620	1500	390	370	590
Zn	480	510	470	450	490	520	440	430	450	420	390	430
Co	2900	3700	3700	3700	4100	3700	3500	3400	3500	3100	2900	3700
Ba	1300	1400	1200	1100	1200	1200	1200	1200	1200	1100	990	1200
Mo	330	330	330	350	310	250	320	320	320	330	260	330
Sr	1200	1100	1200	1200	1100	1000	1100	1200	980	1200	1100	1200
Ce	1100	1200	1200	1100	1300	1100	1200	1200	1300	800	850	870
Y	160	240	180	160	220	120	170	160	170	180	160	170
V	530	420	470	500	410	410	450	520	390	530	500	510
Pb	1400	870	1200	1400	870	1100	1100	1400	820	1500	1400	1400
Cr	8.1	11	28	3.2	40	6.0	15	< 2	4.0	< 2	11	7.4
Cd	2.6	2.8	2.0	2.0	2.1	2.3	2.0	1.6	2.8	3.0	1.6	1.8
As	210	120	170	200	130	150	160	210	110	230	220	200
Pt ppb	140	590	-	-	-	-	250	110	390	100	100	110
Pd	<4	<4	-	-	-	-	<4	<4	<4	<4	<4	<4
Rh	11	30	-	-	-	-	14	8.6	20	7.4	7.4	9.1
Ru	15	18	-	-	-	-	15	15	16	12	13	15
Ir	3.5	8.0	-	-	-	-	5.3	4.0	6.7	3.4	3.1	3.7
Interval[2]	L 0-30	L 30-50	B 0-55	L 0-28	L 28-57	B 0-13	B 0-72	L 0-32	L 32-73	B 0-20	L 0-7	L 7-20
Type	Crust	Crust	Crust	Crust	Crust	Nodule	Crust	Crust	Crust	Crust	Crust	Crust

•Major and minor elements determined by Inductively Coupled Plasma-Atomic Emission Spectrometry (ICP-AES), except K, Zn, Pb by Flame Atomic Absorption Spectroscopy, and As, Cr, Cd by Graphite-Furnace Atomic Absorption Spectroscopy; Pt group elements determined by ICP - Mass Spectroscopy; Samples were air dried before being ground; analysts: J.H. Bullock, W. M. d'Angelo, and H. Smith

[1]Sample numbers that are identical except for suffixes -A, -B, -C, -D, etc. represent different sample intervals from the same crust

[2]Intervals measured from the outer surface of crust; B=bulk, which means the entire crust thickness was sampled and analyzed; L=crust layer

Table 7. Hygroscopic water-free (0% H_2O^-) composition of Fe-Mn crusts from Table 6

	D9-11	D9-22A	D9-25A	D9-25B	D10-1A	D12-3A	D13-13A	D14-11	D14-17A	D14-19A	D15-1A	D15-1B
Fe Wt%	16.4	17.3	17.4	19.6	19.0	18.9	19.0	17.4	17.0	18.6	12.9	9.1
Mn	26.0	21.3	24.1	19.6	27.1	24.3	23.1	22.8	19.6	24.0	20.6	15.3
Si	3.3	4.7	4.0	5.1	3.1	4.7	5.6	5.4	6.7	5.1	3.6	2.2
Na	1.6	1.9	1.7	1.7	1.8	1.8	1.8	1.6	2.0	1.3	1.5	1.1
Al	0.56	1.28	0.71	1.44	0.55	1.03	0.88	1.09	1.70	0.97	0.79	0.75
K	0.55	0.65	0.55	0.60	0.53	0.62	0.56	0.60	0.74	0.56	0.50	0.42
Mg	0.93	0.89	0.88	0.88	1.11	1.08	1.09	0.88	0.89	1.06	0.86	0.86
Ca	2.6	2.7	2.5	2.4	2.7	2.6	2.5	2.4	2.4	2.5	7.5	16.5
Ti	1.21	1.08	1.18	1.24	1.19	1.28	0.98	1.30	1.23	1.30	0.91	0.73
P	0.33	0.45	0.35	0.35	0.32	0.39	0.39	0.32	0.31	0.35	2.19	5.52
H_2O^+	8.0	9.4	11.6	8.6	10.3	9.7	9.5	10.5	9.7	9.7	10.4	6.2
H_2O^-	0.0	0.0	0.0	0.0	0.0	0.0	0.0	0.0	0.0	0.0	0.0	0.0
CO_2	0.47	0.47	0.55	0.41	0.47	0.47	0.52	0.44	0.39	0.52	1.27	2.59
Ni ppm	5479	4255	4144	3399	5007	4189	3804	3887	3394	3856	4247	4935
Cu	945	2793	1310	2745	2165	2568	652	1609	2219	1210	1287	1293
Zn	671	758	615	745	920	784	639	643	627	691	798	870
Co	8493	3856	6818	4183	5683	5676	6114	6166	4830	5851	3732	2233
Ba	1507	2261	1471	2222	2165	2162	1495	1609	1697	1862	2831	2468
Mo	507	359	468	340	555	419	462	389	300	452	515	341
Sr	1644	1596	1604	1569	1759	1622	1630	1475	1436	1596	1673	1645
Ce	890	984	936	876	1042	1189	992	1166	1201	1223	1544	999
Y	192	173	214	209	149	176	204	188	170	199	270	458
V	671	652	682	706	825	730	693	670	601	665	721	517
Pb	1507	1223	1471	1046	1353	1351	1902	1475	1305	1596	2059	1410
Cr	13.7	12.8	12.2	14.4	6.5	9.9	10.9	10.1	12.1	7.9	3.6	95.2
Cd	4.5	3.3	3.1	2.5	2.7	2.7	2.7	3.4	3.0	3.2	3.1	4.4
As	233	226	254	222	257	230	299	228	196	253	180	90
Pt ppb	-	-	-	-	338	473	326	-	-	293	-	-
Pd	-	-	-	-	<5.41	<5.41	<5.43	-	-	<5.32	-	-
Rh	-	-	-	-	16.2	20.3	17.7	-	-	16.0	-	-
Ru	-	-	-	-	21.7	25.7	24.5	-	-	21.3	-	-
Ir	-	-	-	-	6.2	7.4	7.2	-	-	5.7	-	-
Interval[2]	B 0-30	B 0-41	L 0-23	L 23-43	B 0-49	B 0-45	B 0-14	B 0-30	B 0-15	B 0-29	B 0-29	B 0-20
Type	Crust	Crust	Crust	Crust	Crust	Crust	Crust	Crust	Crust	Crust	Crust	Crust

Table 7 Continued

	D15-4A	D15-4B	D15-4C	D15-4D	D18-1A	D18-1B	D18-1C	D18-5A	D19-1	D19-2	D21-3A	D21-4
Fe Wt%	14.4	18.1	16.6	9.2	15.2	18.8	13.5	18.8	17.2	16.1	18.1	17.3
Mn	20.9	25.0	27.6	16.1	29.0	24.1	30.9	21.5	19.9	24.2	18.1	20.0
Si	3.4	5.0	3.6	1.9	3.3	4.6	2.1	5.0	6.8	5.1	7.9	5.9
Na	1.4	1.9	1.1	1.4	1.5	1.7	1.4	2.0	1.7	1.7	2.1	1.7
Al	0.76	0.85	0.86	0.60	0.65	0.68	0.46	0.78	1.21	1.11	1.68	1.25
K	0.47	0.61	0.58	0.42	0.62	0.54	0.62	0.56	0.62	0.68	0.74	0.64
Mg	1.01	1.15	1.21	0.81	1.24	1.11	1.31	0.94	0.85	0.97	1.29	0.97
Ca	9.4	2.5	2.8	17.4	2.9	2.5	2.8	2.6	2.3	2.6	2.3	2.4
Ti	0.97	1.15	1.38	0.61	1.13	1.03	1.32	0.90	1.06	1.34	1.26	1.25
P	2.87	0.36	0.36	6.09	0.40	0.40	0.32	0.44	0.37	0.35	0.36	0.36
H_2O^+	7.6	4.0	9.4	5.0	10.1	8.2	10.3	10.2	7.9	7.9	6.6	10.0
H_2O^-	0.0	0.0	0.0	0.0	0.0	0.0	0.0	0.0	0.0	0.0	0.0	0.0
CO_2	1.44	0.47	0.47	2.73	0.50	0.54	0.48	0.51	0.45	0.46	0.40	0.43
Ni ppm	4308	4590	5655	3851	6777	4021	8158	3629	3046	4295	2710	2929
Cu	1305	932	1931	1366	1798	791	2250	430	689	1879	1265	1252
Zn	601	626	772	522	761	590	830	565	556	644	542	546
Co	4961	7371	7034	2609	6777	5764	8298	5645	5033	6174	4774	4927
Ba	1567	1530	2069	1366	1798	1475	1969	12500	1325	1611	1419	1332
Mo	392	487	497	298	609	523	647	484	397	376	271	346
Sr	1697	1669	1793	1615	1660	1743	1688	1613	1457	1477	1277	1465
Ce	901	946	1145	795	1231	952	1392	847	1007	1302	1419	1332
Y	248	167	138	348	235	214	197	228	212	161	194	200
V	535	640	648	385	622	684	605	753	675	658	606	652
Pb	1305	1808	1379	845	1798	1877	1688	1882	1722	1879	1677	1731
Cr	12.5	13.9	12.4	8.0	10.1	8.3	10.3	7.1	5.8	14.8	154.8	36.0
Cd	2.9	3.5	3.4	3.5	4.3	2.5	4.8	3.0	2.8	3.9	3.0	2.7
As	183	292	248	116	263	308	239	336	278	228	219	253
Pt ppb	614	306	897	733	802	201	1181	-	-	-	-	-
Pd	<5.22	<5.56	<5.52	<4.97	<5.53	<5.36	<5.63	-	-	-	-	-
Rh	23.5	16.7	40.0	23.6	29.0	12.9	39.4	-	-	-	-	-
Ru	20.9	26.4	29.0	14.9	26.3	18.8	32.3	-	-	-	-	-
Ir	8.2	7.4	11.4	8.7	9.5	5.9	12.4	-	-	-	-	-
Interval[2]	B 0-93	L 0-33	L 30-62	L 62-95	B 0-68	L 0-18	L 18-56	B 0-8	B 0-26	B 0-20	B 0-15	B 0-15
Type	Crust	Crust	Crust	Crust	Crust	Crust	Crust	Crust	Crust	Crust	Crust	Crust

Table 7 Continued

	D22-1A	D22-2	D23-1A	D23-1B,C	D23-1D	D23-5A	D25-1	D25-2A	D25-3A	D25-3B	D25-3C	D25-3D
Fe Wt%	18.7	17.4	17.6	18.7	15.2	17.2	17.6	14.3	17.7	19.9	13.7	15.1
Mn	20.1	18.7	23.0	21.3	27.6	25.1	23.0	18.2	24.5	22.6	28.8	23.4
Si	7.5	6.8	5.8	7.5	4.1	2.1	4.9	7.3	4.8	5.0	4.1	5.6
Na	1.9	1.7	1.8	1.7	1.4	1.5	1.9	2.6	1.8	2.1	1.4	1.5
Al	1.47	1.47	1.10	1.17	0.98	0.40	0.89	2.08	1.03	0.77	1.09	1.79
K	0.71	0.71	0.66	0.60	0.70	0.42	0.64	1.11	0.65	0.53	0.73	0.92
Mg	1.22	0.95	1.14	1.01	1.20	0.87	0.95	0.98	1.17	1.08	1.29	1.20
Ca	2.4	3.1	2.6	2.3	2.9	7.0	2.4	2.3	2.7	2.4	2.9	3.3
Ti	0.99	0.92	1.18	1.08	1.32	1.18	1.16	1.07	1.27	1.17	1.32	1.25
P	0.40	0.47	0.39	0.36	0.40	1.85	0.36	0.35	0.41	0.37	0.37	0.59
H_2O^+	8.0	7.4	8.9	8.4	9.2	9.1	9.2	9.0	9.3	10.1	11.0	10.7
H_2O^-	0.0	0.0	0.0	0.0	0.0	0.0	0.0	0.0	0.0	0.0	0.0	0.0
CO_2	0.47	1.31	0.49	0.48	0.48	1.11	0.45	0.40	0.46	0.48	0.44	0.49
Ni ppm	3342	3614	4465	3067	6069	3038	4054	3641	4490	3187	6593	4808
Cu	922	696	1488	853	2483	1162	1203	1560	1497	797	2473	1923
Zn	508	509	663	573	786	753	635	559	680	598	783	714
Co	4947	5355	5142	4267	6069	3038	4865	4681	5306	4781	6319	4121
Ba	1243	1151	1759	1467	2069	3435	1622	1430	1769	1461	1923	2473
Mo	374	348	447	400	497	647	446	312	463	452	522	426
Sr	1471	1339	1624	1467	1517	2114	1486	1183	1497	1594	1511	1511
Ce	842	830	1353	1120	1655	2246	1338	1092	1497	1262	1511	1786
Y	187	174	203	187	193	396	216	182	218	212	206	302
V	588	616	622	627	593	793	676	559	626	664	577	577
Pb	1604	1606	1759	1867	1517	2510	1757	1560	1769	1859	1277	1648
Cr	40.1	16.1	8.5	14.7	8.1	7.5	7.4	15.6	15.0	9.6	31.6	24.7
Cd	2.4	3.2	2.8	2.7	4.1	2.0	3.2	3.0	2.6	3.2	4.0	2.5
As	294	268	257	267	221	238	243	195	245	279	192	192
Pt ppb	281	-	595	200	966	687	-	-	803	159	893	2060
Pd	<5.35	-	<5.41	<5.33	<5.52	<5.28	-	-	<5.44	<5.31	<5.49	<5.49
Rh	16.0	-	25.7	13.3	37.2	26.4	-	-	32.7	11.3	35.7	75.5
Ru	22.7	-	23.0	20.0	27.6	13.1	-	-	21.8	19.9	27.5	27.5
Ir	7.0	-	8.7	5.5	11.9	8.2	-	-	9.7	5.2	11.0	17.9
Interval[2]	B 0-30	B 0-22	B 0-70	L 0-25	L 25-70	B 0-40	B 0-55	B 0-19	B 0-83	L 0-24	L 24-46	L 46-80
Type	Crust	Crust	Crust	Crust	Crust	Crust	Crust	Crust	Crust	Crust	Crust	Crust

Table 7 Continued

	D27-1A	D27-1B	D27-1C	D27-4	D27-5A	D27-5B	D27-5C	D27-5D	D27-5E	D27-5F	D28-1A	D30-1
Fe Wt%	17.3	21.4	14.3	15.8	16.4	19.5	18.4	14.1	17.4	13.8	15.6	18.5
Mn	22.6	22.7	20.8	19.7	21.9	18.2	19.7	25.4	21.4	16.4	18.2	19.8
Si	2.9	4.8	2.6	6.2	3.6	6.6	6.2	4.1	2.8	2.4	8.4	6.2
Na	1.7	1.7	1.6	1.8	1.2	1.2	1.6	1.4	1.3	1.0	1.6	1.7
Al	0.52	0.74	0.49	1.84	0.78	1.10	1.29	1.18	0.58	0.53	2.59	1.25
K	0.41	0.45	0.39	0.81	0.51	0.53	0.66	0.69	0.43	0.36	1.43	0.65
Mg	0.95	1.08	0.78	0.95	0.93	0.95	0.96	1.20	0.84	0.62	0.89	0.87
Ca	5.9	2.3	7.5	2.6	4.9	2.1	2.2	2.7	5.1	11.3	2.2	2.2
Ti	1.19	1.10	1.20	1.31	1.24	1.06	1.45	1.18	1.26	1.13	1.17	1.09
P	1.46	0.39	2.60	0.38	1.37	0.43	0.37	0.41	1.47	4.28	0.32	0.34
H_2O^+	9.2	9.8	7.9	8.4	7.1	10.3	10.4	7.3	7.8	6.4	9.1	10.7
H_2O^-	0.0	0.0	0.0	0.0	0.0	0.0	0.0	0.0	0.0	0.0	0.0	0.0
CO_2	0.95	0.51	1.24	0.45	0.82	0.51	0.38	0.79	0.79	1.89	0.39	0.46
Ni ppm	3063	3209	2731	3548	3825	2597	3022	6347	3217	1887	3243	3034
Cu	1052	722	1183	1708	1503	727	1314	1834	1475	868	1556	897
Zn	679	602	676	644	710	571	604	748	764	616	584	607
Co	3595	4412	3121	5125	3962	4935	5125	5501	3217	2138	4799	5013
Ba	2929	1471	3251	1577	3005	1558	1840	2116	3351	3774	1427	1451
Mo	546	401	559	289	505	325	276	395	603	453	259	356
Sr	1864	1604	2081	1288	1776	1558	1577	1551	2011	2138	1167	1451
Ce	1864	1203	2081	1314	2049	1104	1445	1551	2279	1887	1180	976
Y	266	214	299	171	260	221	210	226	255	465	169	198
V	732	655	767	552	738	662	604	564	871	704	519	646
Pb	1997	1738	2341	1445	2049	1818	1708	1410	2413	1887	1427	1715
Cr	6.8	8.4	4.4	15.8	4.8	10.5	12.6	9.9	7.8	2.5	19.5	8.3
Cd	2.1	3.1	2.6	3.0	2.6	2.5	2.4	4.4	2.3	1.8	3.1	2.5
As	240	281	143	171	205	273	223	197	228	138	169	264
Pt ppb	533	281	455	-	874	156	447	959	1005	390	-	-
Pd	<5.33	<5.35	<5.20	-	<5.46	<5.19	<5.26	<5.64	<5.36	<5.03	-	-
Rh	20.0	17.4	18.2	-	36.9	11.7	26.3	46.5	42.9	13.8	-	-
Ru	14.6	20.1	11.4	-	17.8	19.5	30.2	29.6	16.1	8.7	-	-
Ir	7.9	6.7	6.9	-	11.1	5.1	8.5	13.0	11.7	5.5	-	-
Interval[2]	B 0-62	L 0-14	L 14-51	B 0-18	B 0-114	L 0-11	L 11-23	L 23-53	L 53-84	L 83-114	B 0-11	B 0-21
Type	Crust	Crust	Crust	Crust	Crust	Crust	Crust	Crust	Crust	Crust	Crust	Crust

Table 7 Continued

	D31-1A	D32-2	D32-5	D32-6B	D32-8B	D32-8C	D32-8D	D32-8E	D32-9C	D32-9D	D32-9E	D32-9F
Fe Wt%	16.1	16.3	15.0	18.1	16.0	16.5	17.2	14.8	15.1	18.5	17.4	13.7
Mn	21.4	21.7	26.0	18.1	22.6	16.5	21.2	25.5	23.3	21.2	24.1	28.7
Si	6.2	6.3	4.1	9.0	5.7	10.6	5.2	3.8	4.7	6.1	3.6	2.1
Na	1.6	1.6	1.4	1.9	1.7	2.0	1.7	1.5	1.5	1.7	1.5	1.8
Al	1.34	1.36	0.92	1.68	1.05	1.77	0.81	0.74	1.03	1.08	0.54	0.34
K	0.68	0.69	0.66	0.56	0.59	0.66	0.52	0.55	0.62	0.54	0.44	0.48
Mg	0.95	0.96	1.04	1.10	1.01	0.91	0.97	1.09	1.11	1.12	1.02	1.08
Ca	2.7	2.7	3.0	2.1	2.3	2.0	2.3	2.6	2.6	2.4	2.5	2.7
Ti	1.26	1.28	1.17	1.03	1.16	0.82	1.19	1.34	1.33	0.89	1.14	1.34
P	0.31	0.31	0.41	0.39	0.39	0.41	0.38	0.35	0.41	0.45	0.41	0.36
H_2O^+	10.2	10.3	10.2	8.3	7.5	6.6	6.2	6.8	5.9	10.1	7.8	9.2
H_2O^-	0.0	0.0	0.0	0.0	0.0	0.0	0.0	0.0	0.0	0.0	0.0	0.0
CO_2	0.42	0.42	0.49	0.41	0.47	0.49	0.49	0.47	0.44	0.54	0.52	0.52
Ni ppm	4155	4212	5601	2713	4128	2281	3714	5638	5075	2778	4284	6019
Cu	1475	1495	1639	1421	1198	659	915	1745	1783	847	1138	1642
Zn	643	652	738	646	599	494	570	711	686	608	656	698
Co	6434	6522	5328	3876	5459	3295	5305	6711	6036	3968	5221	6019
Ba	1609	1630	1913	1421	1598	1267	1592	1879	1920	1204	1740	1778
Mo	362	367	519	284	413	292	438	470	412	370	602	657
Sr	1340	1359	1503	1421	1598	1394	1724	1611	1509	1587	1740	1778
Ce	1019	1033	1503	1034	1225	900	1180	1611	1509	1204	1111	1286
Y	188	190	246	155	200	190	225	188	233	198	241	192
V	603	611	669	620	639	596	663	631	617	701	803	739
Pb	1609	1630	1776	1938	1731	1774	1989	1745	1783	1984	2008	1915
Cr	9.1	9.2	4.6	7.1	16.0	11.2	7.2	5.6	7.7	4.8	5.9	2.7
Cd	3.2	3.3	3.8	2.3	3.7	2.2	2.8	3.9	3.8	2.9	2.8	4.0
As	228	231	232	258	240	241	252	228	219	304	281	233
Pt ppb	-	-	-	-	439	177	212	899	754	-	161	205
Pd	-	-	-	-	<5.33	<5.07	<5.31	<5.37	<5.49	-	<5.35	<5.47
Rh	-	-	-	-	24.0	11.2	15.9	38.9	39.8	-	11.5	12.0
Ru	-	-	-	-	25.3	17.7	21.2	29.5	31.6	-	21.4	20.5
Ir	-	-	-	-	7.5	4.1	6.1	10.3	10.8	-	5.0	5.6
Interval[2]	B 0-45	B 0-22	B 0-72	B 0-3	B 0-40	L 0-5	L 5-20	L 20-40	B 0-60	L 0-2	L 2-17	L 17-30
Type	Crust	Crust	Crust	Crust	Crust	Crust	Crust	Crust	Crust	Crust	Crust	Crust

Table 7 Continued

	D32-9G	D32-9H	D33-1A	D33-2A	D36-1	D36-3A	D36-3B	D36-3C	D36-3D	D36-4	D37-2	D37-4A
Fe Wt%	13.3	15.3	17.1	17.9	13.6	13.2	17.2	16.3	9.4	13.7	16.2	17.3
Mn	26.3	25.1	18.4	16.6	27.5	22.4	21.1	24.5	22.1	26.1	21.6	22.6
Si	3.6	3.8	8.5	9.0	2.9	3.4	6.2	4.9	1.6	3.7	6.4	5.0
Na	1.4	1.4	2.5	2.3	1.5	1.5	1.3	1.5	1.7	1.6	1.8	1.5
Al	0.87	1.06	1.71	1.66	0.55	0.61	1.09	0.89	0.40	0.70	1.49	0.93
K	0.62	0.64	0.72	0.56	0.58	0.49	0.55	0.57	0.47	0.60	0.77	0.57
Mg	1.14	1.06	1.13	1.05	1.16	1.03	1.00	1.08	1.00	1.14	1.11	1.04
Ca	2.8	3.6	2.2	2.0	4.8	6.6	2.4	2.3	10.7	5.3	2.8	2.7
Ti	1.30	1.26	0.92	0.90	1.09	0.90	0.79	1.01	0.85	0.95	1.32	1.22
P	0.39	0.75	0.37	0.41	1.10	1.98	0.51	0.44	3.65	1.37	0.53	0.49
H_2O^+	6.9	5.7	7.1	4.9	9.1	6.9	3.8	8.0	2.2	7.3	7.6	6.6
H_2O^-	0.0	0.0	0.0	0.0	0.0	0.0	0.0	0.0	0.0	0.0	0.0	0.0
CO_2	0.42	0.53	0.45	0.45	0.77	1.29	0.62	0.54	1.95	0.86	0.46	0.60
Ni ppm	6648	4742	2756	2305	6327	5013	3166	4496	5859	5761	3514	3851
Cu	2355	2092	971	986	1513	778	383	790	1211	864	1486	1328
Zn	803	753	551	679	853	607	449	545	716	700	635	637
Co	6510	4045	4331	3713	5777	5013	5277	5722	4297	5761	5405	4515
Ba	2216	2929	1312	1408	2063	1451	1135	1362	1693	1646	1622	1726
Mo	526	460	302	294	619	515	501	504	495	590	365	438
Sr	1662	1674	1312	1408	1788	1715	1583	1635	1693	1783	1486	1594
Ce	1662	2092	984	922	1513	1240	897	1090	1432	1372	1622	1461
Y	208	391	184	166	344	317	211	177	417	274	243	239
V	637	669	577	602	674	594	686	654	508	631	595	664
Pb	1524	1813	1706	1793	1926	1847	1979	2044	1563	1920	1486	1594
Cr	8.9	4.7	10.5	14.1	6.1	6.9	2.6	9.7	14.3	16.5	8.5	11.8
Cd	4.3	2.9	2.2	1.8	4.1	3.6	2.4	4.1	3.8	3.7	2.8	2.8
As	194	181	223	256	248	224	356	300	143	247	203	252
Pt ppb	970	2650	-	230	-	620	264	490	951	-	-	385
Pd	<5.54	<5.58	-	<5.12	-	<5.28	<5.28	<5.45	<5.21	-	-	<5.31
Rh	41.6	97.6	-	12.8	-	31.7	18.5	28.6	39.1	-	-	22.6
Ru	29.1	29.3	-	19.2	-	18.5	19.8	23.2	16.9	-	-	21.2
Ir	11.6	22.3	-	5.5	-	9.4	6.7	9.4	11.3	-	-	7.0
Interval[2]	L 30-50	L 50-60	B 0-10	B 0-10	B 0-72	B 0-78	L 0-18	L 18-49	L 18-49	B 0-76	B 0-50	B 0-50
Type	Crust	Crust	Crust	Crust	Crust	Crust	Crust	Crust	Crust	Crust	Crust	Crust

Table 7 Continued

	D37-4B	D37-4C	D38-1A	D38-1B	D38-1C	D38-2-2A	D41-1A	D41-1B	D41-1C	D42-1A	D42-1B	D42-1C
Fe Wt%	18.5	12.7	17.3	19.2	19.1	14.4	16.2	20.2	12.6	19.9	19.9	18.7
Mn	21.1	22.9	22.6	23.3	21.8	22.3	21.6	21.5	23.2	19.9	18.6	21.3
Si	5.0	5.1	5.6	4.9	5.2	6.7	5.3	4.3	6.1	5.2	5.4	5.1
Na	1.5	1.5	1.5	1.3	1.5	2.1	1.5	1.3	1.8	1.3	1.7	1.3
Al	0.78	1.32	1.21	0.88	0.80	1.83	1.35	0.89	1.77	0.88	1.12	0.92
K	0.49	0.82	0.69	0.56	0.50	0.89	0.72	0.47	0.93	0.48	0.57	0.49
Mg	0.98	1.14	1.11	1.08	1.01	1.15	1.11	1.03	1.26	1.02	1.04	1.03
Ca	2.4	4.0	2.9	2.5	2.5	2.6	2.7	2.3	3.1	2.3	2.1	2.4
Ti	1.21	1.18	1.26	1.26	1.25	1.22	1.27	1.34	1.19	1.00	1.00	1.19
P	0.40	1.01	0.53	0.38	0.41	0.43	0.46	0.39	0.53	0.44	0.44	0.41
H_2O^+	7.4	5.1	8.4	9.4	7.6	8.8	5.0	8.3	4.5	6.1	6.6	7.6
H_2O^-	0.0	0.0	0.0	0.0	0.0	0.0	0.0	0.0	0.0	0.0	0.0	0.0
CO_2	0.55	0.65	0.55	0.49	0.57	0.41	0.46	0.51	0.42	0.63	0.54	0.60
Ni ppm	3034	5384	3862	3557	3134	4194	4049	2957	5321	2793	2258	3333
Cu	937	2019	1318	793	967	2097	1484	833	2046	519	491	787
Zn	633	686	626	616	654	682	594	578	614	559	518	573
Co	3826	4980	4927	5062	3951	4849	4723	4570	4775	4122	3851	4933
Ba	1715	1884	1598	1505	1771	1573	1619	1613	1637	1463	1315	1600
Mo	435	444	439	479	450	328	432	430	437	439	345	440
Sr	1583	1480	1598	1642	1635	1311	1484	1613	1337	1596	1461	1600
Ce	1451	1615	1598	1505	1499	1442	1619	1613	1774	1064	1129	1160
Y	211	323	240	219	218	157	229	215	232	239	212	227
V	699	565	626	684	722	537	607	699	532	705	664	680
Pb	1847	1171	1598	1915	1907	1442	1484	1882	1119	1995	1859	1867
Cr	10.7	14.8	37.3	4.4	11.0	7.9	20.2	2.7	5.5	2.7	14.6	9.9
Cd	3.4	3.8	2.7	2.7	3.5	3.0	2.7	2.2	3.8	4.0	2.1	2.4
As	277	162	226	274	286	197	216	282	150	306	292	267
Pt ppb	185	794	-	-	-	-	337	148	532	133	133	147
Pd	<5.28	<5.38	-	-	-	-	<5.40	<5.38	<5.46	<5.32	<5.31	<5.33
Rh	14.5	40.4	-	-	-	-	18.9	11.6	27.3	9.8	9.8	12.1
Ru	19.8	24.2	-	-	-	-	20.2	20.2	21.8	16.0	17.3	20.0
Ir	4.6	10.8	-	-	-	-	7.2	5.4	9.1	4.5	4.1	4.9
Interval[2]	L 0-30	L 30-50	B 0-55	L 0-28	L 28-57	B 0-13	B 0-72	L 0-32	L 32-73	B 0-20	L 0-7	L 7-20
Type	Crust	Crust	Crust	Crust	Crust	Nodule	Crust	Crust	Crust	Crust	Crust	Crust

Table 8. Statistics for 46 bulk Fe-Mn crusts from Tunes 6 cruise; data from table 6

Element	N	Mean	Median	SD[1]	Min[2]	Max[3]
Fe Wt %	46	12.4	13.0	1.46	7.7	15.0
Mn	46	16.5	16.5	1.91	13.0	21.0
Fe/Mn[4]	46	0.77	0.76	0.13	0.50	1.08
Si	46	4.0	3.9	1.4	1.6	7.0
Na	46	1.3	1.3	0.2	0.9	2.0
Al	46	0.9	0.8	0.4	0.3	2.0
K	46	0.48	0.46	0.13	0.31	1.10
Mg	46	0.77	0.77	0.08	0.64	1.00
Ca	46	2.7	1.9	2.1	1.6	14.0
Ti	46	0.85	0.88	0.11	0.62	1.00
P	46	0.57	0.30	0.76	0.23	4.70
H_2O^+	46	6.4	6.6	1.1	3.7	8.1
H_2O^-	46	24.8	24.9	2.1	14.9	27.7
CO_2	46	0.48	0.35	0.33	0.30	2.20
LOI	46	37.2	37.5	2.4	26.1	40.7
Ni ppm	46	2993	2900	702	1800	4900
Cu	46	1016	1000	380	320	2100
Zn	46	493	480	73	380	740
Co	46	3802	3800	739	1900	6200
Ba	46	1498	1200	1235	860	9300
Mo	46	316	310	70	200	490
Sr	46	1158	1100	135	900	1600
Ce	46	950	920	230	620	1700
Y	46	166	150	50	110	390
V	46	483	480	47	400	610
Pb	46	1270	1300	183	920	1900
Cr	45	13	7	20	2	120
Cd	46	2.0	2.3	0.5	1.4	8.1
As	46	176	175	29	77	250
Pt ppb	19	373	350	159	100	640
Pd	19	<4	<4	0	<4	<4
Rh	19	17.2	17.0	5.9	7.4	29.0
Ru	19	15.9	16.0	3.1	9.9	23.0
Ir	19	5.8	5.6	1.3	3.4	8.1
Depth[5]	46	1450	7238	2261	1450	13025
Thickness[6]	46	40	59	26	3	114

[1]Standard deviation; [2]Minimum; [3]Maximum; [4]Ratio of the Fe and Mn means, not a mean of the summation of ratios; [5]Water depth in meters; [6]Crust thickness in millimeters

Table 9. Statistics for 46 bulk Fe-Mn crusts from Tunes 6 cruise; data from table 7 (hygroscopic water-free)

Element	N	Mean	Median	SD[1]	Min[2]	Max[3]
Fe Wt%	46	16.7	17.2	1.7	12.9	19.9
Mn	46	22.1	22.1	2.8	16.6	29.0
Si	46	5.4	5.3	1.7	2.1	9.0
Na	46	1.7	1.7	0.3	1.2	2.6
Al	46	1.15	1.07	0.46	0.40	2.59
K	46	0.65	0.62	0.17	0.41	1.43
Mg	46	1.02	1.02	0.11	0.85	1.29
Ca	46	3.2	2.6	1.6	2.0	9.4
Ti	46	1.14	1.18	0.14	0.90	1.34
P	46	0.63	0.40	0.58	0.31	2.87
H_2O^+	46	8.6	9.0	1.6	4.9	11.6
CO_2	46	0.59	0.47	0.28	0.39	1.44
Ni ppm	46	3992	3875	960	2305	6777
Cu	46	1369	1323	499	430	2793
Zn	46	652	643	86	508	920
Co	46	5177	5023	1002	3038	8493
Ba	46	1978	1610	1656	1151	12500
Mo	46	422	416	98	259	647
Sr	46	1538	1506	183	1167	2114
Ce	46	1260	1224	315	830	2246
Y	46	215	202	50	149	396
V	46	645	635	65	519	825
Pb	46	1689	1711	245	1223	2510
Cr	46	15.3	10.1	22.5	2.7	154.8
Cd	46	3.1	3.0	0.6	1.8	4.5
As	46	237	236	34	169	336
Pt ppb	19	501	473	218	133	874
Pd	19	<5.36	<5.35	0.10	<5.12	<5.53
Rh	19	23.2	22.6	8.1	9.8	39.8
Ru	19	21.3	21.3	4.4	13.1	31.6
Ir	19	7.8	7.5	1.8	4.5	11.1
Depth[4]	46	1450	7238	2261	1450	13025
Thickness[5]	46	40	59	26	3	114

[1]Standard deviation; [2]Minimum; [3]Maximum; [4]Ratio of the Fe and Mn means, not a mean of the summation of ratios; [5]Water depth in meters; [6]Crust thickness in millimeters

Table 10. Statistics for 38 Fe-Mn crust layers from the Tunes 6 cruise; data from table 7 (hygroscopic water-free)

Element	N	Mean	Median	SD[1]	Min[2]	Max[3]
Fe Wt. %	38	16.2	16.9	3.2	9.1	21.4
Mn	38	22.6	22.4	3.6	15.3	30.9
Fe/Mn[4]	38	0.7	0.8	0.2	0.4	1.1
Si	38	4.6	4.9	1.8	1.6	10.6
Na	38	1.5	1.5	0.2	1.0	2.1
Al	38	0.93	0.88	0.36	0.34	1.79
K	38	0.57	0.55	0.13	0.36	0.93
Mg	38	1.04	1.05	0.15	0.62	1.31
Ca	38	4.0	2.5	3.7	2.0	17.4
Ti	38	1.15	1.19	0.19	0.61	1.45
P	38	0.99	0.41	1.45	0.32	6.09
H_2O^+	38	7.7	7.8	2.1	2.2	11.0
CO_2	38	0.73	0.52	0.58	0.38	2.73
Ni ppm	38	4209	3783	1492	1887	8158
Cu	38	1332	1161	641	383	2745
Zn	38	654	630	100	449	870
Co	38	4837	4857	1380	2138	8298
Ba	38	1887	1728	603	1135	3774
Mo	38	453	451	92	276	657
Sr	38	1639	1612	163	1337	2138
Ce	38	1374	1339	366	795	2279
Y	38	243	214	78	138	465
V	38	647	659	86	385	871
Pb	38	1722	1816	332	845	2413
Cr	38	12.1	9.7	15.0	2.5	95.2
Cd	38	3.2	3.0	0.8	1.8	4.8
As	38	233	240	61	90	356
Pt ppb	33	612	447	566	133	2650
Pd	33	<5.36	<5.36	0.2	<4.97	<5.64
Rh	33	27.7	18.5	19.6	9.8	97.6
Ru	33	22.2	20.5	5.7	8.7	32.3
Ir	33	8.7	7.4	4.1	4.1	22.3

[1]Standard deviation; [2]Minimum; [3]Maximum; [4]Ratio of the Fe and Mn means, not a mean of the summation of ratios

Table 11. Concentrations of rare earth elements (ppm) in Fe-Mn crusts from the Tunes 6 cruise

	D10-1A	D12-3A	D13-3A	D14-19A	D15-4A	D15-4B	D15-4C	D15-4D	D18-1A	D18-1B	D18-1C	D22-1A	D23-1A
La	320	320	260	360	250	310	230	240	320	310	280	290	290
Ce	980	1100	790	1100	650	840	980	810	1000	710	1300	780	1100
Pr	59	62	44	71	40	54	42	32	60	58	55	55	57
Nd	230	240	180	280	160	220	170	130	240	240	210	220	230
Sm	46	48	36	58	32	43	33	24	47	47	44	45	48
Eu	10.0	11.0	8.6	13.0	7.3	9.8	7.3	5.9	11.0	11.0	10.0	10.0	11.0
Gd	44	50	40	55	36	45	33	31	50	50	43	47	48
Tb	7.4	7.9	6.6	9.1	5.7	7.3	5.4	4.8	8.0	8.4	7.4	7.7	8.0
Dy	42	46	39	54	35	44	33	33	49	49	42	47	47
Ho	8.4	9.3	8.6	11.0	7.9	8.9	6.6	8.1	10.0	10.0	8.5	9.3	9.1
Er	23	25	23	29	24	25	19	25	28	27	24	27	25
Tm	3.4	3.7	3.5	4.3	3.5	3.7	2.8	3.7	4.0	3.9	3.6	3.8	3.7
Yb	20	23	21	27	21	22	17	24	25	24	22	23	22
Σ REE	1793	1946	1460	2071	1272	1633	1579	1372	1852	1548	2050	1565	1899
Ce*	1.61	1.78	1.64	1.57	1.43	1.45	2.25	1.95	1.63	1.20	2.39	1.40	1.95
Interval	B 0-49	B 0-45	B 0-14	B 0-29	B 0-93	L 0-43	L 30-62	L 62-95	B 0-68	L 0-18	L 18-56	B 0-30	B 0-70

	D23-1B,C	D23-1D	D23-5A	D25-3A	D25-3C	D25-3D	D27-1A	D27-1B	D27-1C	D27-5A	D27-5B	D27-5C	D27-5D
La	300	280	540	320	310	420	430	360	430	410	270	280	260
Ce	960	1400	2000	1300	1400	1700	1500	1100	1900	2200	920	1100	1600
Pr	59	54	77	65	65	82	72	70	68	65	53	52	48
Nd	230	210	290	250	260	320	280	270	260	260	220	210	200
Sm	47	44	51	53	55	65	52	57	47	48	47	43	39
Eu	11.0	10.0	12.0	12.0	12.0	15.0	12.0	13.0	12.0	11.0	12.0	11.0	10.0
Gd	50	44	58	53	49	66	57	59	51	52	54	47	41
Tb	8.3	7.1	9.0	8.5	8.4	9.8	8.8	9.6	7.8	7.9	8.5	7.5	6.8
Dy	48	43	56	50	51	59	54	58	48	47	50	46	41
Ho	9.5	8.6	12.0	9.7	9.7	11.0	11.0	11.0	11.0	10.0	9.9	9.5	8.6
Er	26	25	34	26	27	31	31	30	31	29	27	27	23
Tm	3.8	3.6	5.0	3.8	3.9	4.3	4.4	4.3	4.3	4.0	3.8	3.8	3.5
Yb	23	22	30	22	23	25	26	26	27	24	23	24	22
Σ REE	1776	2151	3174	2173	2274	2808	2538	2068	2897	3168	1698	1861	2303
Ce*	1.65	2.59	2.11	2.07	2.27	2.09	1.89	1.58	2.44	2.96	1.75	2.06	3.24
Interval	L 0-25	L 25-70	B 0-40	B 0-83	L 24-46	L 46-80	B 0-62	L 0-14	L 14-51	B 0-114	L 0-11	L 11-23	L 23-53

Table 11 Continued

	D27-5E	D27-5F	D32-8B	D32-8C	D32-8D	D32-8E	D32-9C	D32-9D	D32-9E	D32-9F	D32-9G	D32-9H	D33-2A
La	370	500	260	240	330	270	330	280	370	320	240	400	240
Ce	2100	2400	1100	820	1100	1600	1500	1000	1100	1200	1500	1700	790
Pr	63	73	49	47	63	52	66	59	77	69	48	80	46
Nd	240	280	200	190	250	200	260	240	300	260	180	320	180
Sm	44	50	41	41	51	43	55	51	64	58	39	62	38
Eu	11.0	12.0	10.0	11.0	13.0	11.0	14.0	13.0	17.0	15.0	10.0	17.0	11.0
Gd	48	61	47	46	59	41	57	56	68	53	38	71	41
Tb	7.2	9.0	7.3	7.5	9.6	7.1	9.5	9.0	11.0	9.5	6.5	11.0	7.0
Dy	44	60	45	45	55	42	54	51	64	55	38	62	39
Ho	8.8	14.0	8.9	9.2	12.0	9.3	11.0	10.0	13.0	11.0	8.0	13.0	7.9
Er	25	39	24	24	29	26	29	26	35	30	23	35	22
Tm	3.6	5.5	3.4	3.3	4.3	3.7	4.2	3.7	5.1	4.2	3.4	4.8	3.3
Yb	22	35	22	21	27	24	26	23	30	27	20	29	20
Σ REE	2987	3539	1818	1505	2003	2329	2416	1822	2154	2113	2154	2805	1445
Ce*	3.06	2.71	2.21	1.76	1.73	3.07	2.33	1.79	1.50	1.87	3.20	2.17	1.71
Interval	L 53-84	L 83-114	B 0-40	L 0-5	L 5-20	L 20-40	B 0-60	L 0-2	L 2-17	L 17-30	L 30-50	L 50-60	B 0-10

	D36-3A	D36-3B	D36-3C	D36-3D	D37-4A	D37-4B	D37-4C	D41-1A	D41-1B	D41-1C	D42-1A	D42-1B	D42-1C
La	290	280	240	290	350	340	290	300	350	260	330	330	390
Ce	1200	780	960	1300	1400	1300	1500	1500	1400	1600	920	950	1100
Pr	49	51	44	47	74	73	58	68	78	57	68	66	78
Nd	200	200	170	190	290	280	220	260	290	220	270	260	310
Sm	41	42	37	39	63	59	47	57	64	49	59	56	64
Eu	11.0	12.0	10.0	11.0	18.0	17.0	14.0	16.0	18.0	13.0	17.0	16.0	19.0
Gd	47	50	41	48	68	63	53	61	69	48	64	59	72
Tb	7.8	8.3	6.7	7.5	11.0	11.0	8.9	10.0	11.0	8.3	11.0	9.9	12.0
Dy	45	48	38	45	61	56	50	53	60	45	58	53	64
Ho	10.0	9.9	8.6	11.0	12.0	11.0	11.0	11.0	12.0	9.1	12.0	11.0	14.0
Er	29	28	25	31	33	32	31	29	33	26	33	29	39
Tm	4.2	4.1	3.5	4.6	4.8	4.5	4.2	4.2	4.5	3.7	4.6	3.9	5.2
Yb	25	23	22	27	29	28	26	25	28	22	28	25	33
Σ REE	1959	1536	1606	2051	2414	2275	2313	2394	2418	2361	1875	1869	2200
Ce*	2.24	1.47	2.11	2.46	2.01	1.91	2.65	2.45	1.97	3.05	1.41	1.47	1.44
Interval	B 0-78	L 0-18	L 18-49	L 18-49	B 0-50	L 0-30	L 30-50	B 0-72	L 0-32	L 32-73	B 0-20	L 0-7	L 7-20

- Analysis by Inductively Coupled Plasma-Mass Spectrometry (ICP-MS); analysts: G. O. Riddle and M. J. Malcolm
- Intervals are measured from the outer surface of the crust; B=bulk, the entire crust thickness was sampled and analyzed; L=layer
- Ce* = 2 Ce/La+Pr from chondrite-normalized data

Table 12. Correlation coefficient matrix for 46 bulk crusts listed in Table 6; n=46, except for Pt, Rh, Ru, and Ir =19; the zero correlations for 46 points and 19 points at the 99% confidence level are |0.374| and |0.568|, respectively

	Depth	Lat.	Long.	Fe	Mn	Fe/Mn	Si	Na	Al	K	Mg	Ca	Ti	P	H2O+	H2O-	CO2	LOI	Ni
Lat.	-0.014																		
Long.	-0.410	-0.748																	
Fe	-0.048	-0.221	0.435																
Mn	-0.106	-0.261	0.447	-0.102															
Fe/Mn	0.025	0.132	-0.085	0.685	-0.747														
Si	0.087	0.235	-0.179	0.423	-0.714	0.747													
Na	-0.179	0.076	0.104	0.509	-0.436	0.630	0.707												
Al	0.143	0.310	-0.302	0.318	-0.725	0.693	0.945	0.583											
K	0.097	0.341	-0.211	0.166	-0.200	0.201	0.631	0.257	0.752										
Mg	-0.180	0.131	0.138	0.114	0.042	0.004	0.483	0.357	0.506	0.788									
Ca	-0.329	-0.034	0.011	-0.481	-0.007	-0.274	-0.584	-0.359	-0.557	-0.717	-0.572								
Ti	0.453	-0.101	-0.082	0.133	0.378	-0.186	-0.302	-0.434	-0.139	0.118	-0.186	-0.288							
P	-0.333	-0.012	-0.038	-0.504	-0.099	-0.224	-0.514	-0.334	-0.491	-0.694	-0.573	0.993	-0.344						
H2O+	-0.321	-0.478	0.755	0.370	0.715	-0.291	-0.441	-0.091	-0.556	-0.257	0.054	0.030	0.128	-0.053					
H2O-	0.258	-0.159	0.092	-0.126	0.573	-0.537	-0.358	-0.436	-0.269	0.295	0.265	-0.383	0.462	-0.428	0.323				
CO2	-0.389	0.012	-0.030	-0.494	-0.050	-0.249	-0.529	-0.341	-0.538	-0.725	-0.569	0.978	-0.374	0.985	-0.010	-0.453			
LOI	0.248	-0.247	0.183	-0.089	0.703	-0.585	-0.424	-0.399	-0.364	0.203	0.249	-0.404	0.503	-0.461	0.422	0.970	-0.469		
Ni	-0.135	-0.130	0.181	-0.582	0.666	-0.833	-0.437	-0.424	-0.380	0.155	0.421	-0.044	0.074	-0.075	0.237	0.606	-0.054	0.658	
Cu	-0.125	-0.324	0.331	0.060	0.467	-0.251	-0.269	-0.129	-0.115	0.194	0.146	-0.228	0.585	-0.273	0.229	0.445	-0.324	0.517	0.423
Zn	-0.169	-0.419	0.571	0.266	0.585	-0.149	-0.415	0.020	-0.452	-0.378	-0.190	-0.046	0.315	-0.107	0.466	0.154	-0.097	0.321	0.181
Co	-0.037	-0.424	0.421	-0.115	0.421	-0.456	0.040	-0.109	0.028	0.423	0.651	-0.428	0.027	-0.441	0.302	0.515	-0.420	0.553	0.730
Ba	0.139	-0.096	0.038	0.072	0.315	-0.106	-0.634	-0.340	-0.614	-0.665	-0.774	0.396	0.433	0.341	0.286	0.087	0.320	0.126	-0.260
Mo	-0.075	0.011	0.156	-0.191	0.763	-0.584	-0.836	-0.480	-0.877	-0.577	-0.392	0.374	0.163	0.295	0.543	0.305	0.352	0.392	0.303
Sr	0.175	-0.106	0.196	-0.084	0.365	-0.248	-0.711	-0.323	-0.788	-0.849	-0.763	0.701	-0.004	0.651	0.390	-0.196	0.683	-0.135	-0.154
Ce	0.336	0.321	-0.438	-0.171	0.181	-0.171	-0.537	-0.473	-0.449	-0.422	-0.712	0.298	0.521	0.264	-0.054	0.159	0.251	0.142	-0.216
Y	-0.094	0.393	-0.339	-0.472	0.139	-0.359	-0.576	-0.467	-0.562	-0.592	-0.635	0.719	-0.055	0.702	-0.060	-0.192	0.736	-0.228	-0.086
V	0.016	-0.345	0.375	0.481	0.406	0.061	-0.424	-0.055	-0.511	-0.532	-0.557	0.017	0.336	-0.038	0.463	0.074	-0.005	0.188	-0.273
Pb	0.174	0.362	-0.287	-0.070	0.003	-0.009	-0.202	-0.055	-0.310	-0.487	-0.559	0.266	-0.092	0.259	0.002	-0.112	0.285	-0.140	-0.355
Cr	-0.018	0.313	-0.203	0.228	-0.436	0.370	0.587	0.365	0.640	0.632	0.535	-0.255	-0.287	-0.227	-0.224	-0.143	-0.261	-0.257	-0.250
Cd	0.142	-0.147	-0.022	-0.649	0.422	-0.739	-0.216	-0.433	-0.200	0.161	0.298	-0.109	0.062	-0.106	0.012	0.415	-0.073	0.450	0.829
As	-0.069	0.064	0.257	0.644	-0.005	0.374	0.500	0.546	0.279	0.277	0.452	-0.557	-0.326	-0.565	0.316	-0.027	-0.489	-0.001	-0.224
Pt	-0.042	0.106	-0.148	-0.631	0.354	-0.635	-0.613	-0.511	-0.520	-0.290	-0.263	0.420	0.196	0.401	0.087	0.428	0.356	0.388	0.445
Rh	0.090	0.153	-0.323	-0.716	0.206	-0.638	-0.464	-0.548	-0.370	-0.153	-0.229	0.265	0.224	0.274	-0.174	0.435	0.248	0.371	0.451
Ru	0.136	-0.303	0.180	-0.110	0.091	-0.249	0.311	0.078	0.336	0.580	0.606	-0.550	0.104	-0.535	-0.069	0.434	-0.562	0.418	0.511
Ir	0.042	0.148	-0.306	-0.710	0.160	-0.594	-0.475	-0.507	-0.374	-0.156	-0.196	0.333	0.113	0.341	-0.125	0.480	0.296	0.388	0.433
Thick	-0.040	0.116	-0.273	-0.656	0.132	-0.468	-0.552	-0.600	-0.370	-0.150	-0.205	0.472	0.198	0.474	-0.115	0.333	0.417	0.275	0.419

	Cu	Zn	Co	Ba	Mo	Sr	Ce	Y	V	Pb	Cr	Cd	As	Pt	Rh	Ru	Ir
Zn	0.630																
Co	0.302	0.022															
Ba	0.185	0.507	-0.601														
Mo	0.063	0.474	-0.156	0.670													
Sr	-0.095	0.385	-0.522	0.797	0.774												
Ce	0.010	0.163	-0.639	0.840	0.578	0.585											
Y	-0.353	-0.088	-0.547	0.561	0.614	0.738	0.695										
V	0.264	0.731	-0.347	0.756	0.574	0.641	0.462	0.152									
Pb	-0.496	0.010	-0.591	0.597	0.500	0.577	0.677	0.717	0.329								
Cr	-0.262	-0.627	0.011	-0.509	-0.483	-0.471	-0.409	-0.276	-0.444	-0.247							
Cd	0.158	-0.120	0.742	-0.381	0.072	-0.250	-0.251	-0.064	-0.429	-0.269	-0.169						
As	-0.363	-0.064	0.166	-0.309	-0.068	-0.209	-0.395	-0.343	0.112	0.116	0.400	-0.199					
Pt	0.199	0.111	-0.066	0.430	0.453	0.306	0.526	0.509	-0.061	0.370	-0.430	0.287	-0.570				
Rh	0.122	-0.055	0.018	0.247	0.262	0.110	0.470	0.455	-0.177	0.316	-0.375	0.434	-0.567	0.904			
Ru	0.362	-0.114	0.822	-0.609	-0.483	-0.693	-0.575	-0.601	-0.449	-0.542	0.150	0.636	0.089	-0.057	0.133		
Ir	0.090	-0.112	-0.013	0.261	0.274	0.126	0.445	0.442	-0.211	0.316	-0.306	0.355	-0.549	0.933	0.961	0.081	
Thick	0.239	-0.050	-0.102	0.233	0.241	0.141	0.385	0.300	-0.194	-0.063	-0.281	0.214	-0.769	0.756	0.693	-0.165	0.756

Table 13. Correlation coefficient matrix for 9 bulk crusts ≥70mm listed in table 6; n=9, except for Pt, Rh, Ru, and Ir = 5; the zero correlations for 9 points and 5 points at the 95% confidence level are |0.665| and |0.883|, respectively

	Depth	Lat.	Long.	Fe	Mn	Fe/Mn	Si	Na	Al	K	Mg	Ca	Ti	P	H2O+	H2O-	CO2	LOI	N
Lat.	0.534																		
Long.	-0.591	-0.877																	
Fe	0.546	0.251	0.065																
Mn	-0.322	0.208	0.134	0.413															
Fe/Mn	0.837	0.281	-0.161	0.733	-0.286														
Si	0.717	0.588	-0.291	0.846	0.148	0.866													
Na	0.036	0.138	0.310	0.840	0.764	0.327	0.620												
Al	0.970	0.550	-0.491	0.725	-0.140	0.896	0.850	0.275											
K	0.869	0.712	-0.539	0.794	0.141	0.798	0.917	0.466	0.948										
Mg	0.467	0.502	-0.164	0.917	0.652	0.513	0.792	0.854	0.648	0.815									
Ca	-0.636	-0.802	0.513	-0.775	-0.447	-0.589	-0.884	-0.637	-0.765	-0.929	-0.905								
Ti	0.834	0.493	-0.352	0.876	0.210	0.764	0.821	0.533	0.922	0.943	0.857	-0.841							
P	-0.647	-0.775	0.484	-0.803	-0.447	-0.610	-0.893	-0.655	-0.780	-0.937	-0.920	0.999	-0.862						
H2O+	-0.512	-0.422	0.777	0.433	0.698	-0.124	0.061	0.789	-0.304	-0.161	0.388	-0.035	-0.012	-0.057					
H2O-	0.598	0.685	-0.383	0.859	0.538	0.573	0.857	0.733	0.747	0.909	0.970	-0.980	0.886	-0.986	0.174				
CO2	-0.728	-0.686	0.423	-0.871	-0.372	-0.707	-0.917	-0.654	-0.856	-0.969	-0.930	0.975	-0.935	0.984	-0.059	-0.982			
LOI	0.510	0.668	-0.356	0.833	0.635	0.470	0.791	0.761	0.667	0.854	0.978	-0.960	0.846	-0.966	0.236	0.992	-0.951		
N	-0.895	-0.126	0.191	-0.639	0.353	-0.871	-0.618	-0.127	-0.889	-0.718	-0.424	0.426	-0.807	0.457	0.254	-0.461	0.598	-0.374	
Cu	0.707	-0.002	0.112	0.865	-0.030	0.854	0.702	0.504	0.798	0.701	0.639	-0.501	0.841	-.0540	0.177	0.590	-0.678	0.529	-0.905
Zn	-0.299	-0.112	0.524	0.626	0.854	0.000	0.293	0.932	-0.068	0.134	0.663	-0.358	0.254	-0.376	0.939	0.486	-0.363	0.549	0.142
Co	-0.780	-0.500	0.750	0.076	0.709	-0.512	-0.310	0.542	-0.627	-0.471	0.120	0.223	-0.320	0.212	0.915	-0.093	0.245	0.002	0.561
Ba	0.359	-0.008	0.331	0.963	0.429	0.643	0.710	0.873	0.554	0.603	0.823	-0.589	0.739	-0.624	0.617	0.707	-0.707	0.691	-0.560
Mo	-0.504	0.446	-0.338	-0.422	0.498	-0.676	-0.266	-0.027	-0.492	-0.242	-0.062	-0.076	-0.412	-0.035	0.002	-0.003	0.138	0.076	0.821
Sr	-0.794	-0.608	0.505	-0.767	-0.299	-0.598	-0.718	-0.456	-0.860	-0.917	-0.845	0.856	-0.966	0.870	0.100	-0.893	0.916	-0.874	0.694
Ce	0.698	0.919	-0.800	0.513	0.304	0.425	0.685	0.303	0.738	0.873	0.724	-0.909	0.768	-0.898	-0.308	0.858	-0.862	0.844	-0.392
Y	-0.638	-0.110	-0.124	-0.958	-0.151	-0.855	-0.822	-0.692	-0.782	-0.759	-0.773	0.641	-0.856	0.675	-0.321	-0.721	0.781	-0.668	0.794
V	0.260	0.838	-0.498	0.518	0.663	0.202	0.655	0.616	0.400	0.666	0.777	-0.889	0.522	-0.872	0.139	0.847	-0.773	0.869	0.033
Pb	-0.410	0.495	-0.173	0.023	0.764	-0.400	0.103	0.444	-0.285	0.028	0.340	-0.389	-0.120	-0.359	0.351	0.349	-0.201	0.423	0.665
Cr	0.830	0.219	-0.463	0.329	-0.319	0.510	0.281	-0.180	0.738	0.578	0.267	-0.305	0.693	-0.325	-0.517	0.335	-0.439	0.286	-0.839
Cd	-0.703	-0.068	-0.026	-0.874	-0.115	-0.748	-0.652	-0.528	-0.793	-0.730	-0.722	0.561	-0.901	0.599	-0.179	-0.668	0.728	-0.628	0.875
As	0.024	0.584	-0.130	0.578	0.746	0.186	0.641	0.807	0.225	0.504	0.757	-0.770	0.382	-0.759	0.470	0.756	-0.665	0.783	0.153
Pt	-0.716	-0.461	0.669	0.100	0.764	-0.545	-0.339	0.528	-0.576	-0.419	0.181	0.182	-0.230	0.169	0.871	-0.034	0.193	0.072	0.503
Rh	-0.767	-0.090	0.287	-0.144	0.826	-0.756	-0.392	0.364	-0.663	-0.418	0.113	0.081	-0.361	0.093	0.620	-0.012	0.200	0.109	0.781
Ru	0.174	-0.319	0.612	0.774	0.157	0.629	0.561	0.721	0.350	0.322	0.502	-0.262	0.440	-0.299	0.656	0.365	-0.397	0.327	-0.472
Ir	-0.838	-0.234	0.443	-0.145	0.783	-0.743	-0.421	0.382	-0.723	-0.501	0.054	0.177	-0.427	0.185	0.710	-0.096	0.279	0.020	0.788
Thick	-0.493	-0.884	0.645	-0.348	-0.090	-0.491	-0.761	-0.266	-0.556	-0.699	-0.473	0.779	-0.427	0.755	0.265	-0.643	0.674	-0.593	0.146

	Cu	Zn	Co	Ba	Mo	Sr	Ce	Y	V	Pb	Cr	Cd	As	Pt	Rh	Ru	Ir
Zn	0.281																
Co	-0.182	0.808															
Ba	0.854	0.732	0.276														
Mo	-0.805	0.091	0.255	-0.498													
Sr	-0.689	-0.204	0.330	-0.598	0.223												
Ce	0.311	0.037	-0.451	0.270	0.197	-0.869											
Y	-0.964	-0.458	0.065	-0.939	0.655	0.702	-0.384										
V	0.085	0.443	0.016	0.346	0.509	-0.603	0.820	-0.291									
Pb	-0.480	0.497	0.441	-0.036	0.878	0.000	0.327	0.248	0.763								
Cr	0.617	-0.370	-0.639	0.205	-0.568	-0.716	0.488	-0.440	-0.070	-0.619							
Cd	-0.970	-0.328	0.138	-0.844	0.707	0.803	-0.422	0.928	-0.170	0.401	-0.695						
As	0.105	0.690	0.309	0.497	0.448	-0.390	0.550	-0.357	0.915	0.807	-0.358	-0.134					
Pt	-0.146	0.798	0.977	0.282	0.253	0.204	-0.357	0.055	0.037	0.416	-0.491	0.055	0.269				
Rh	-0.520	0.622	0.835	-0.056	0.708	0.234	-0.132	0.381	0.300	0.756	-0.618	0.391	0.420	0.861			
Ru	0.769	0.627	0.318	0.891	-0.639	-0.219	-0.123	-0.837	0.021	-0.214	-0.015	-0.662	0.296	0.246	-0.175		
Ir	-0.493	0.662	0.909	-0.016	0.621	0.338	-0.277	0.356	0.192	0.691	-0.691	0.395	0.376	0.911	0.985	-0.065	
Thick	-0.094	0.022	0.452	-0.136	-0.302	0.432	-0.738	0.256	-0.789	-0.463	0.014	0.054	-0.685	0.509	0.223	0.009	0.305

Table 14. Correlation coefficient matrix for 5 bulk crusts ≤11mm listed in table 6; the zero correlation for 5 points at the 95% confidence level is |0.883|

	Depth	Lat.	Long.	Fe	Mn	Fe/Mn	Si	Na	Al	K	Mg	Ca	Ti	P	H2O+	H2O-
Lat.	-0.854															
Long.	-0.414	0.362														
Fe	0.136	0.248	0.484													
Mn	-0.091	-0.088	0.840	0.153												
Fe/Mn	0.124	0.178	-0.272	0.563	-0.663											
Si	0.357	-0.160	-0.946	-0.218	-0.945	0.520										
Na	-0.419	0.822	0.076	0.443	-0.313	0.363	0.191									
Al	0.210	-0.409	-0.888	-0.786	-0.653	0.007	0.721	-0.374								
K	-0.024	-0.419	-0.477	-0.947	-0.147	-0.436	0.197	-0.660	0.820							
Mg	0.237	0.260	-0.407	0.379	-0.563	0.467	0.624	0.757	-0.032	-0.547						
Ca	-0.430	0.166	0.866	0.000	0.932	-0.685	-0.972	-0.221	-0.585	-0.021	-0.667					
Ti	0.528	-0.808	-0.685	-0.698	-0.273	-0.182	0.437	-0.772	0.850	0.826	-0.307	-0.343				
P	-0.149	0.413	0.703	0.941	0.313	0.453	-0.456	0.410	-0.879	-0.879	0.130	0.254	-0.803			
H2O+	0.286	-0.590	0.396	-0.240	0.820	-0.771	-0.641	-0.734	-0.151	0.304	-0.662	0.684	0.318	-0.173		
H2O-	-0.323	0.173	0.855	0.094	0.951	-0.721	-0.933	-0.078	-0.676	-0.176	-0.454	0.959	-0.433	0.285	0.678	
CO2	-0.528	0.658	0.900	0.682	0.542	0.055	-0.717	0.469	-0.933	-0.723	-0.056	0.606	-0.922	0.863	-0.031	0.628
LOI	-0.390	0.358	0.948	0.358	0.888	-0.490	-0.928	0.141	-0.857	-0.438	-0.302	0.899	-0.671	0.546	0.475	0.953
Ni	-0.063	-0.333	0.558	-0.297	0.868	-0.797	-0.795	-0.670	-0.208	0.356	-0.835	0.856	0.177	-0.113	0.933	0.783
Cu	0.610	-0.670	-0.929	-0.533	-0.629	0.131	0.793	-0.424	0.899	0.606	0.147	-0.724	0.888	-0.747	-0.073	-0.743
Zn	0.352	-0.112	-0.459	0.408	-0.713	0.953	0.637	0.117	0.221	-0.236	0.394	-0.787	0.113	0.250	-0.641	-0.837
Co	-0.324	-0.060	0.704	-0.230	0.886	-0.762	-0.893	-0.484	-0.340	0.257	-0.832	0.953	-0.046	0.020	0.805	0.865
Ba	-0.283	0.142	0.969	0.377	0.917	-0.369	-0.982	-0.169	-0.795	-0.321	-0.573	0.910	-0.487	0.594	0.585	0.873
Mo	-0.338	0.288	0.997	0.499	0.866	-0.280	-0.951	0.025	-0.892	-0.480	-0.415	0.864	-0.648	0.703	0.447	0.859
Sr	-0.006	0.253	0.760	0.932	0.480	0.294	-0.557	0.284	-0.929	-0.870	0.074	0.358	-0.741	0.970	0.041	0.418
Ce	0.431	-0.638	-0.853	-0.768	-0.490	-0.124	0.642	-0.539	0.958	0.820	-0.080	-0.514	0.949	-0.902	0.084	-0.571
Y	-0.573	0.413	0.949	0.203	0.854	-0.494	-0.962	0.037	-0.741	-0.247	-0.513	0.955	-0.595	0.470	0.456	0.926
V	-0.065	0.201	0.888	0.803	0.694	0.047	-0.753	0.137	-0.958	-0.746	-0.133	0.587	-0.696	0.895	0.272	0.631
Pb	0.350	0.097	0.318	0.958	0.090	0.516	-0.069	0.440	-0.693	-0.938	0.543	-0.135	-0.585	0.812	-0.208	0.021
Cr	-0.261	-0.078	-0.564	-0.760	-0.522	0.042	0.420	-0.349	0.835	0.838	-0.361	-0.294	0.623	-0.670	-0.209	-0.504
Cd	0.096	-0.558	0.213	-0.559	0.628	-0.769	-0.514	-0.856	0.167	0.651	-0.847	0.612	0.531	-0.428	0.904	0.508
As	-0.067	0.277	0.829	0.886	0.568	0.190	-0.645	0.265	-0.961	-0.839	0.007	0.462	-0.760	0.953	0.114	0.520
Thick	-0.847	0.542	-0.023	-0.592	-0.171	-0.192	-0.044	0.095	0.327	0.523	-0.366	0.191	-0.007	-0.345	-0.244	0.021

	CO2	LOI	Ni	Cu	Zn	Co	Ba	Mo	Sr	Ce	Y	V	Pb	Cr	Cd	As
LOI	0.829															
Ni	0.147	0.599														
Cu	-0.980	-0.899	-0.276													
Zn	-0.211	-0.672	-0.734	0.394												
Co	0.357	0.730	0.960	-0.492	-0.780											
Ba	0.771	0.910	0.719	-0.811	-0.491	0.813										
Mo	0.876	0.945	0.585	-0.901	-0.450	0.711	0.980									
Sr	0.839	0.639	0.049	-0.738	0.125	0.139	0.688	0.777								
Ce	-0.988	-0.793	-0.050	0.948	0.140	-0.245	-0.711	-0.834	-0.883							
Y	0.806	0.953	0.668	-0.893	-0.675	0.830	0.926	0.933	0.524	-0.727						
V	0.864	0.795	0.307	-0.809	-0.111	0.394	0.851	0.907	0.964	-0.880	0.703					
Pb	0.511	0.254	-0.359	-0.362	0.408	-0.351	0.222	0.346	0.839	-0.629	0.034	0.697				
Cr	-0.601	-0.637	-0.067	0.552	0.160	-0.075	-0.497	-0.596	-0.792	0.693	-0.386	-0.783	-0.831			
Cd	-0.227	0.256	0.926	0.095	-0.609	0.817	0.421	0.245	-0.274	0.327	0.357	-0.032	-0.577	0.220		
As	0.877	0.724	0.142	-0.798	0.011	0.243	0.760	0.843	0.993	-0.910	0.618	0.986	0.784	-0.799	-0.198	
Thick	0.010	-0.035	0.070	-0.119	-0.281	0.241	-0.073	-0.093	-0.492	0.110	0.219	-0.421	-0.760	0.716	0.117	-0.441

Table 15. Correlation coefficient matrix for 5 layers from D27-5 listed in table 6; the zero correlation for 5 points at the 95% confidence level is |0.883|

	Fe	Mn	Fe/Mn	Si	Na	Al	K	Mg	Ca	Ti	P	H2O+	H2O-	CO2	LOI	N
Mn	-0.414															
Fe/Mn	0.916	-0.673														
Si	0.740	-0.127	0.700													
Na	0.330	0.312	0.017	0.478												
Al	0.337	0.277	0.233	0.857	0.642											
K	0.093	0.540	-0.078	0.656	0.705	0.946										
Mg	0.029	0.758	-0.156	0.524	0.454	0.798	0.886									
Ca	-0.444	-0.565	-0.197	-0.718	-0.594	-0.803	-0.806	-0.897								
Ti	0.281	-0.093	0.049	0.164	0.831	0.210	0.244	-0.114	-0.078							
P	-0.410	-0.604	-0.151	-0.683	-0.604	-0.787	-0.808	-0.905	0.999	-0.087						
H2O+	0.909	-0.283	0.822	0.936	0.541	0.681	0.459	0.294	-0.615	0.365	-0.580					
H2O-	-0.365	0.993	-0.608	-0.044	0.288	0.341	0.581	0.815	-0.626	-0.161	-0.661	-0.224				
CO2	-0.570	-0.481	-0.283	-0.721	-0.680	-0.745	-0.734	-0.791	0.977	-0.232	0.975	-0.693	-0.530			
LOI	-0.241	0.971	-0.492	0.043	0.284	0.370	0.580	0.845	-0.704	-0.195	-0.735	-0.124	0.989	-0.616		
N	-0.537	0.945	-0.692	-0.069	0.191	0.380	0.619	0.806	-0.513	-0.250	-0.545	-0.321	0.956	-0.372	0.918	
Cu	-0.519	0.916	-0.811	-0.327	0.441	0.118	0.427	0.523	-0.337	0.210	-0.385	-0.400	0.865	-0.303	0.803	0.816
Zn	-0.536	0.598	-0.722	-0.789	-0.131	-0.584	-0.316	-0.051	0.158	-0.085	0.111	-0.723	0.528	0.145	0.488	0.419
Co	0.315	0.476	0.164	0.799	0.575	0.955	0.938	0.926	-0.926	0.053	-0.918	0.609	0.547	-0.855	0.596	0.541
Ba	-0.439	-0.351	-0.322	-0.874	-0.502	-0.942	-0.871	-0.870	0.918	0.006	0.902	-0.700	-0.434	0.855	-0.502	-0.419
Mo	-0.290	0.014	-0.317	-0.837	-0.489	-0.933	-0.819	-0.575	0.547	-0.183	0.521	-0.653	-0.051	0.479	-0.061	-0.168
Sr	-0.202	-0.590	-0.044	-0.706	-0.516	-0.909	-0.930	-0.972	0.926	0.036	0.924	-0.491	-0.659	0.836	-0.701	-0.656
Ce	-0.352	-0.038	-0.422	-0.868	-0.219	-0.880	-0.731	-0.667	0.644	0.190	0.613	-0.640	-0.136	0.540	-0.189	-0.231
Y	-0.401	-0.648	-0.107	-0.603	-0.611	-0.706	-0.749	-0.873	0.984	-0.114	0.991	-0.531	-0.694	0.977	-0.770	-0.549
V	0.242	-0.403	0.228	-0.469	-0.351	-0.816	-0.865	-0.737	0.482	0.038	0.479	-0.169	-0.449	0.334	-0.407	-0.626
Pb	0.372	-0.446	0.330	-0.348	-0.228	-0.724	-0.797	-0.714	0.406	0.154	0.406	-0.024	-0.490	0.237	-0.438	-0.686
Cr	0.567	0.412	0.307	0.805	0.751	0.852	0.824	0.798	-0.963	0.311	-0.957	0.756	0.462	-0.980	0.536	0.344
Cd	-0.469	0.859	-0.560	0.079	0.117	0.488	0.672	0.858	-0.557	-0.371	-0.579	-0.220	0.895	-0.390	0.870	0.973
As	0.870	0.000	0.736	0.768	0.275	0.482	0.307	0.427	-0.749	-0.024	-0.724	0.818	0.076	-0.802	0.216	-0.105
Pt	-0.544	0.787	-0.797	-0.637	0.109	-0.323	-0.021	0.203	-0.065	0.030	-0.116	-0.622	0.722	-0.061	0.674	0.620
Rh	-0.438	0.909	-0.743	-0.404	0.309	-0.048	0.250	0.451	-0.325	0.095	-0.374	-0.431	0.861	-0.310	0.825	0.753
Ru	0.135	0.605	-0.108	0.607	0.807	0.897	0.979	0.874	-0.842	0.363	-0.849	0.462	0.631	-0.802	0.634	0.618
Ir	-0.451	0.919	-0.757	-0.383	0.344	-0.007	0.294	0.475	-0.338	0.121	-0.387	-0.420	0.870	-0.320	0.830	0.772
Thick	-0.826	0.309	-0.799	-0.974	-0.485	-0.757	-0.524	-0.333	0.587	-0.286	0.549	-0.978	0.239	0.630	0.153	0.277

	Cu	Zn	Co	Ba	Mo	Sr	Ce	Y	V	Pb	Cr	Cd	As	Pt	Rh	Ru	Ir
Zn	0.704																
Co	0.250	-0.392															
Ba	-0.091	0.491	-0.984														
Mo	0.138	0.795	-0.800	0.809													
Sr	-0.349	0.273	-0.988	0.959	0.729												
Ce	0.238	0.755	-0.842	0.891	0.907	0.799											
Y	-0.449	-0.005	-0.858	0.836	0.408	0.872	0.501										
V	-0.281	0.401	-0.758	0.691	0.832	0.769	0.759	0.383									
Pb	-0.315	0.310	-0.685	0.611	0.744	0.717	0.700	0.313	0.987								
Cr	0.255	-0.291	0.909	-0.905	-0.633	-0.872	-0.639	-0.938	-0.461	-0.351							
Cd	0.662	0.231	0.635	-0.540	-0.316	-0.741	-0.424	-0.555	-0.730	-0.787	0.381						
As	-0.254	-0.355	0.586	-0.689	-0.314	-0.532	-0.517	-0.718	0.042	0.138	0.752	-0.020					
Pt	0.884	0.954	-0.135	0.264	0.579	0.015	0.587	-0.221	0.152	0.081	-0.059	0.433	-0.306				
Rh	0.958	0.837	0.145	-0.008	0.347	-0.256	0.362	-0.464	-0.053	-0.099	0.209	0.586	-0.142	0.960			
Ru	0.530	-0.190	0.909	-0.831	-0.717	-0.902	-0.607	-0.815	-0.757	-0.679	0.871	0.629	0.340	0.109	0.377		
Ir	0.973	0.812	0.175	-0.034	0.301	-0.284	0.332	-0.472	-0.103	-0.146	0.229	0.608	-0.158	0.948	0.998	0.417	
Thick	0.449	0.836	-0.658	0.748	0.778	0.540	0.763	0.474	0.324	0.188	-0.721	0.142	-0.744	0.721	0.520	-0.488	0.502

Table 16. Correlation coefficient matrix for 5 layers from D32-9 listed in table 6; the zero correlation for 5 points at the 95% confidence level is |0.883|

	Fe	Mn	Fe/Mn	Si	Na	Al	K	Mg	Ca	Ti	P	H2O+	H2O-	CO2	LOI	Ni
Mn	-0.621															
Fe/Mn	0.986	-0.739														
Si	0.454	-0.967	0.580													
Na	-0.093	0.833	-0.246	-0.926												
Al	-0.123	-0.681	0.046	0.748	-0.918											
K	-0.527	-0.317	-0.377	0.440	-0.739	0.908										
Mg	-0.802	0.492	-0.818	-0.253	0.000	-0.030	0.299									
Ca	-0.103	-0.368	0.027	0.289	-0.442	0.734	0.687	-0.408								
Ti	-0.904	0.890	-0.955	-0.791	0.509	-0.276	0.150	0.673	-0.070							
P	0.181	-0.598	0.315	0.490	-0.544	0.751	0.581	-0.596	0.955	-0.361						
H2O+	0.012	0.743	-0.157	-0.780	0.913	-0.992	-0.855	0.157	-0.769	0.367	-0.813					
H2O-	-0.731	0.036	-0.614	0.059	-0.411	0.702	0.916	0.337	0.721	0.472	0.523	-0.642				
CO2	0.654	-0.056	0.602	-0.200	0.450	-0.372	-0.578	-0.893	0.192	-0.354	0.307	0.258	-0.457			
LOI	-0.906	0.379	-0.839	-0.268	-0.108	0.418	0.747	0.519	0.514	0.750	0.250	-0.337	0.937	-0.483		
Ni	-0.892	0.671	-0.924	-0.461	0.183	-0.132	0.254	0.969	-0.344	0.834	-0.579	0.256	0.391	-0.777	0.624	
Cu	-0.803	0.032	-0.693	0.148	-0.509	0.683	0.921	0.622	0.446	0.479	0.257	-0.591	0.923	-0764	0.882	0.609
Zn	-0.729	-0.060	-0.622	0.276	-0.602	0.674	0.876	0.711	0.266	0.367	0.118	-0.575	0.795	-0.893	0.742	0.639
Co	-0.442	0.597	-0.541	-0.421	0.358	-0.525	-0.279	0.827	-0.841	0.507	-0.944	0.620	-0.235	-0.592	0.024	0.796
Ba	-0.180	-0.500	-0.023	0.494	-0.687	0.912	0.866	-0.208	0.945	-0.115	0.909	-0.922	0.803	-0.100	0.557	-0.211
Mo	0.168	0.626	0.000	-0.680	0.869	-0.994	-0.924	0.051	-0.798	0.212	-0.794	0.987	-0.757	0.328	-0.485	0.127
Sr	0.456	0.408	0.302	-0.543	0.816	-0.935	-0.991	-0.302	-0.631	-0.052	-0.555	0.884	-0.855	0.620	-0.662	-0.224
Ce	-0.377	-0.355	-0.225	0.391	-0.648	0.896	0.934	-0.015	0.901	0.070	0.811	-0.881	0.907	-0.252	0.708	-0.007
Y	0.292	-0.663	0.422	0.541	-0.553	0.725	0.511	-0.667	0.916	-0.462	0.993	-0.798	0.426	0.363	0.137	-0.665
V	0.777	0.000	0.661	-0.162	0.522	-0.720	-0.944	-0.550	-0.527	-0.455	-0.341	0.636	-0.952	0.704	-0.895	-0.546
Pb	0.758	0.000	0.663	-0.225	0.552	-0.615	-0.837	-0.764	-0.198	-0.412	-0.041	0.510	-0.767	0.919	-0.739	-0.695
Cr	0.035	-0.609	0.124	0.786	-0.819	0.568	0.452	0.372	-0.139	-0.401	-0.034	-0.524	0.092	-0.715	-0.089	0.138
Cd	-0.843	0.717	-0.894	-0.514	0.269	-0.244	0.137	0.960	-0.445	0.826	-0.670	0.365	0.281	-0.733	0.538	0.993
As	0.727	0.000	0.605	-0.107	0.459	-0.731	-0.938	-0.363	-0.703	-0.446	-0.512	0.668	-0.998	0.503	-0.926	-0.402
Pt	-0.159	-0.487	-0.005	0.467	-0.651	0.888	0.838	-0.252	0.962	-0.117	0.927	-0.904	0.789	-0.044	0.546	-0.245
Rh	-0.166	-0.497	-0.010	0.485	-0.672	0.902	0.852	-0.232	0.953	-0.120	0.919	-0.915	0.794	-0.071	0.549	-0.231
Ru	-0.350	-0.515	-0.190	0.645	-0.883	0.962	0.967	0.245	0.610	-0.070	0.571	-0.919	0.784	-0.602	0.561	0.142
Ir	-0.201	-0.475	-0.046	0.469	-0.669	0.903	0.868	-0.198	0.949	-0.089	0.905	-0.912	0.815	-0.100	0.577	-0.196
Thick	-0.272	0.056	-0.290	0.169	-0.224	-0.045	0.053	0.787	-0.681	0.107	-0.686	0.136	-0.129	-0.823	-0.055	0.626

	Cu	Zn	Co	Ba	Mo	Sr	Ce	Y	V	Pb	Cr	Cd	As	Pt	Rh	Ru	Ir
Zn	0.965																
Co	0.076	0.216															
Ba	0.635	0.519	-0.719														
Mo	-0.703	-0.665	0.567	-0.950													
Sr	-0.896	-0.885	0.256	-0.841	0.936												
Ce	0.773	0.656	-0.574	0.978	-0.939	-0.899											
Y	0.163	0.040	-0.966	0.866	-0.761	-0.496	0.749										
V	-0.996	-0.942	0.013	-0.698	0.746	0.913	-0.826	-0.247									
Pb	-0.955	-0.997	-0.291	-0.452	0.604	0.845	-0.600	0.038	0.926								
Cr	0.389	0.599	0.203	0.181	-0.477	-0.566	0.192	-0.014	-0.347	-0.591							
Cd	0.509	0.550	0.855	-0.327	0.243	-0.110	-0.126	-0.748	-0.441	-0.612	0.102						
As	-0.942	-0.829	0.215	-0.805	0.779	0.884	-0.910	-0.417	0.968	0.801	-0.157	-0.291					
Pt	0.600	0.473	-0.751	0.998	-0.931	-0.808	0.971	0.886	-0.668	-0.405	0.127	-0.359	-0.788				
Rh	0.616	0.495	-0.737	1.000	-0.942	-0.825	0.974	0.878	-0.681	-0.428	0.157	-0.346	-0.794	1.000			
Ru	0.839	0.851	-0.287	0.834	-0.952	-0.992	0.873	0.525	-0.856	-0.808	0.640	0.030	-0.818	0.800	0.818		
Ir	0.643	0.522	-0.713	1.000	-0.944	-0.839	0.982	0.860	-0.707	-0.456	0.161	-0.312	-0.816	0.998	0.999	0.829	
Thick	0.262	0.486	0.819	-0.410	0.129	-0.137	-0.304	-0.688	-0.176	-0.534	0.728	0.648	0.077	-0.464	-0.436	0.161	-0.418

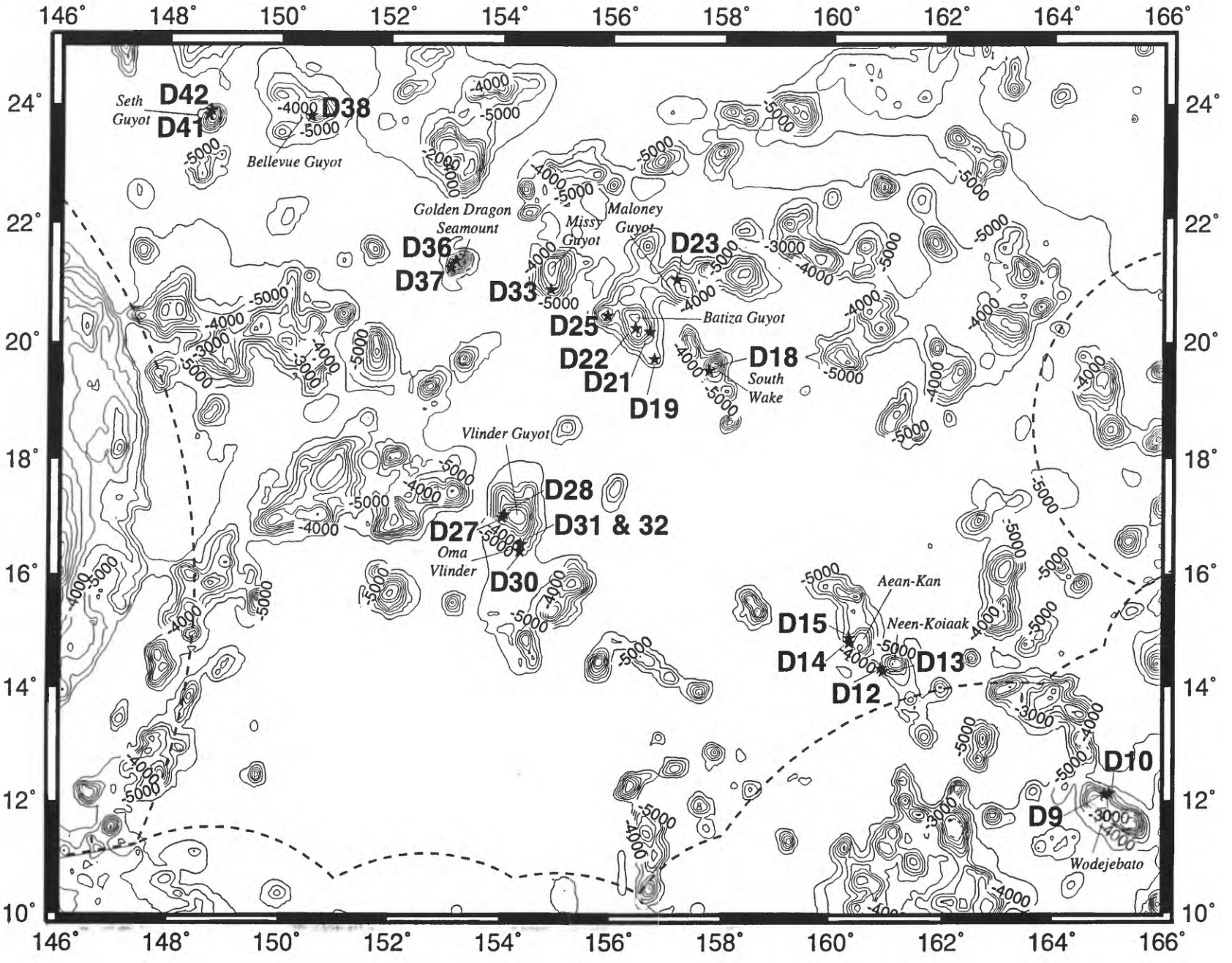

Figure 1. Bathymetry, seamount and guyot names, and dredge locations for Tunes 6 cruise; dashed EEZ boundaries: west = Commonwealth of the Northern Mariana Islands; southwest = Federated States of Micronesia; southeast = Republic of the Marshall Islands; and east = Wake Island; contour interval = 500 m

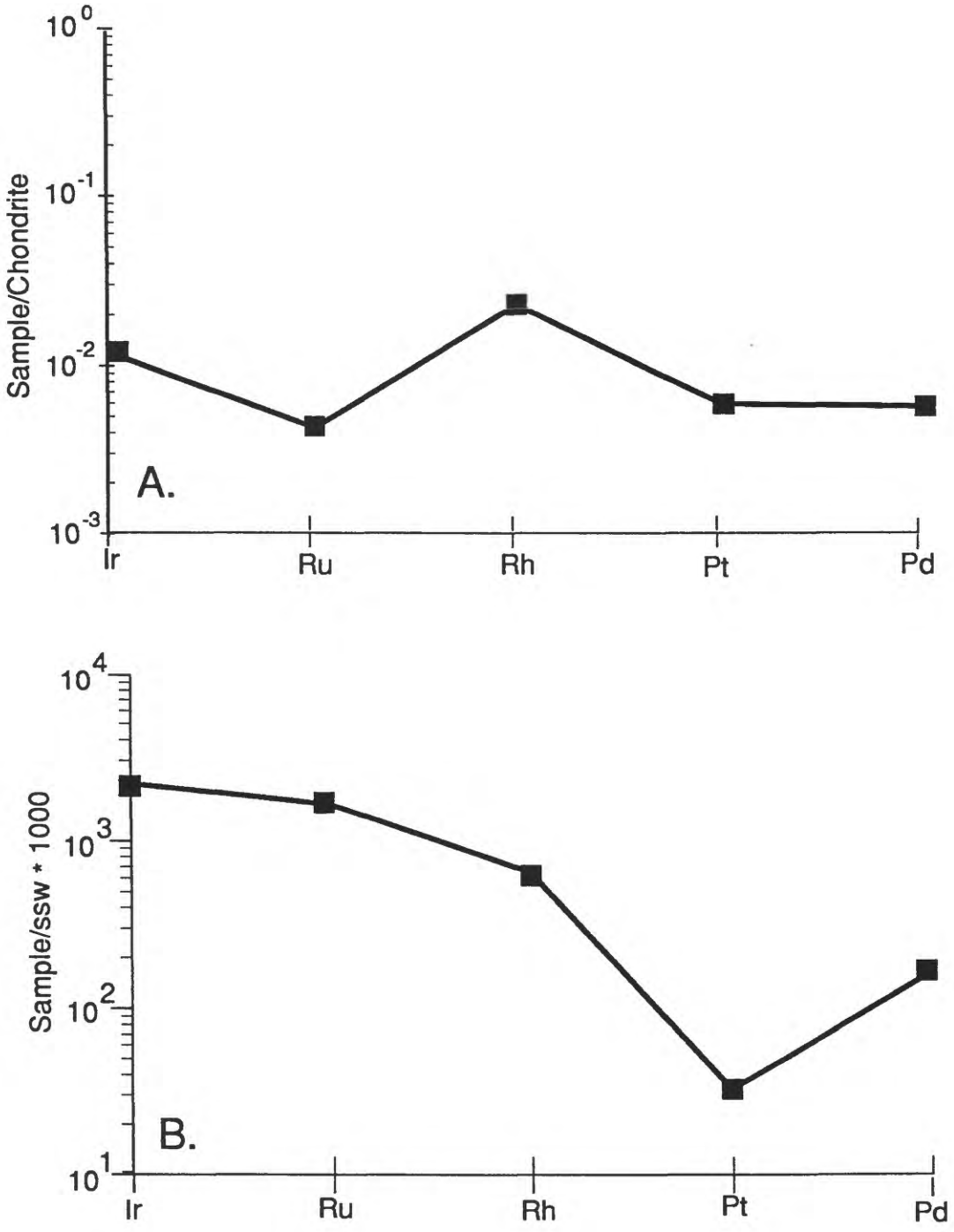

Figure 2. Mean PGE concentrations in 46 bulk crusts (A) normalized to chondrites (Anders and Grevesse, 1989) and (B) to surface seawater abundance (Goldberg, 1987; Bertine et al., 1993); Pd contents of the Fe-Mn crusts are less than the limit of detection, therefore the Pd points are maximum ratios

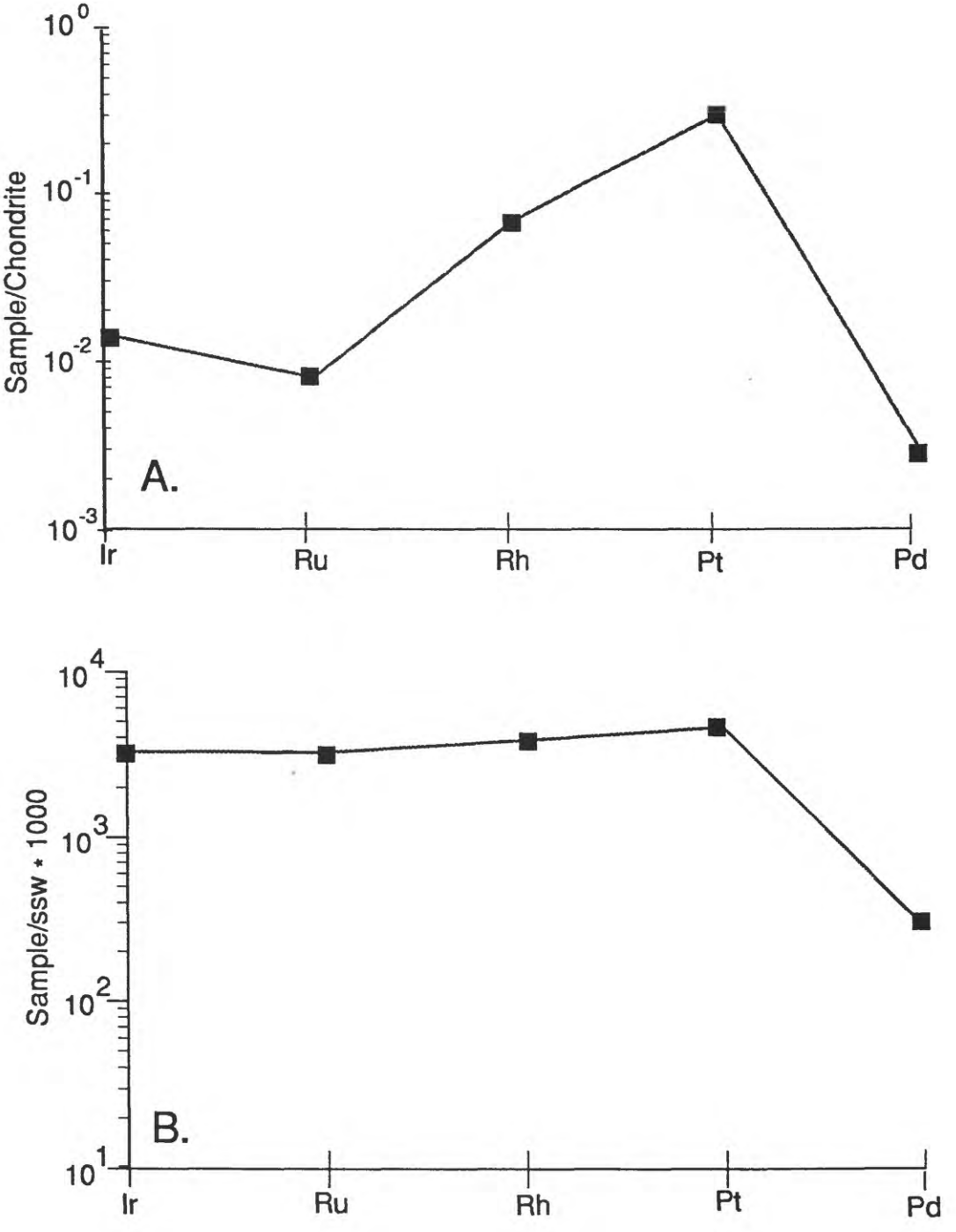

Figure 3. Mean PGE concentrations in D32-9H, 50-60 mm (A) normalized to chondrites (Anders and Grevesse, 1989) and (B) to surface seawater abundance (Goldberg,1987; Bertine et al., 1993); Pd contents of the Fe-Mn crusts are less than the limit of detection, therefore the Pd points are maximum ratios.

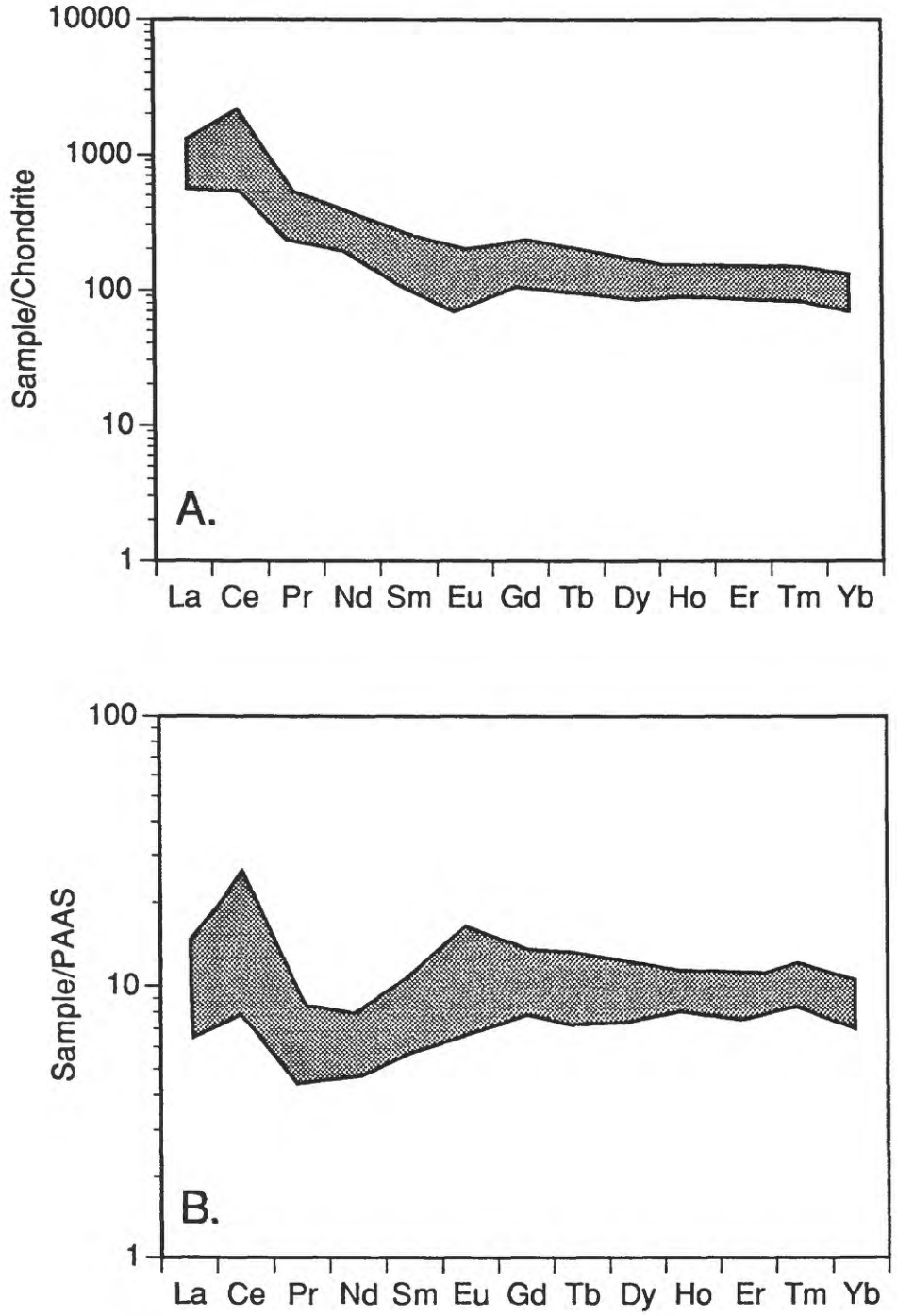

Figure 4. REE range plots for all 52 Fe-Mn crust samples: (A) Chondrite normalized, and (B) PAAS normalized

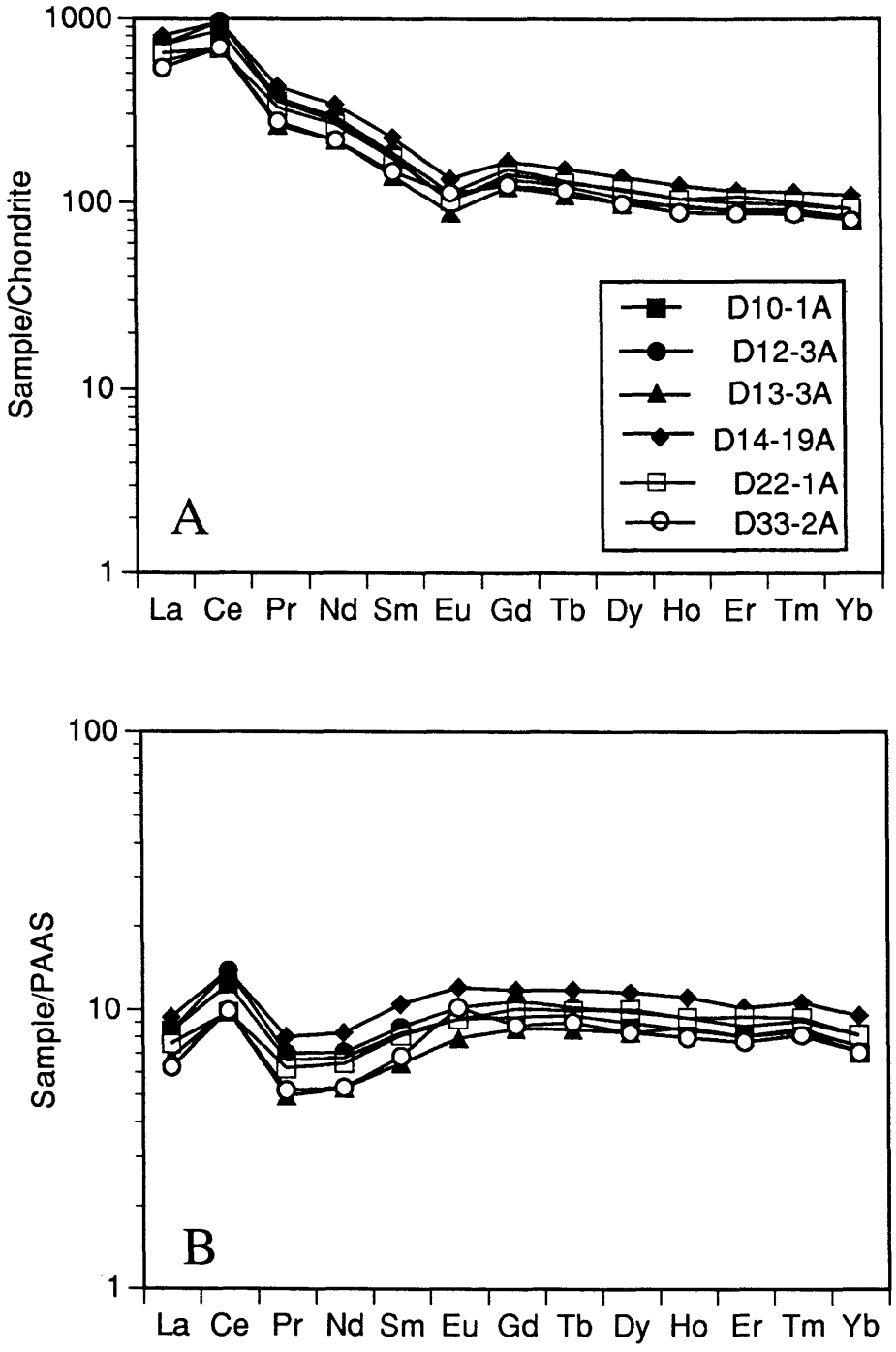

Figure 5. REE plots of bulk crusts from Wodejebato, Neen-Kiaakk, Batiza, Missy, and Aean-Kan Guyots: (A) Chondrite normalized, and (B) PAAS normalized

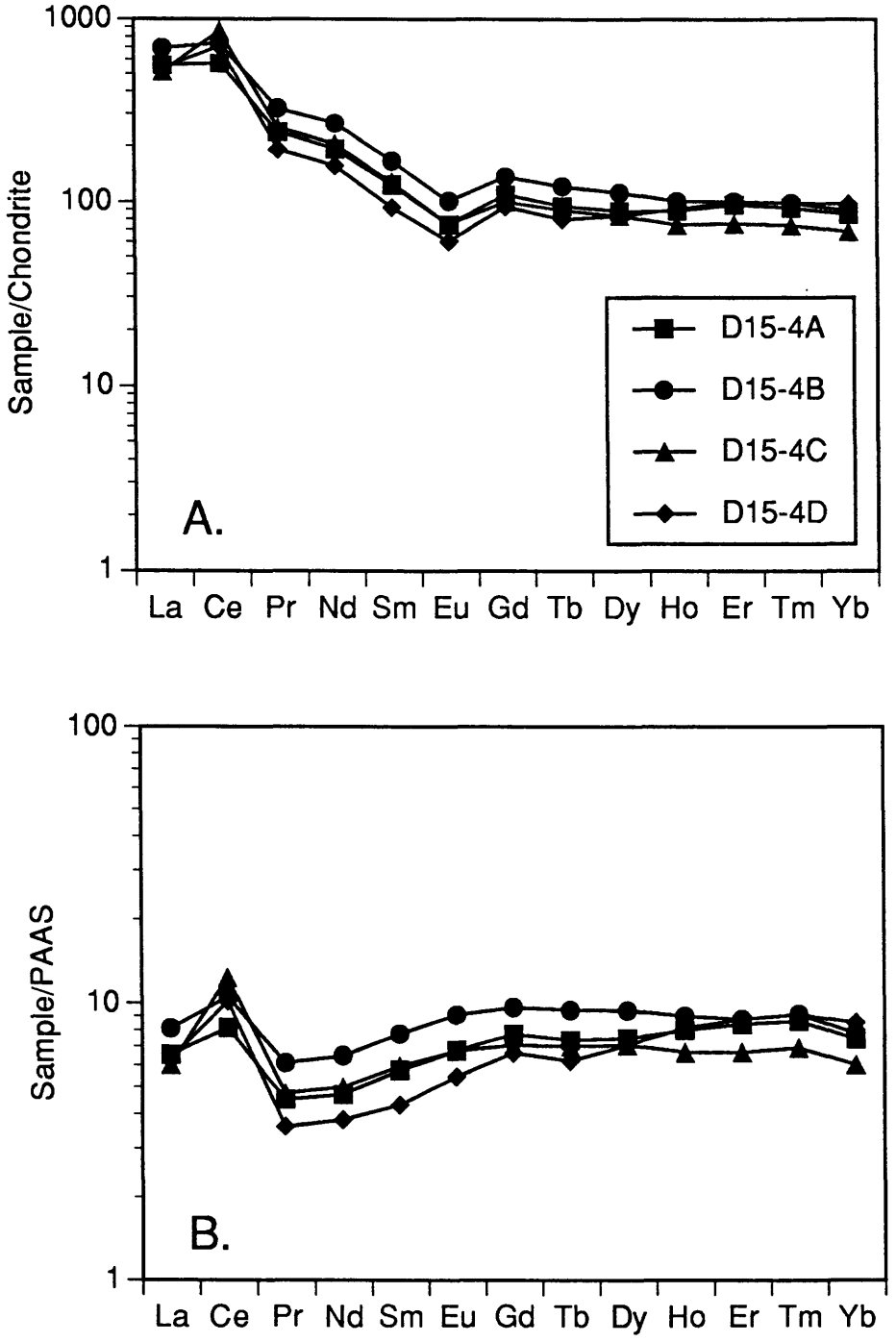

Figure 6. REE plots of crust samples from D15-4, Aean-Kan Guyot: (A) chondrite normalized, and (B) PAAS normalized

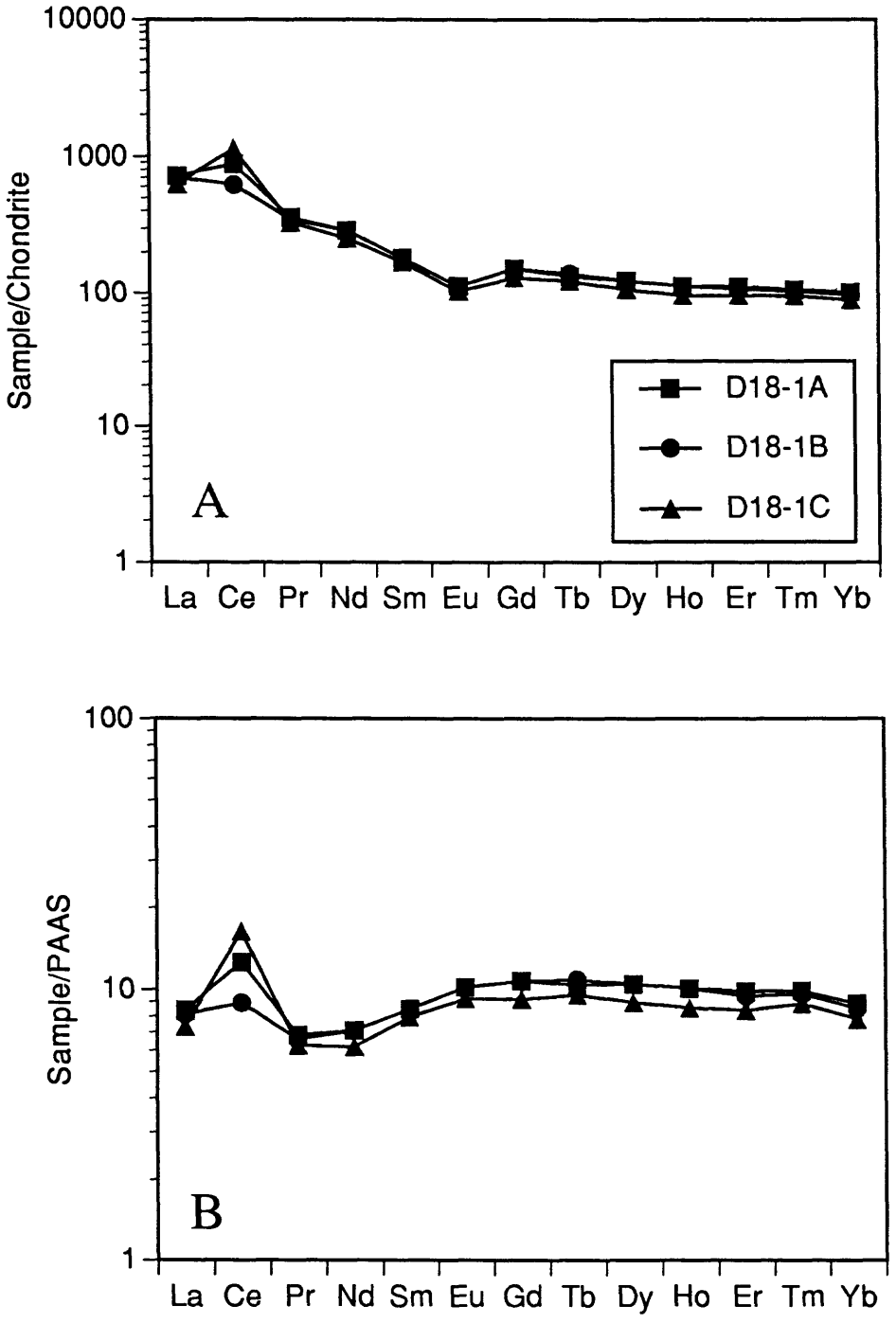

Figure 7. REE plots of crust samples from D18-1, South Wake Guyot: (A) Chondrite normalized, and (B) PAAS normalized

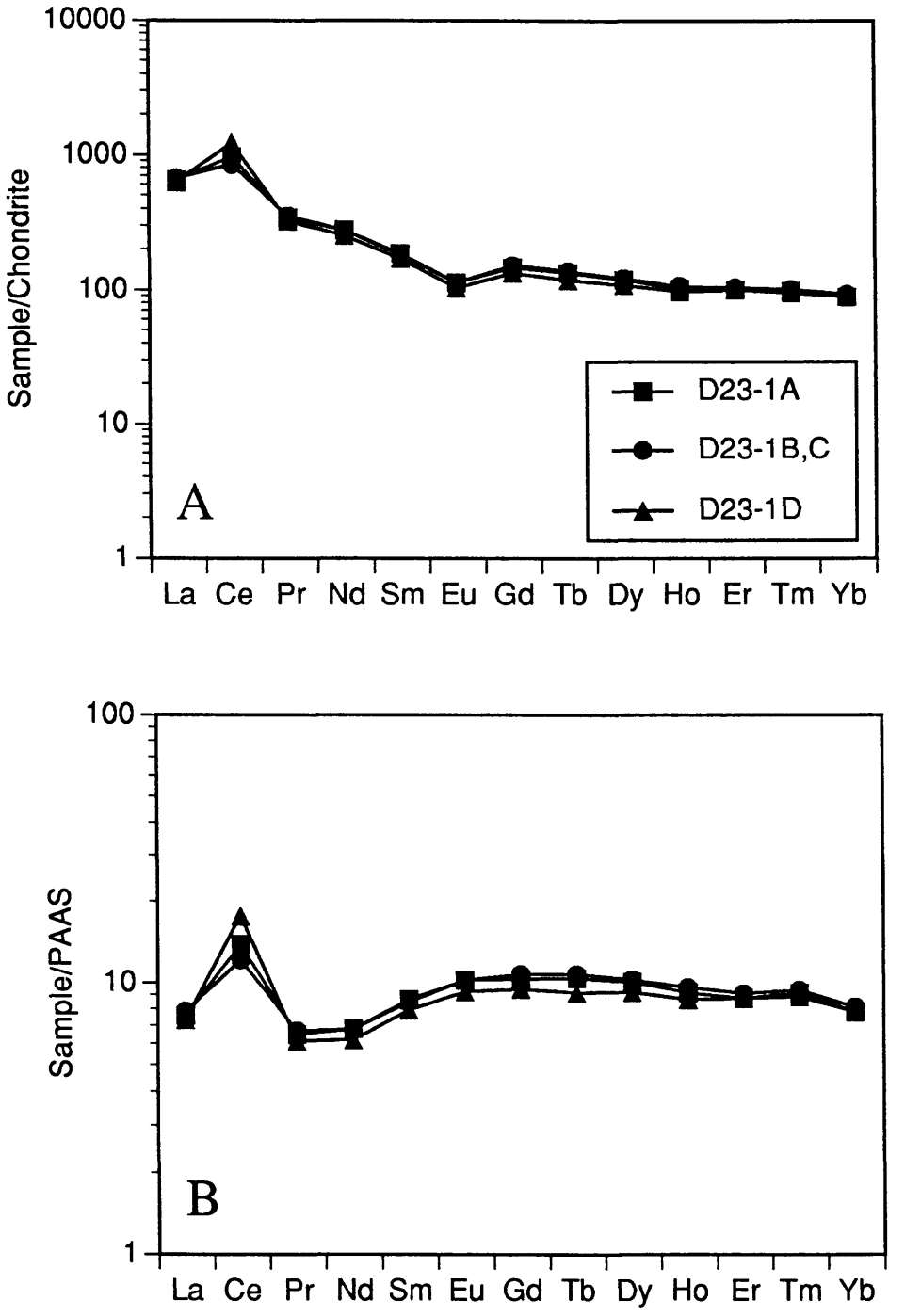

Figure 8. REE plots of crust samples from D23-1, Maloney Guyot: (A) Chondrite normalized, and (B) PAAS normalized

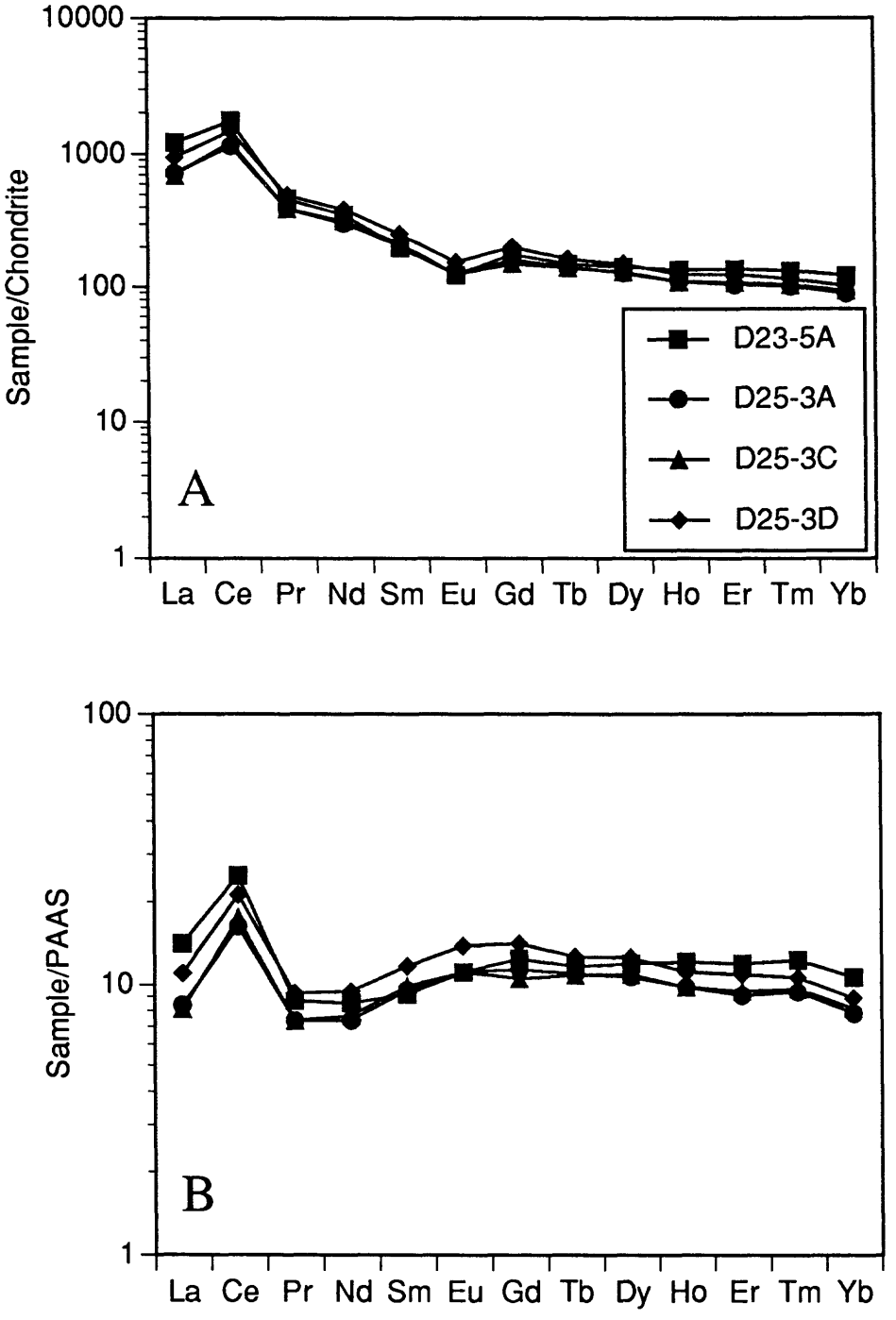

Figure 9. REE plots of crust samples from D25-3, West Batiza Guyot: (A) Chondrite normalized, and (B) PAAS normalized

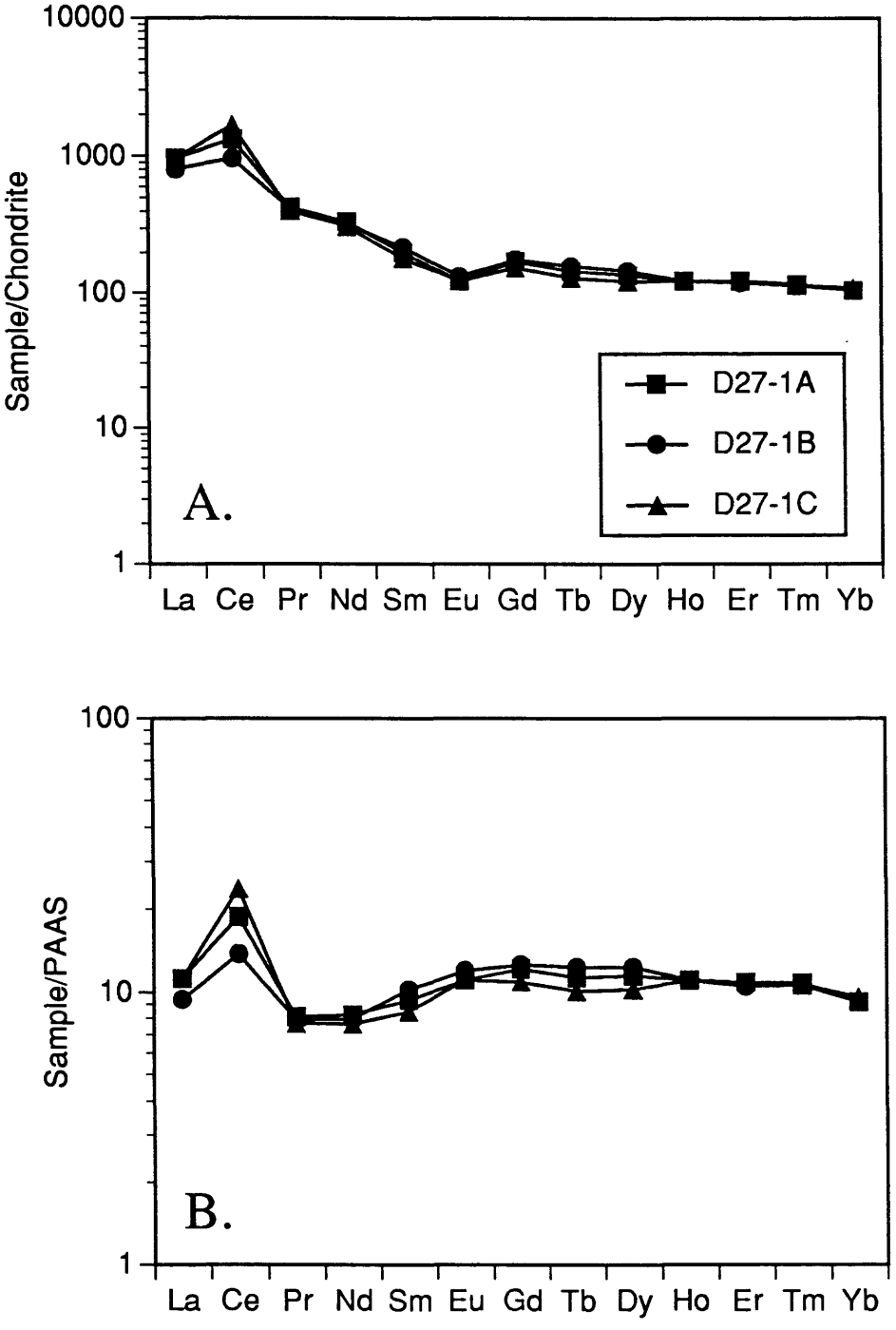

Figure 10. REE plots of crust samples from D27-1, Vlinder Guyot: (A) chondrite normalized, and (B) PAAS normalized

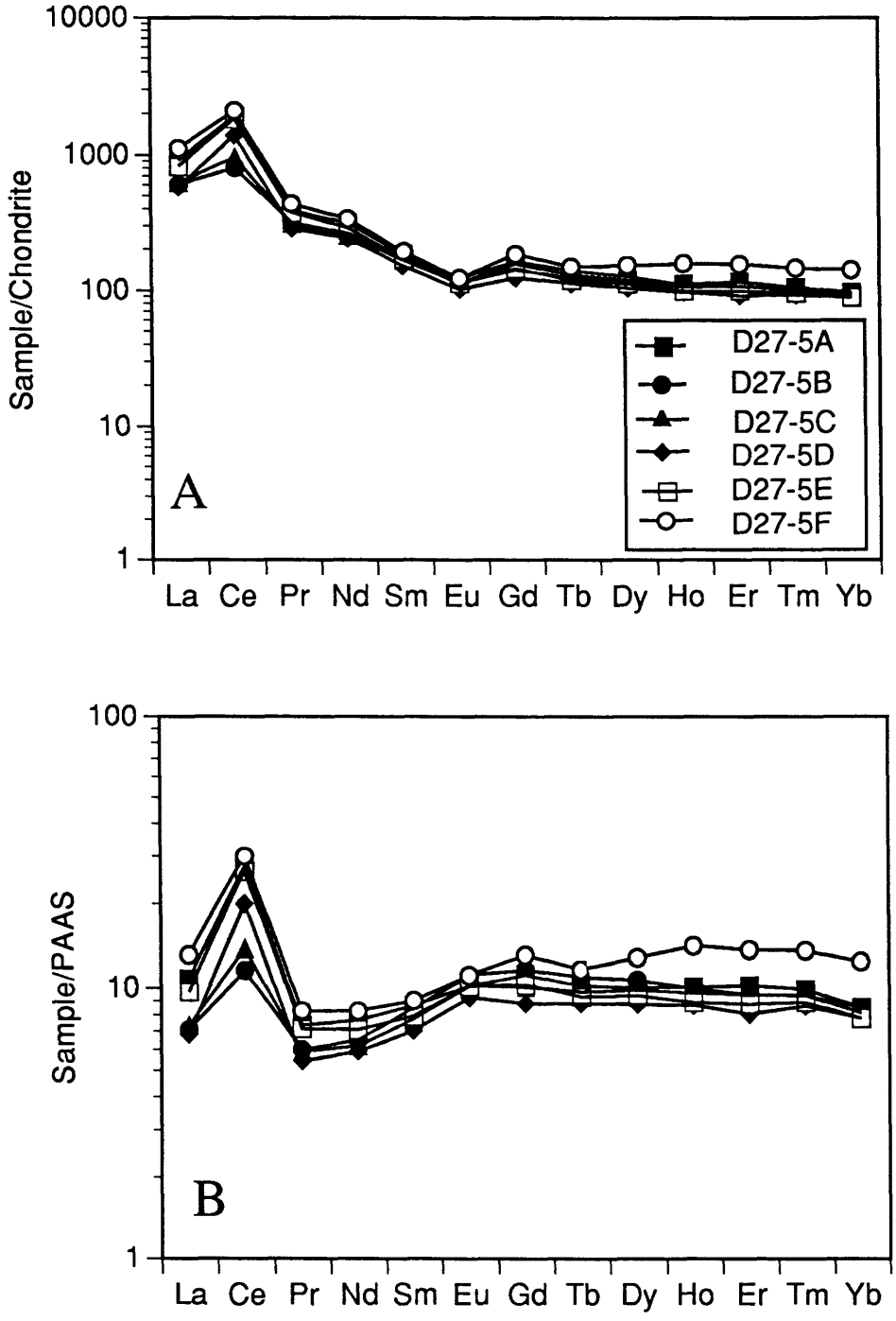

Figure 11. REE plots of crust samples from D27-5, Vlinder Guyot: (A) Chondrite normalized, and (B) PAAS normalized

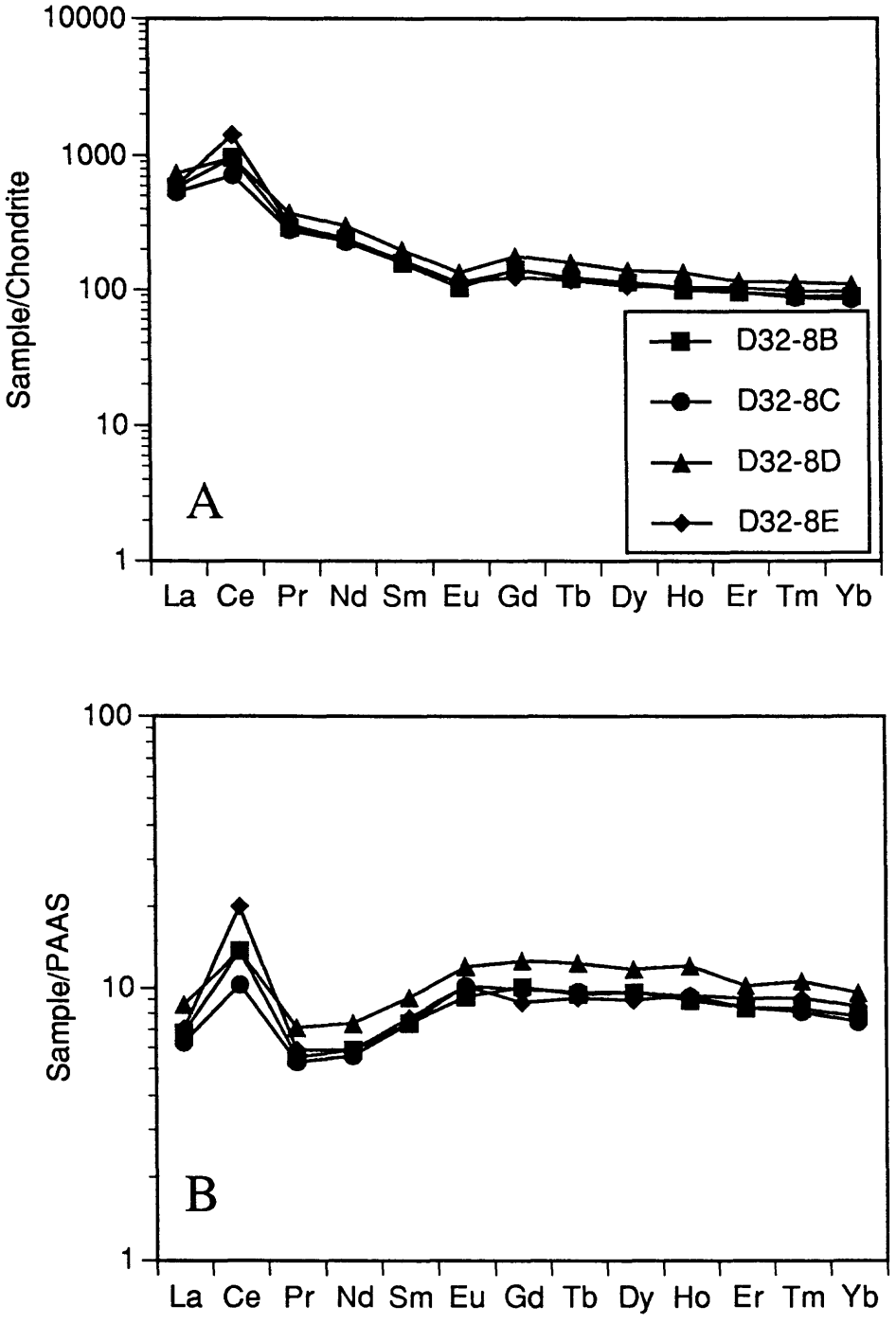

Figure 12. REE plots of crust samples from D32-8, Oma Vlinder Guyot: (A) Chondrite normalized, and (B) PAAS normalized

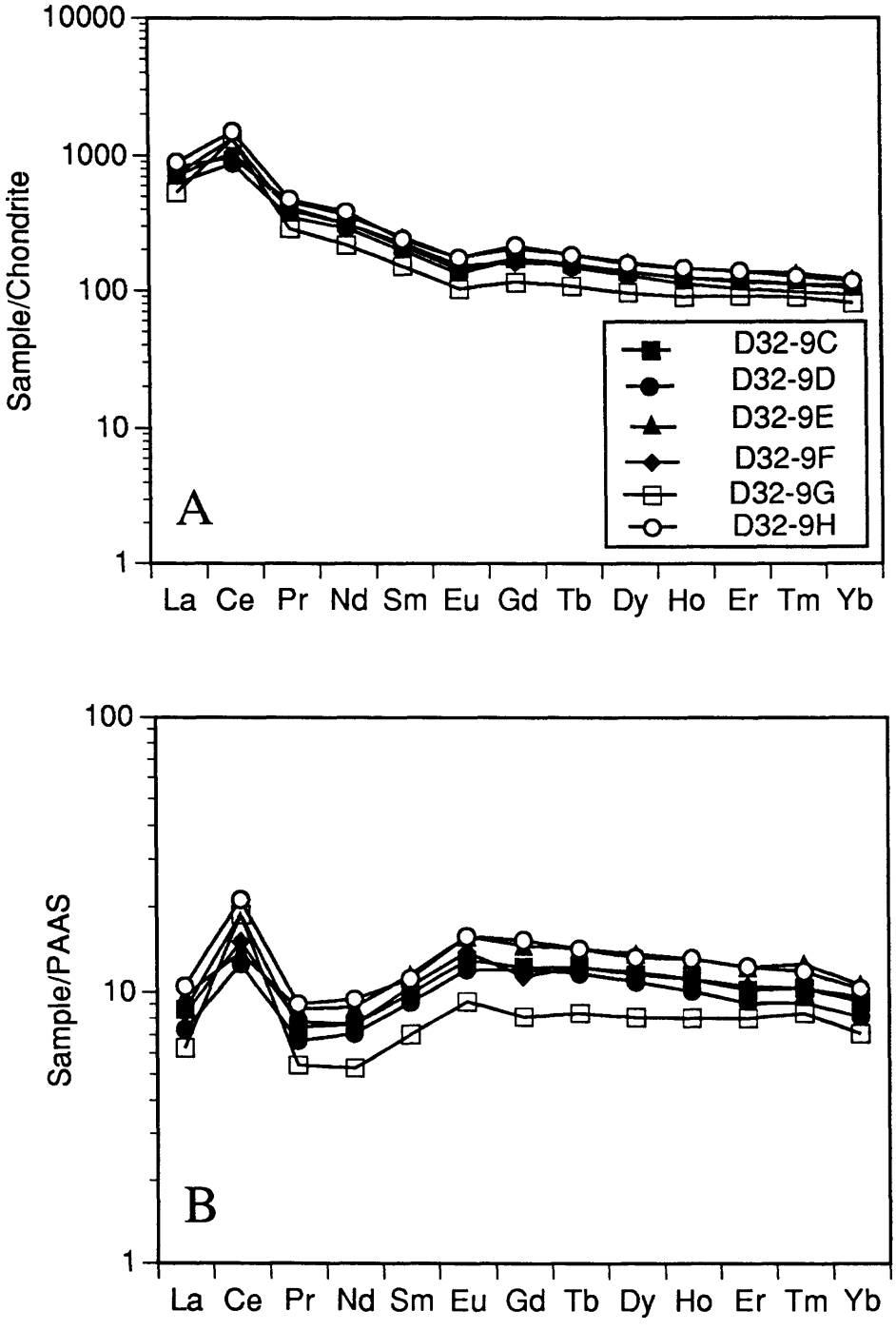

Figure 13. REE plots of crust samples from D32-9, Oma Vlinder Guyot: (A) Chondrite normalized, and (B) PAAS normalized

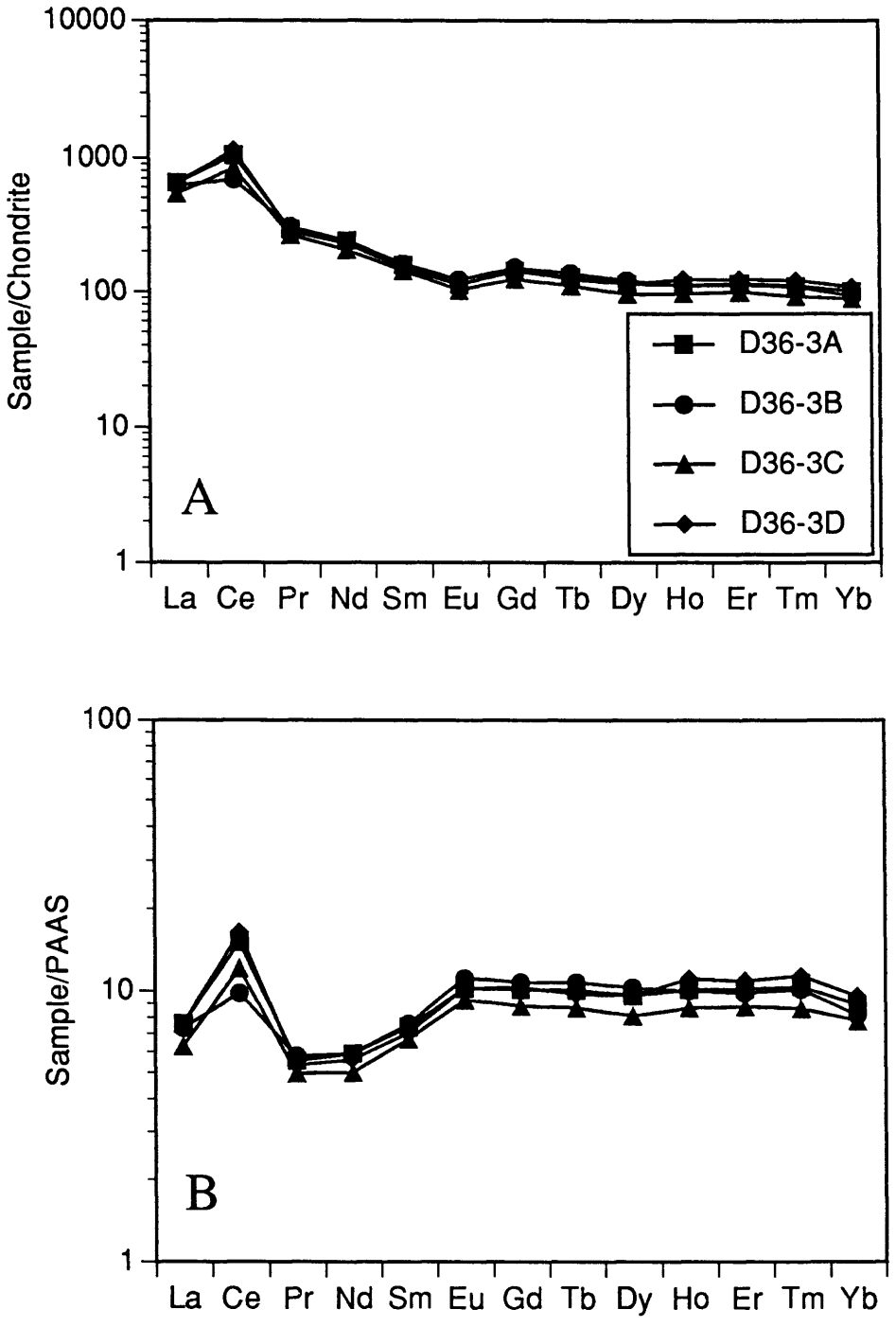

Figure 14. REE plots of crust samples from D36-3, Golden Dragon Seamount: (A) Chondrite normalized, and (B) PAAS normalized

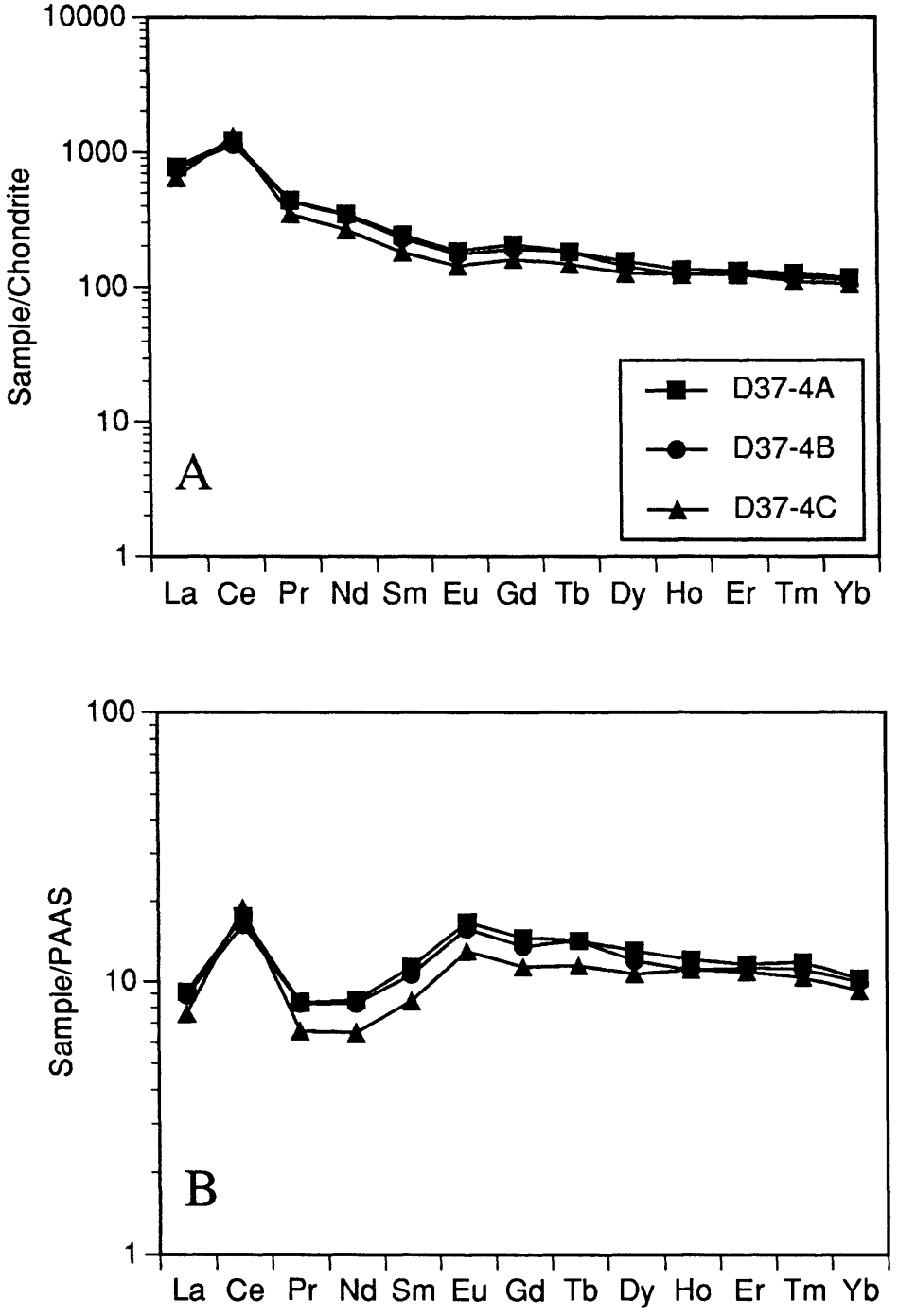

Figure 15. REE plots of crust samples from D37-4, Golden Dragon Seamount: (A) Chondrite normalized, and (B) PAAS normalized

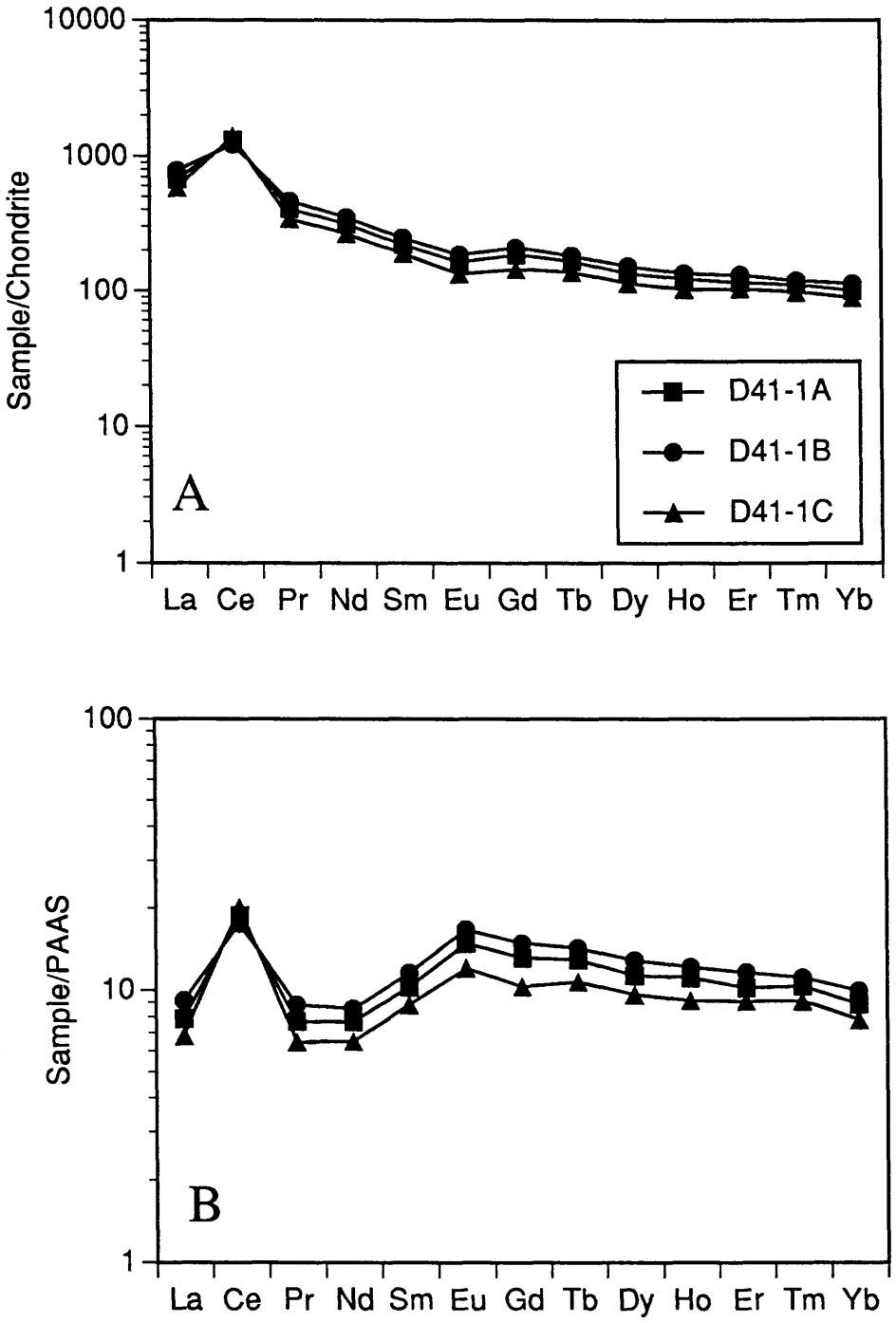

Figure 16. REE plots of crust samples from D41-1, Seth Guyot: (A) Chondrite normalized, and (B) PAAS normalized

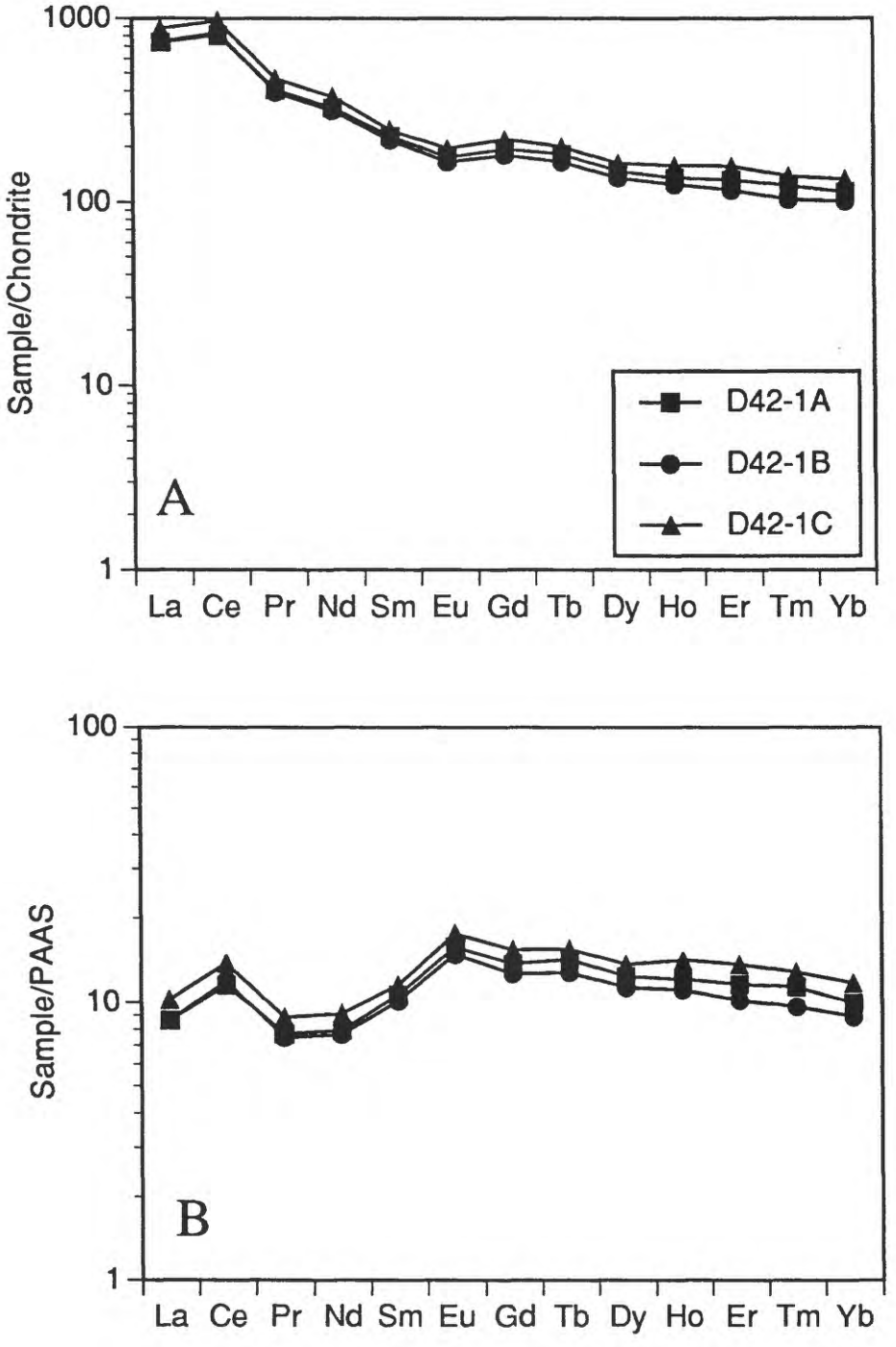

Figure 17. REE plots of crust samples from D42-1, Seth Guyot: (A) Chondrite normalized, and (B) PAAS normalized

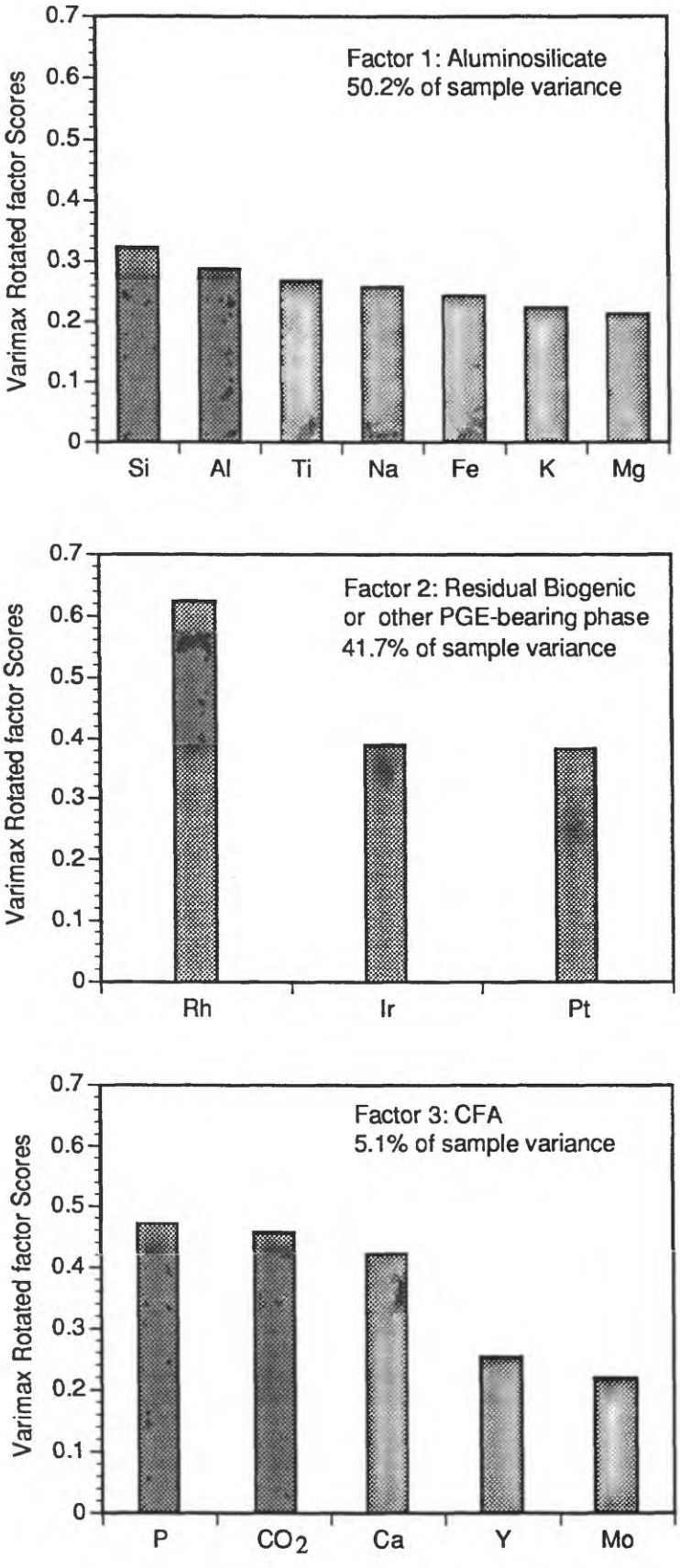

Figure 18. Three of five Q-mode factors for 46 bulk crusts (see figure 19 for other two). Factor scores between 0 and I0.20I are not included because random noise makes it difficult to resolve the orientation of the factor to within 10° of an absolute direction in variable space.

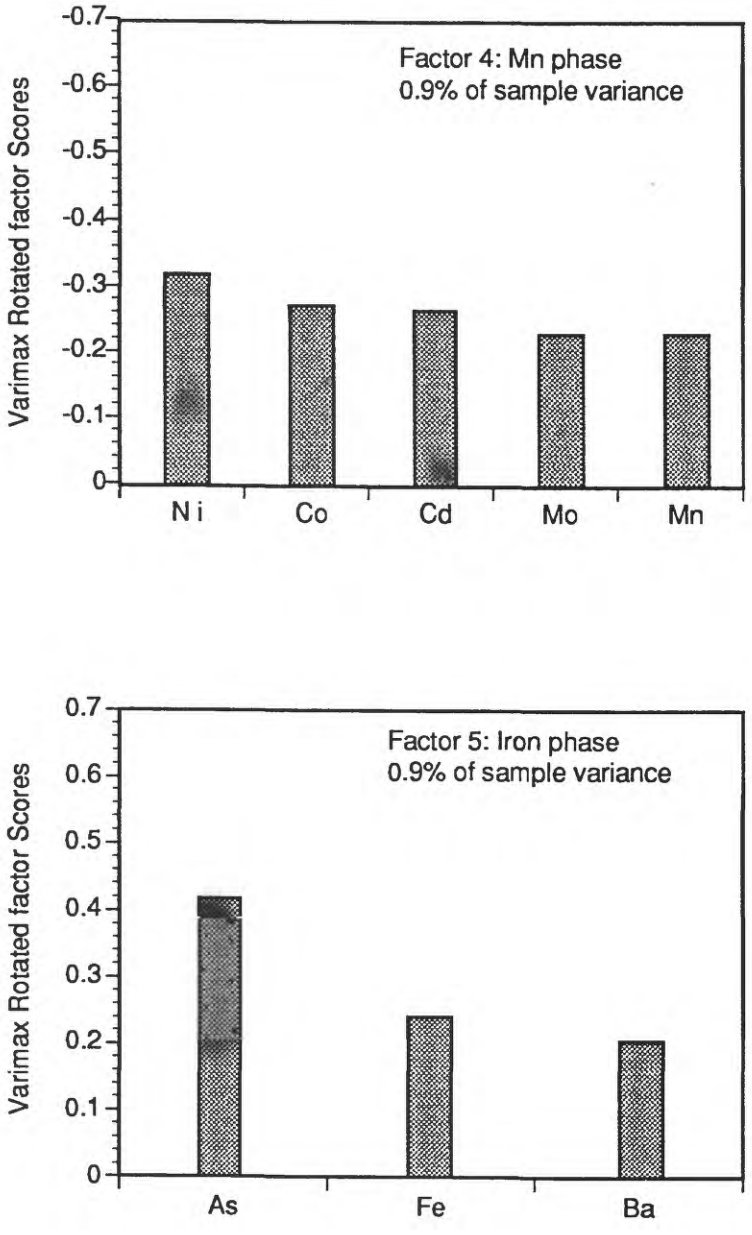

Figure 19. Two of five Q-mode factors for 46 bulk crusts (see figure 18 for other three). The five factors account for 98.8% of the dataset.